VOLUME 42 [J. CELL. AND COMP. PHYSIOL.] NUMBER 1

JOURNAL OF CELLULAR AND COMPARATIVE PHYSIOLOGY

BOARD OF EDITORS

DETLEV W. BRONK, Managing Editor
The Johns Hopkins University

W. R. AMBERSON
University of Maryland

M. H. JACOBS
University of Pennsylvania

A. C. REDFIELD
Harvard University

E. NEWTON HARVEY
Princeton University

E. K. MARSHALL, JR.
The Johns Hopkins University

H. W. SMITH
New York University

L. IRVING
Arctic Health Research Center

G. H. PARKER
Harvard University

RAYMOND E. ZIRKLE
The University of Chicago

AUGUST 1953

PUBLISHED BIMONTHLY BY
THE WISTAR INSTITUTE OF ANATOMY AND BIOLOGY
WOODLAND AVENUE AND THIRTY-SIXTH STREET, PHILADELPHIA 4, PA.

Entered as second-class matter February 19, 1932, at the post office at Philadelphia, Pa., under Act of March 3, 1879. Acceptance for mailing at special rate of postage provided for in section 1103, Act of October 3, 1917, authorized on July 2, 1918

Price, $7.50 per volume, Domestic; $8.00 per volume, Foreign

Publications of The Wistar Institute

JOURNAL OF MORPHOLOGY

Devoted to the publication of original research on animal morphology, including cytology, protozoology, and the embryology of vertebrates and invertebrates. Articles do not usually exceed 50 pages in length.

Issued bimonthly, 2 vols. annually: $20.000 Domestic, $21.00 Foreign, per year.

THE JOURNAL OF COMPARATIVE NEUROLOGY

Publishes the result of original investigations on the comparative anatomy and physiology of the nervous system.

Issued bimonthly, 2 vols. annually: $150.00 Domestic, $16.00 Foreign, per year.

THE AMERICAN JOURNAL OF ANATOMY

Publishes the results of comprehensive investigations in vertebrate anatomy — descriptive, analytical, experimental.

Issued bimonthly, 2 vols. annually: $15.00 Domestic, $16.00 Foreign, per year.

THE ANATOMICAL RECORD

Organ of the American Association of Anatomists and the American Society of Zoologists

For the prompt publication of concise original articles on vertebrate anatomy, preliminary reports; technical notes; critical notes of interest to anatomists and short reviews of noteworthy publications.

Issued monthly, 3 vols. annually: $22.50 Domestic, $24.00 Foreign, per year.

THE JOURNAL OF EXPERIMENTAL ZOOLOGY

Publishes papers embodying the results of original researches of an experimental or analytical nature in the field of zoology.

Issued 9 times a year, 3 vols. annually: $22.50 Domestic, $24.00 Foreign, per year.

AMERICAN JOURNAL OF PHYSICAL ANTHROPOLOGY

Organ of the American Association of Physical Anthropologists

Publishes original articles on comparative human morphology and physiology as well as on the history of this branch of science and the techniques used herein. In addition it gives comprehentive reviews of books and papers, an annual bibliography, and informal communications.

Issued quarterly, 1 vol. annually: $7.50 Domestic, $8.00 Foreign, per year.

JOURNAL OF CELLULAR AND COMPARATIVE PHYSIOLOGY

Publishes papers which embody the results of original research of a quantitative or analytical nature in general and comparative physiology, including both their physical and chemical aspects.

Issued bimonthly, 2 vols. annually: $15.00 Domestic, $16.00 Foreign, per year.

THE JOURNAL OF NUTRITION

Organ of the American Institute of Nutrition

Publishes original researches in the field of nutrition and occasional reviews of literature on topics with which the journal is concerned.

Issued monthly, 3 vols. annually: $22.50 Domestic, $24.00 Foreign, per year.

THE AMERICAN ANATOMICAL MEMOIRS

Publishes original monographs based on experimental or descriptive investigations in the field of anatomy which are too extensive to appear in the current periodicals. Each number contains only one monograph. List of monographs already published, with prices, sent on application.

ADVANCE ABSTRACT CARD SERVICE

Every paper accepted for publication in one of the above periodicals is accompanied by the author's abstract. The abstract and the complete bibliography reference to the paper as it will eventually appear is printed on the face of a standard library catalogue card. This Advance Abstract Card Service is issued promptly, in advance of the journal containing the paper, and is offered in three styles.

Prices per year $2.00, $2.50 and $3.00, postpaid.

These publications enjoy the largest circulation of any similar journals published.

THE WISTAR INSTITUTE OF ANATOMY AND BIOLOGY
WOODLAND AVENUE AND THIRTY-SIXTH STREET, PHILADELPNIA 4, PA.

THE ELECTRICAL POTENTIALS PRODUCED BY THE CHICK EMBRYO DURING ITS INCUBATION PERIOD

B. W. SHUMWAY, M. SABLE AND H. R. BIERMAN

Laboratory of Experimental Oncology, National Cancer Institute, National Institutes of Health, Public Health Service, Federal Security Agency and the Department of Medicine and Cancer Research Institute, University of California School of Medicine, San Francisco

SIX FIGURES

Electrical field variations have been related to the growth or activity of various embryos. Herman and von Gendre in 1885 found that during the first 150 hours of incubation the chick embryo was always positive with respect to the white and to the yolk. Their readings were of the order of 1 mv. at 10 hours, 5 at 40 hours, a maximum of about 10 at 80 hours, 5 at 120 hours, and approximately 2 at 150 hours.

Hyde ('04) found "with few exceptions the direction of the current in the turtle egg was from the animal toward the vegetative pole." She also found between the poles of *Fundulus* an electrical potential that rhythmically became positive and negative and "might be compared with certain phases in the egg during the interval between fertilization and cleavage."

Hyman and Bellamy ('22) postulated that the steady state potential differences in organisms were due to differences of metabolic rate with the regions of high rates being more negative than those of lower rates.

Gayda ('25) found potentials in *Bufo vulgaris* of the order of 20 to 30 mv. in the fertilized egg, 50 mv. just prior to hatch-

JOURNAL OF CELLULAR AND COMPARATIVE PHYSIOLOGY, VOL. 42, NO. 1
AUGUST 1953

ing, and one week after hatching the tadpole had a potential difference of about 22 mv. between the head and tail end.

Burr and Hovland ('37) studied the cephalo-caudad potential gradients of Amblystoma during development from stages 0 to 50, and of chick embryos between head and tail during the first 72 hours of incubation. In each case the electrical potential appeared to increase in the same manner as a growth curve. Burr ('41) later correlated potential gradients with the longitudinal axis of frog embryos.

Romanoff and Cottrell ('39) measured the potential differences of chick embryos between one point in the albumen several millimeters beyond the yolk and another point on top of the yolk at various distances from the center of the blastoderm. These potential differences, which were measured during the first 24 hours of incubation, gradually increased over this period from 1 to 8 mv.

The work of Burr and coworkers has further demonstrated that the presence of neoplastic growth whether spontaneous, chemically induced, or transplanted, markedly affects the bioelectric field of the animal involved. In 1949 Langman and Burr applied these findings and used field measurements to detect malignant lesions in the genital tract of women.

These considerations suggested that long-time recordings could be obtained of the electrical potential field of normal, growing tissue which might be employed as an estimate of the growth process. An initial study was undertaken to obtain reproducible potential recordings for normal tissue which would serve as a baseline for later studies of neoplastic tissues growing upon chick embryos.

The chick embryo was selected for such a study because of the large amount of knowledge concerning its development (Lillie, '08; Needham, '31). Furthermore, it was of convenient size, a rapidly growing organism completely enclosed in a protective shell which could be easily studied in a controlled environment, and neoplastic tissue could be implanted upon the embryo for future investigation.

PROCEDURE

Several methods for measuring the electrical potentials from the egg were attempted. Initially, small glass capillaries containing cotton wicks were placed at the head and tail of the chick embryo but proved unsatisfactory because of high mortality. Moreover, the technical difficulties in making a window for visual control of the electrode placement and sealing the capillaries firmly into the shell made this procedure undesirable.

Further studies revealed that potential readings could be obtained by placement of the electrodes on the external surface of the egg shell.

Finally two-inch lengths of glass tubing bent in the center to form a 90° angle were employed. One end of each ''elbow'' was sealed to the blunt (base) and to the pointed end (apex) of the egg with dental and ceresin waxes taking care that no wax separated the hollow opening of the elbow from the shell. The elbows, with the free ends pointing upward, were first completely filled with isotonic saline and then silver-silver chloride electrodes were introduced several millimeters into the free ends (fig. 1). Excessive wax to prevent leakage at the egg-elbow junction caused high mortality of the eggs as a result of occluding a large portion of the air space. Duco Household Cement used in small amounts was found to be satisfactory for securing the elbows to the egg, preventing leakage and holding the elbows securely though very little of the shell surface was covered.

Measurements of the direct-current series resistance of the electrode assembly and egg were made using an RCA Voltohmist. This resistance was measured for detecting difficulties within the apparatus. Open circuits due to the presence of air bubbles, the clogging of shell pores by the cement, the evaporation of saline from the elbows, or the incomplete permeation of the shell area by the saline were thus rapidly detected. It was of further interest to determine if the resistance had a time relationship.

The electrical differences appearing between the electrodes were amplified by a two-stage, direct-coupled, balanced amplifier and recorded on an Esterline-Angus recorder of one milliampere full-scale sensitivity (fig. 1). The amplifiers originally employed tubes of the electrometric type, but these were unable to drive a recorder directly, and new amplifiers were built using balanced 6SF5 tubes in the input and a 6SN7 tube in the output. No grid resistor was used for the input tubes, the egg and electrode assembly serving as a grid return. Degeneration was incorporated to improve stability, and at the sensitivity level required the zero remained constant for hours at a time. A circuit which recorded calibration potentials of ± 20 mv. by the manual operation of a front panel switch was included in each amplifier. The gain and balance controls of the amplifiers could be adjusted to set the output current to correspond to the known input voltages. These amplifiers, which had grid currents of less than 10^{-9} ampere,

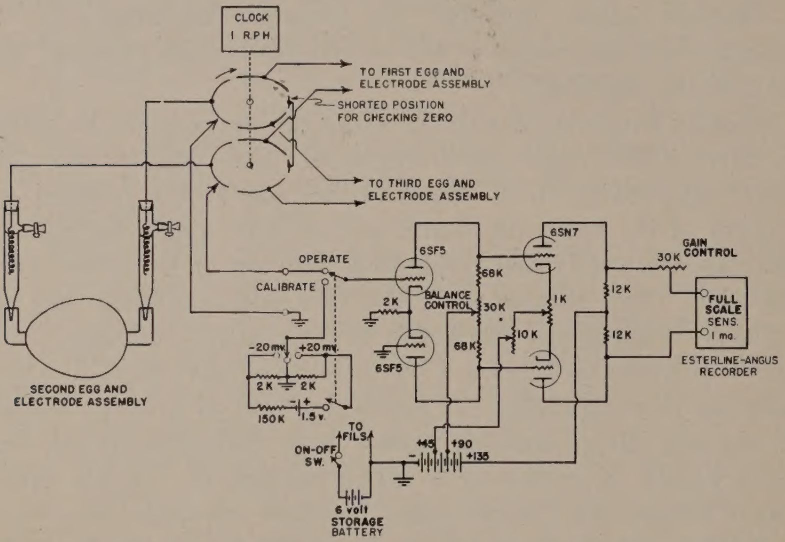

Fig. 1 Circuit and assembly for measuring electrical potentials of the chick embryo.

were checked extensively against the original electrometers and no appreciable difference was ever noted.

An armature-type switch which rotated once each hour was used. The amplifier and recorder were switched serially to three eggs, each for 19 minutes and then to a shorting circuit for three minutes, thus completing the switching cycle. The Esterline-Angus recorder had a paper speed of one and one-half to 6 inches per hour. Two amplifiers and two recorders allowed records to be made of 6 eggs in concert. A comparison of records thus obtained with several continuous recordings revealed that negligible error had been introduced by the switching technic.

For the shorting circuit to render a valid reference of zero potential difference, it had to be assured that no standing potential existed between the electrodes. This was accomplished by placement of the electrodes into a beaker of physiological saline. A Leeds and Northrup Type 8667 portable potentiometer was used to measure the potential. Although several sets of electrodes were used and measurements of their standing potentials were made over several days prior to actual use and then at the beginning and end of each experiment, at no time was there a potential difference greater than 1 mv.

The overall error was estimated to be ± 1.2 mv. which included the recorder writing error, variations of the standing potential of the electrodes, error from grid current in the amplifier input and thermoelectric variations.

The incubator temperature was kept at 37 ± 1°C. and the humidity was approximately 35%.

The use of elbows for making electrode contacts prevented turning the eggs but it was found that this was not essential to the maintenance of viability, although it probably did increase the percentage of mortality.

RESULTS

Of 90 separate studies of the chick egg, 27 afforded continuous records of 10 days or longer. These records were

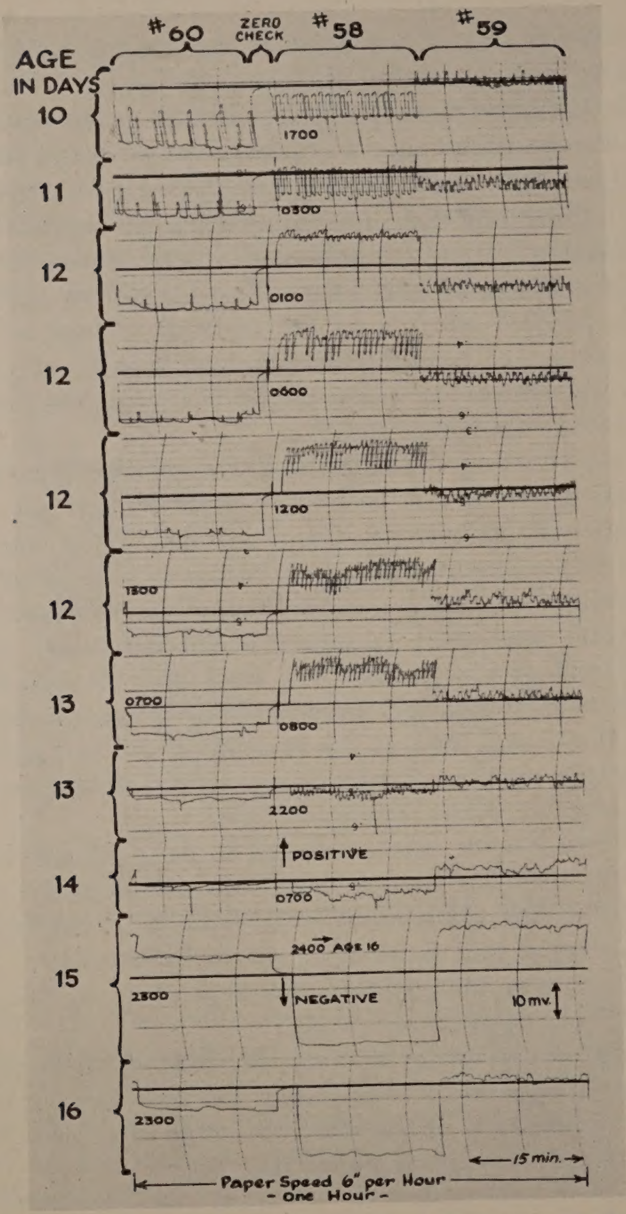

Fig. 2 Represents sections of electrical potential recordings in Eggs nos. 58, 59 and 60. Note the changes with respect to the zero line of the "A" potential upon which is superimposed a more rapidly changing "B" component. The record obtained for Egg no. 58 demonstrates clearly that the "B" component is in reality a complex of several potentials.

begun prior to the 8th or 9th day and were continued until the chick hatched or died. Two records were obtained for the entire 21-day period but the mortality was too great to make many such prolonged studies expedient. The remaining 63 records were for periods of 4 to 9 days and although they were not used in this report, the findings during these short periods were similar to those on the 27 eggs recorded over longer periods.

A consistent pattern of electrical potential variation was observed which was broadly classified into two major components; a basic potential that varied slowly over days upon which was superimposed a rapidly-varying component having an average period of a half to 10 minutes. The slow potentials ranged between — 50 to + 50 mv., apparently related to the growth of the embryo, and were designated arbitrarily as ''A potentials'' (fig. 2). The rapidly-varying component was termed ''B potentials'' and suggested an association with movement of the embryo as observed beneath cover slip preparations over openings in a few eggs. The ''B potentials'' exhibited some rhythmicity in occurrence, of period, and of character (fig. 2). Their amplitude appeared first to increase and then decrease as the embryo approached hatching, but rarely exceeded 10 mv.

For ease of comparison and interpretation, plots of the ''A potentials'' of individual eggs were made by averaging 4 19-minute intervals (the actual record usually being almost a straight line over these 4 intervals) for each plotted point: thus 6 points were plotted for each 24 hours of record. These were later averaged for each 24-hour period and replotted. The resulting curves were smooth and varied slowly.

Typical curves of the ''A potentials'' are plotted in figure 3 a. It is seen that the curves follow a general pattern. By translation of the axes to allow for slight differences in age, in rate of development, and for standing potentials within the egg, many of the curves could be fairly well superimposed. Using this technic a composite curve was made (fig. 3 b).

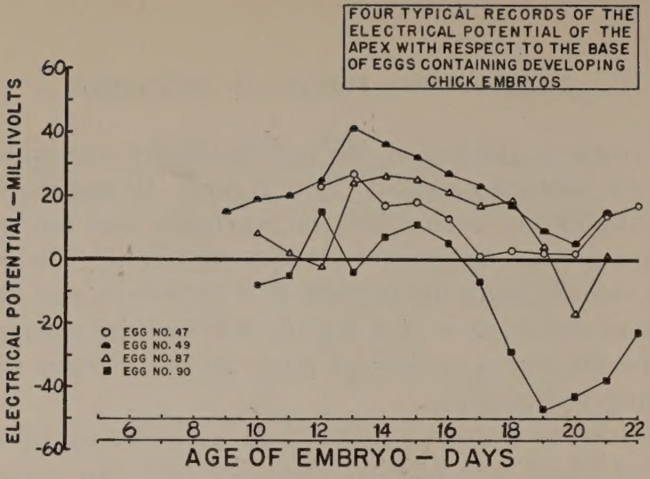

Figure 3 a

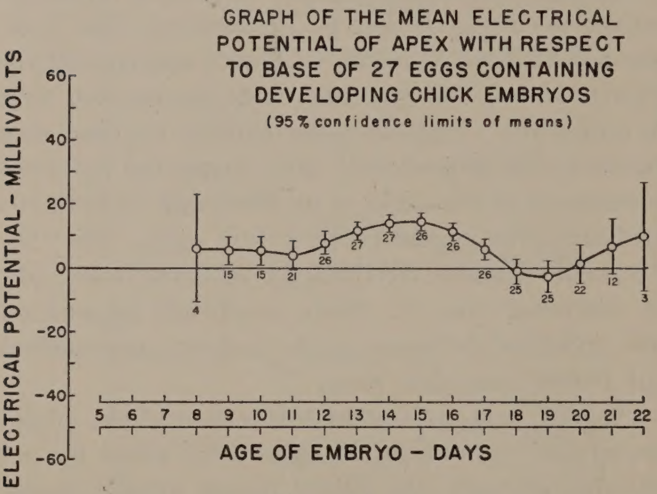

Figure 3 b

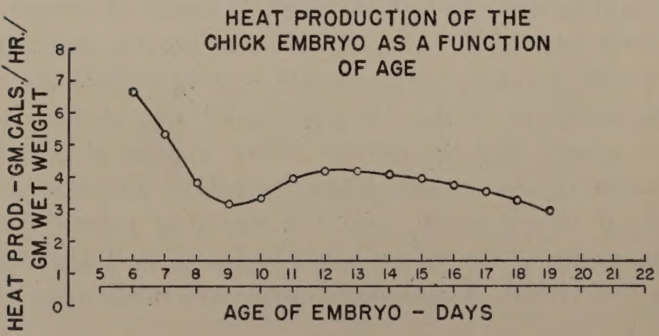

Figure 3 c

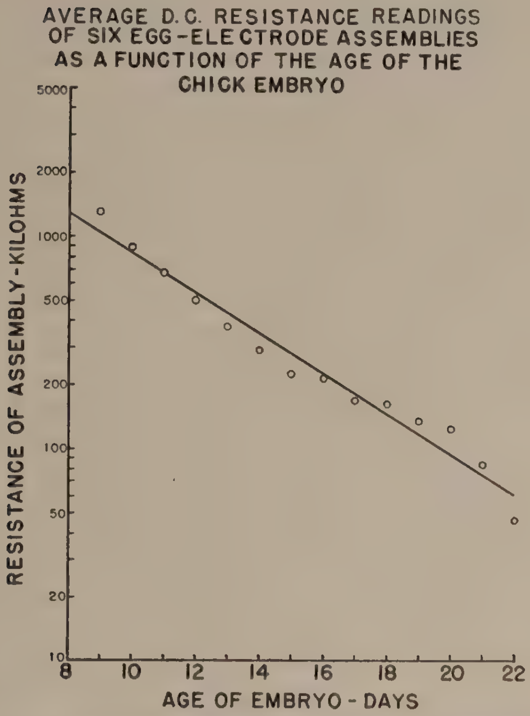

Fig. 4 Average direct current resistance readings of 6 egg-electrode assemblies as a function of the age of the chick embryo.

Fig. 3 (a) Typical records of the electrical potential averaged by days of the apex with respect to the base of eggs containing developing chick embryos. These 4 were selected to indicate the wide variation of the individual readings at any given age. Nearly all other curves obtained fell within the extreme values of these curves except for minor short time excursions similar to that on the 12th day shown by Egg no. 87. Notice that the individual records vary widely, but that a general pattern is evident.

(b) Graph of mean electrical potential of 27 eggs containing chick embryos. The vertical lines represent 95% confidence limits of the means calculated in terms of a *t* distribution and the numerals below each line represent the number of eggs upon which the line is based.

(c) The heat production curve of developing chick embryo as a function of age was calculated from data of Bohr and Hasselbalch ('03) and of H. A. Murray, Jr. ('26).

During the first 5 days no potential of appreciable magnitude was observed. The "A" potential differences slowly increased, apex positive with respect to the base, and reached a maximum about the 14th or 15th day. Subsequently, the potential differences decreased and generally became reversed in polarity during the 18th or 19th day briefly before the apex again became slightly positive with respect to the base. When the eggs died prior to the normal 20- to 22-day period, the small rapid variations (B potentials) in the recordings vanished and the slow "A potentials" approached a constant value approximately zero. Recordings on boiled eggs showed no variations or electrical potential differences.

The curve of the average electrical resistance of 6 eggs was plotted as a function of age of the embryo and showed a logarithmic decrease (fig. 4). This decrease may also be influenced by an increasing saturation of the shell and certain regions of the egg by saline during the initial period of study but more probably reflect an increase in electrolyte concentration from tissue fluids of the developing embryo.

DISCUSSION

Although measurements of electrical potential differences on the external surfaces of fertile chicken eggs yielded a reproducible pattern, attempts to correlate the form of the resultant mean curve with specific developmental changes were inconclusive.

The orientation of the embryo within the shell might also be expected to affect the potential readings. At approximately the 14th day of incubation which corresponded to the period of maximum potential difference, the embryo has become oriented lengthwise along the apicobasal axis (Lillie, '08). On the 19th day, corresponding to the minimum potential difference, the embryo's beak pierces the membranes, enters the air space, and normal breathing begins.

Similarly several other events may be related to the potentials, none of which, however, can be definitely associated. The rate of fluid loss of the chick embryo increases and then decreases during the 11th to the 19th day of incubation in almost precisely the same manner as the potential curve (Needham, '31). It continues, however, to decrease after the 19th day. The specific gravity of the amniotic fluid is maximum about the 14th day which is approximately coincident with the maximum potential difference. The percentage rate of increase of dry substance of the embryo dips slightly around the 10th to 12th days and shows a possible maximum during the 13th to 14th days. If one plots the percentage change of calorific value, a curve similar to that of potential is obtained but the maximum is slightly more pronounced. The plot of per cent change in fat approximates the potential curve still better.

Heat production is of more interest. The data of Bohr and Hasselbalch ('03) for the gram calories lost per hour were taken and divided by the embryo wet weight which were in turn taken from smoothed data of Murray ('26). A least squares solution was first obtained for Murray's values, and the smoothed values of weight were calculated from the resulting empirical equation:

$$\text{Weight (gm)} = 0.00078\ \text{Age (days)}^{3.59}.$$

The curve for the heat production is shown in figure 3 c. The similarity of this curve to the potential curve is striking. It must be emphasized however that many simultaneous processes of the chick embryo produce potentials and the potential as measured can be presumed to be approximately the average algebraic summation of the components projected on the conical surface of the egg delimited by the apex and the rim of the air space at the base. While a single physiological process may be dominant in producing the pattern of variation of potential, many other processes contribute and cannot be excluded from consideration.

Specific interpretation of the potential pattern must be somewhat speculative in the absence of an explicit cause-effect relationship. On the other hand concomitancy between metabolism and externally measured potential lends much interest to the reproducible electrical pattern as a reflection of normal growth.

SUMMARY

1. The bioelectric field potential of the apex of the external shell of the chick embryo with respect to the base was recorded during the incubation period for 90 normal, fertile eggs. Continuous records on 27 chick embryos which were obtained for 10 days or longer are reported.

2. The potentials were of two basic patterns. A low component designated ''A'' potential that varied over days between − 50 and + 50 mv. Superimposed on the ''A'' potential was a more rapid component termed ''B'' potential that varied over minutes and was visibly observed to be associated in part with movements of the embryo.

3. The ''A'' and ''B'' potentials were found to vary in a reproducible pattern in life and to approach a constant value approximating zero with death of the embryo.

4. A similarity was found between the curve for electrical potential and a calculated curve of metabolic rate.

ACKNOWLEDGMENT

The authors wish to acknowledge the technical assistance of R. J. Jenkins for construction of the amplifier and of E. Randolph for his aid in obtaining the records.

LITERATURE CITED

Bohr, C., and K. A. Hasselbalch 1903 Ueber die Warmeproduction und den Stoffwechsel des Embryes. Skandinavisches Archiv fur Physiologie, *14:* 398–429.

Burr, H. S. 1941 Field properties of the developing frog's egg. Proc. Natl. Acad. Sci. Wash., *27:* 276–281.

———— 1941 Changes in the field properties of mice with transplanted tumor. Yale J. Biol. Med., *13:* 783–788.

Burr, H. S., and C. I. Hovland 1937 Bioelectric potential gradients in the chick. Yale J. Biol. Med., *9:* 247–258.

———— 1937 Bioelectric correlates of development in amblystoma. Yale J. Biol. Med., *9:* 541–549.

BURR, H. S., G. M. SMITH AND L. C. STRONG 1938 Bioelectric properties of cancer-resistant and cancer susceptible mice. Am. J. Cancer, *32:* 240–248.

——— 1940 Electrometric studies of tumors induced in mice by the external application of benz-pyrene. Yale J. Biol. Med., *12:* 711–717.

BURR, H. S., L. C. STRONG AND G. M. SMITH 1938 Bioelectric correlates of methylcholanthrene-induced tumors in mice. Yale J. Biol. Med., *10:* 539–544.

GAYDA, T. 1922 Ricerche di elettrofisiologia mello sviluppo ontogenetico del ''Bufo vulgaris.'' Archivio di Scienze Biol., *3:* 1–25.

HERMANN, L., AND A. VON GENDRE 1885 Ueber eine electromotorische Eigenschaft des bebruteten Huhnereies. A. Pflug. Arch. ges. Physiol., *35:* 34–35.

HYDE, E. H. 1904 Difference in electrical potential in developing eggs. Am. J. Physiol., *12:* 241–275.

HYMAN, L. H., AND A. W. BELLAMY 1922 Studies on the correlation between metabolic gradients, electrical gradients, and galvanotaxis. Biol. Bull. Woods Hole, *43:* 313–347.

LANGMAN, L., AND H. S. BURR 1949 A technique to aid in the detection of malignancy of the female genital tract. Am. J. Obstet. and Gyn., *57:* 274–281.

LILLIE, F. R. 1908 The Development of the Chick. Henry Holt and Co., New York.

MURRAY, H. A., JR. 1926 Physiological ontogeny, A. Chicken embryos. VII. The concentration of the organic constituents and the calorific value as functions of age. J. Gen. Physiol., *9:* 405–432.

NEEDHAM, J. 1931 Chemical Embryology. The Cambridge University Press, Cambridge, England.

ROMANOFF, A. L., AND C. L. COTTRELL 1939 Bioelectric potentials of the hen's egg. Science, *90:* 471–472.

THE ULTRASTRUCTURE OF THE OUTER SEGMENTS OF RODS AND CONES OF THE EYE AS REVEALED BY THE ELECTRON MICROSCOPE [1]

FRITIOF S. SJÖSTRAND
Department of Anatomy, Karolinska Institutet, Stockholm

TWELVE FIGURES

In previous papers (F. S. Sjöstrand, '48, '49) the author has reported on an analysis of the outer segments of the rods of the retina of the guinea pig eye. Each outer segment is composed of a pile of rounded discs which are arranged in pairs.

In order to test the validity of the proposed model describing the arrangement of these discs the investigation has been carried on using ultrathin sections through the guinea pig retina. The work has also been extended to include an analysis of the rod and cone outer segments from the retina of perch eyes. A similar but not identical organization of the outer segments of the cones has been revealed.

Earlier investigations on the outer segments of rods and cones by means of light microscopy including polarization optical analysis have been described by W. J. Schmidt ('34).

MATERIAL AND TECHNIQUE

For sectioning the eyes of albino guinea pigs (300–400 gm) were removed from the animals after beheading and were opened along the equator. After removing the vitreous body the eye cup was fixed in buffered 1% osmium tetroxide according to the recommendations of G. E. Palade.

---

[1] This paper is based on a report given at the Scandinavian Electron Microscope Society meeting, June 8, 1952 and at the Electron Microscope Society of America meeting, November 1952.

When dissecting the perch eyes the retina sticks to the rigid vitreous body and in order to obtain as fast fixation as possible the vitreous body with the adhering retina in good shape was removed and fixed as stated above.

As embedding medium n-butylmethacrylate was used mainly according to Newman, Borysko and Swerdlow ('49).

The Spencer rotary microtome model 820 was used for sectioning with the standard adapter to reduce the feed and with modifications similar to those recommended by Hillier and Gettner ('50) for decreasing friction in the horizontal slides. A coil spring was adapted by means of specially made parts to secure a lifting force applied at the center of gravity of the moving system carrying the specimen block. A motor was used to drive the microtome at a speed of 52 revolutions a minute. The mechanical advance mechanism was found to be more convenient than the thermal expansion arrangement for advancing the block. The thermal expansion was realized through cooling the brass holder for the methacrylate block by blowing CO_2 directly on this brass holder.

Special attention was paid to the problem of vibrations which are transferred from the motor and which arise in the microtome due to the repeated change of direction of the parts of the microtome moving vertically. The microtome was mounted on a concrete foundation resting on solid rock and isolated from the laboratory floor. As transmission between motor and microtome a plastic belt was found superior to the arrangement of Hillier and Gettner. The microtome was especially trimmed to give a smooth running. A careful oiling of all sliding surfaces is of the greatest importance.

Schick razor blades were used as knives mounted in a curved position (F. Sjöstrand, '51). They have to be polished very carefully to be useful for really thin sectioning. For polishing Linde B polishing powder, dispersed in a 1% soap solution, was used as abrasive. The razor blade was mounted in a special holder during polishing, which was performed on a plain mirror glass surface. The sections were collected on a liquid surface, using a trough similar to the one originally described by Gettner and Hillier ('50). As liquid 20–30% ethyl alcohol was used.

The sections were floated onto the specimen grids covered with a thin formvar film. They were examined in the electron microscope without dissolving the methacrylate. The examination was performed at a low beam intensity, to avoid subliming the methacrylate.

An RCA EMU 2 c electron microscope was used with compensated standard objective pole piece, with standard objective aperture, with three apertures in the projector lens (according to Hillier's recommendations) and reduced condensor lens aperture.

The magnifications were calibrated by using chromium shadowed replicas of an 1152 lines per millimeter diffraction grating and Dow latex particles, 58 G lot 3584. To reduce the influence of the layer of contamination that is built up during the exposure of the particles to the beam, the double diameter of pairs of particles in contact was measured and the average single diameter of the two particles as measured across the contaminated surfaces was subtracted. At the spot of contact there will not be any increase of the diameter due to contamination and the first measurement will include the diameter of the two particles plus the thickness of two contamination layers. When subtracting the diameter of an individual particle as measured across the free surface the diameter of one particle plus two contaminating layers are subtracted and the diameter of the uncontaminated particle is obtained.

The resolution of the micrographs stated is based on measurements which have determined the minimum distance between image points which are resolved.

Electron microscope observation

Sections through the outer segments of the rods clearly show that these segments are composed of a stack of thin membranes with a diameter corresponding to the diameter of the segment (figs. 1–2). The thin membranes are connected in pairs. All

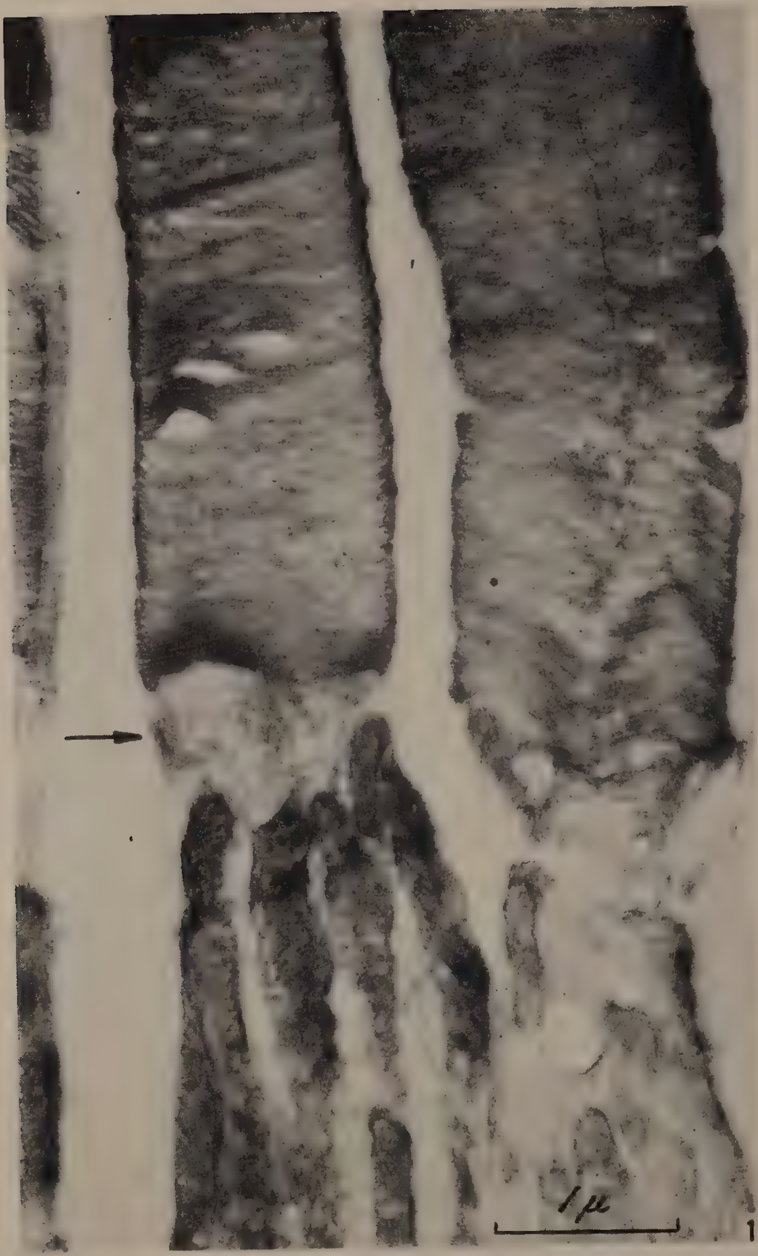

Fig. 1 Rods from the guinea pig retina showing the laminated structure of the outer segments and the border between outer and inner segments. At the base of the outer segments some wrinkled membranes are seen (indicated by the arrow), constituting an artifact. Magnification, × 24,000.

around the circumference the two membranes in such a pair are connected without any discontinuity. These pairs, therefore, constitute discs with a narrow and closed space or compartment in between the two membranes. They will be called *double membrane discs* (figs. 4–5).

The whole outer segment is uniformly organized with a regular and uninterrupted sequence of double membrane discs. There is a sharp demarcation between the inner and outer segments without any interconnection except for a specialized structure joining them. This structure will be described in a following paper.

The pile of discs is surrounded by a thin outer membrane (fig. 6), which is not continuous with the outer membrane of the inner segment. In preparations that are not perfectly preserved there frequently occurs a zone at the base of the outer segment characterized by irregularly wrinkled thin membranes (fig. 1). This is an artifact depending upon a disorganization of the double membrane discs at the base, presumably through not quite ideal fixation and embedding.

The outer segments constitute structures that are extremely sensitive to fixation and embedding procedures. They are easily damaged, and the first indication of a damage is a partial or complete separation of the double membrane discs (figs. 2 and 5).

The connection at the edge between the two membranes of a double membrane disc appears as a fairly resistant and dense marginal U-shaped portion. This seems indicated by the characteristic deformation of the double membrane discs which have swollen due to improper fixation. The narrow cavity between the membranes of a double membrane disc then increases in volume, pushing the membranes apart. The marginal connection then still keeps a U-shaped form (fig. 5).

When cut transversely or obliquely the stack of rod discs appear rounded with an incision towards the center of the discs. The incisions of adjacent discs are oriented in the same direction, and therefore, a narrow groove or fissure runs along the whole outer segment. This groove widens at the base of the

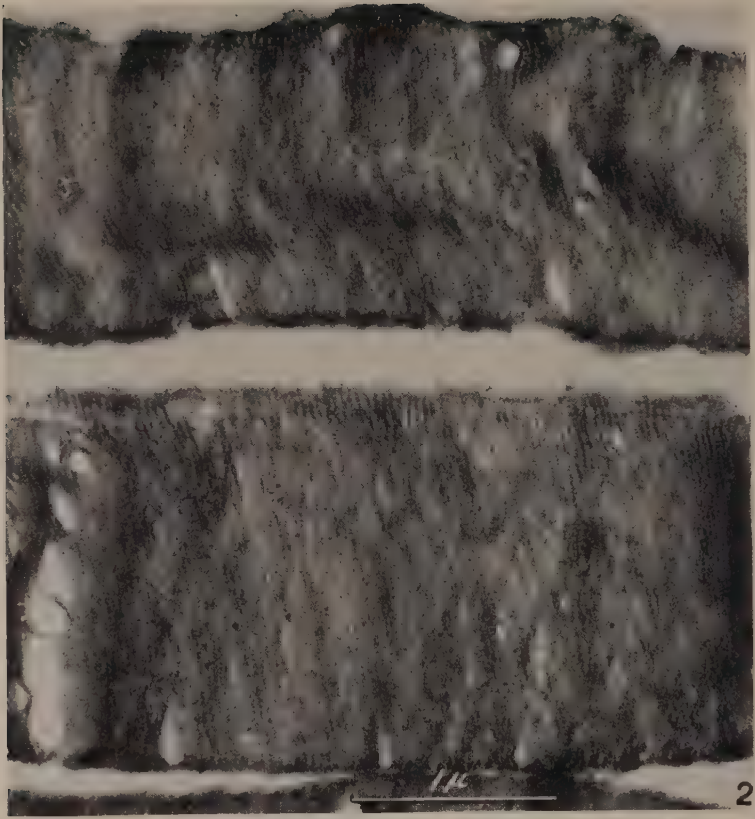

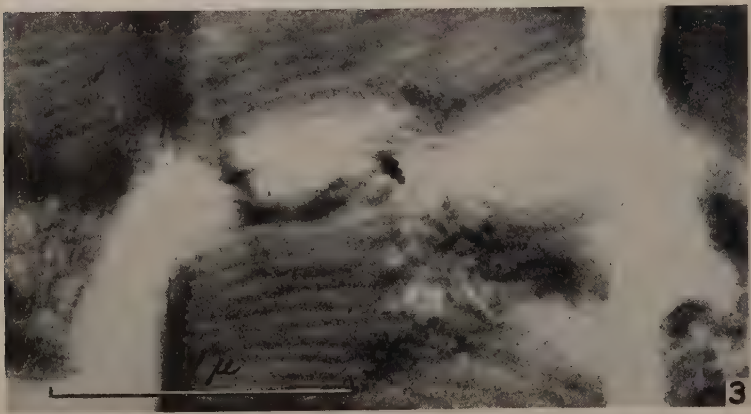

Fig. 2 Guinea pig rod outer segments with laminated structure. At the left side of the lower rod there is an artificial separation of some of the membranes. Magnification, × 28,000.

Fig. 3 Guinea pig rod outer segment showing connections between the double membrane discs. Magnification, ×40,000.

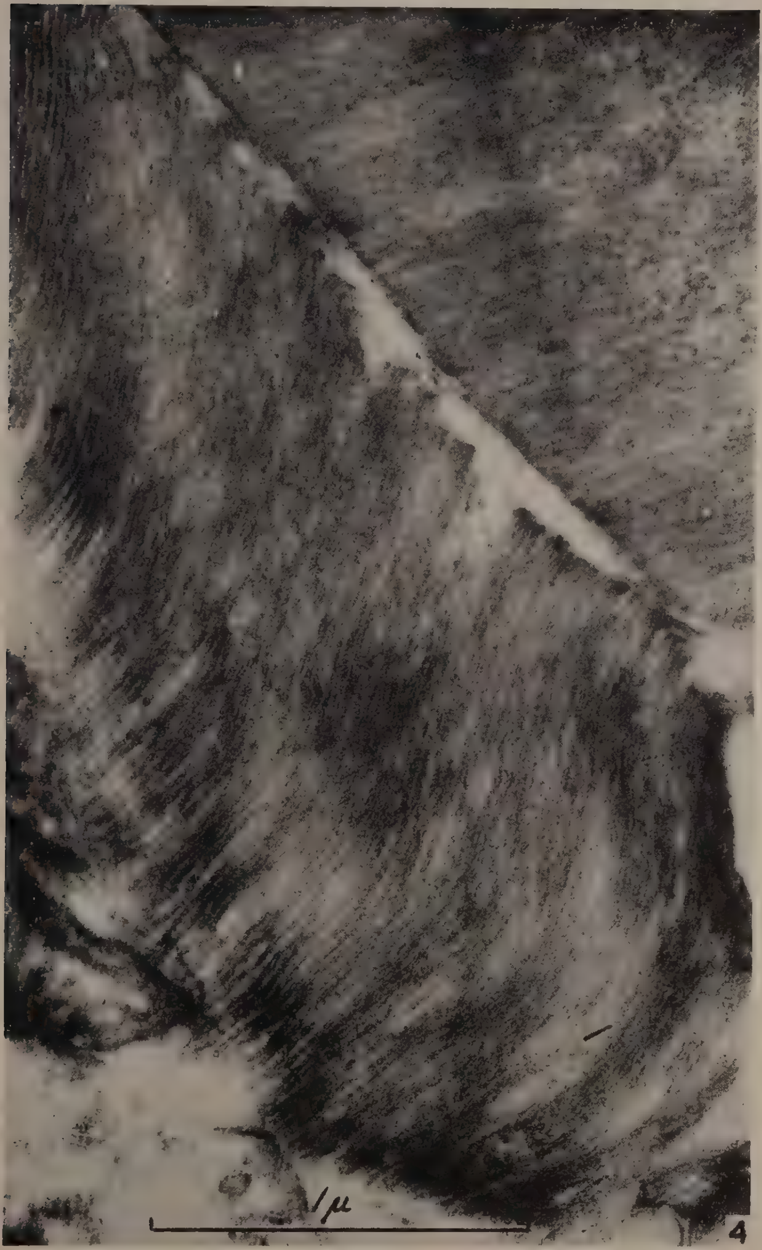

Fig. 4 Guinea pig rod outer segments of a rather well preserved specimen. The double membrane discs are tightly packed. Magnification, × 50,000.

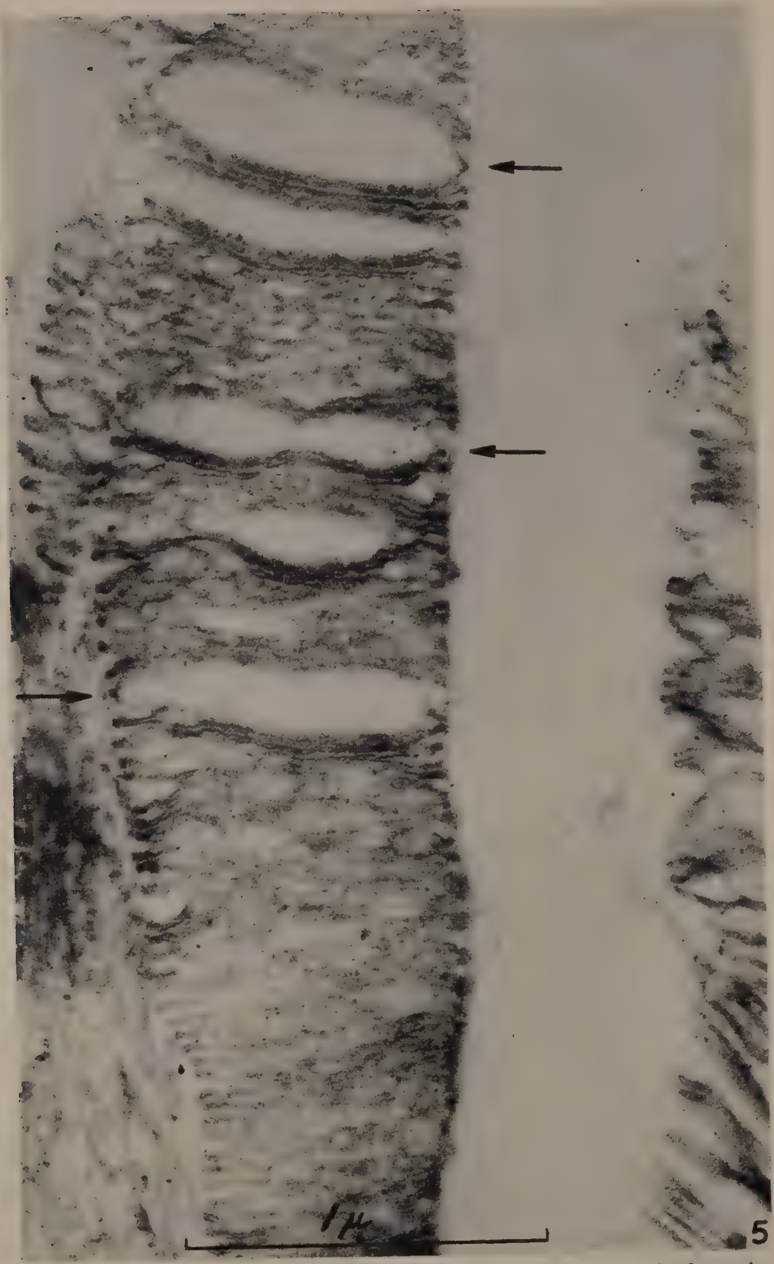

Fig. 5 Guinea pig rod outer segments distorted and showing the loosening of the connections between the double membrane disc (the rod along the right side) and the swelling of some of these discs. The resistant outer edges of these swollen discs are indicated by arrows. Magnification, × 48,000.

segment where the already mentioned specialized structure connects the outer and the inner segments.

When cut obliquely the rods show characteristic structures in connection with the central terminations of the incisions of the discs (fig. 6). There are indications of lengthwise oriented short fibrils with dense edges mutually connecting the double membrane discs. These fibrils seem to correspond to the thin stalks which may be observed extending from the incisions of discs isolated through fragmentation. In sections these structures appear rather complicated (figs. 1, 4 and 6) but the interpretation is facilitated through observing sections of rods where the distance between the double membrane discs have been slightly increased due to a swelling of the rod outer segment when fixed and embedded (fig. 3). The double membrane discs then appear connected in series with criss-cross oriented extensions.

The membranes of the discs exhibit no internal structure that can be observed with the resolution of the best micrographs of these sections, 30 A with the exception of the black dots described in previous papers (F. S. Sjöstrand, '48–'49) on fragmented material.

The distance between the two membranes in a double membrane disc has been measured on 280 double membrane discs in 24 different rods as the distance between the centers of the two dark lines that represent the cross-cut membranes. This distance is 105 ± 2 Å (table 1). The coefficient of variation is 10.5%. This measure includes the thickness of one membrane which according to previous measurements (F. S. Sjöstrand, '48) is about 30 Å. The space between the membranes in such a double disc, therefore measures 70–80 Å.

The thickness of the single membranes cannot be estimated with any great degree of accuracy on these sections as it corresponds to the resolution in these micrographs.

The membranes are best defined due to the enhanced contrast when cut exactly across. They will then be oriented parallel to the electron beam and the pattern of mass distribution in the section will be the same through the whole thickness of

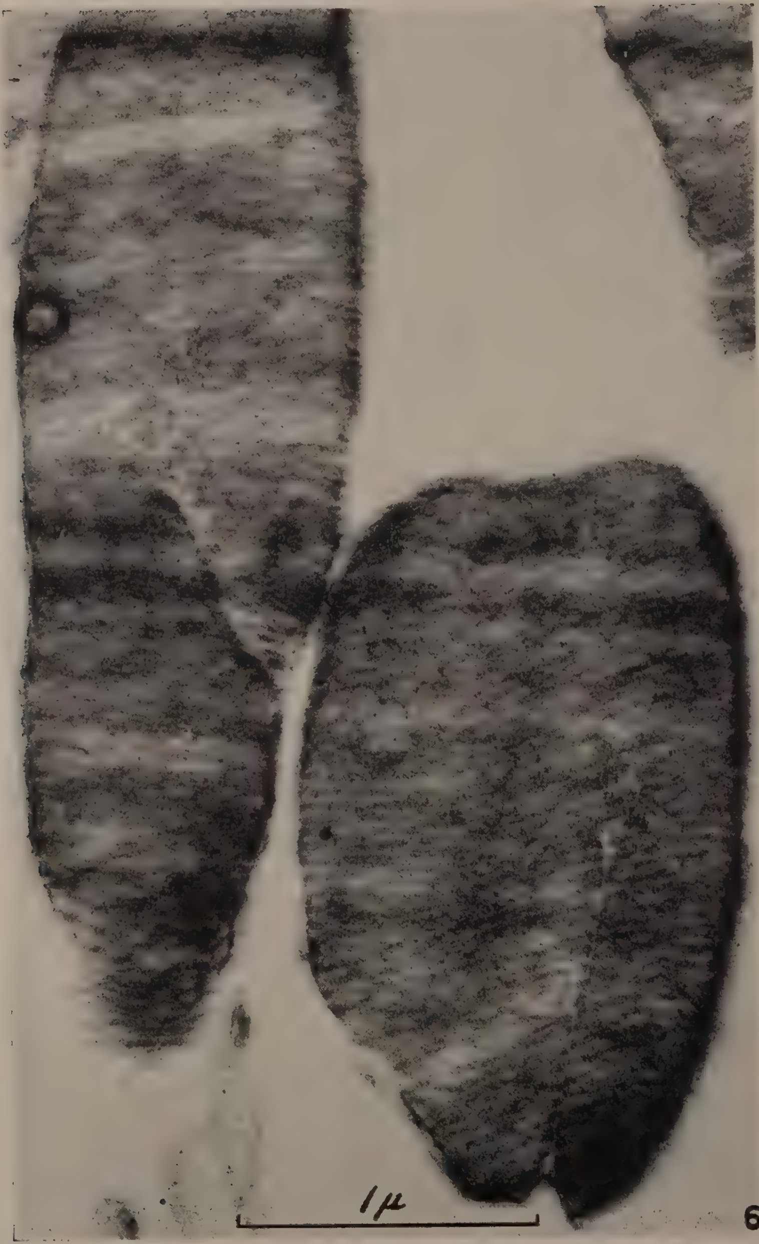

Fig. 6 Guinea pig rod outer segments cut obliquely and showing the groove running along the outer segment due to the incisions of the individual double membrane discs. Magnification, × 40,000.

the section. In such cases it is possible to reveal the membrane structure even in fairly thick, over 0.05 μ sections.

On the thinnest sections with the highest resolution, about 30 Å, and with the discs cut perpendicularly the total thickness of the double membrane discs has been measured. The average thickness from measurements on 200 double discs in 11 different rods was 146 ± 4 Å (table 2). This figure corresponds well to the one obtained when measuring the thickness of isolated double membrane discs on shadowed specimens, 140 Å.

TABLE 1

The distance between the two membranes of the double membrane discs; measured as the distance between the centers of the perpendicularly cut membranes. Each figure represents the mean value of 10–15 measurements.

ROD NO.	DISTANCE IN Å	ROD NO.	DISTANCE IN Å
1	123	13	108
2	105	14	104
3	94	15	95
4	119	16	95
5	105	17	97
6	108	18	103
7	103	19	97
8	103	20	89
9	110	21	100
10	125	22	93
11	118	23	95
12	118	24	102

Mean value 105 ± 2 coefficient of variation = 10.5%.

It seems justified to evaluate the figure representing the distance between the centers of the membranes in a double membrane disc as more reliable than the above reported measurements on sections of the total thickness of the double membrane discs. This figure was 105 Å. Adding the thickness of a membrane 30 Å would give a total thickness of the double membrane disc of about 140 Å.

The distances between the double membrane discs have been estimated by counting the number of double membrane discs

TABLE 2

The total thickness of the double membrane discs of the guinea pig rods

ROD NO.	NUMBER OF MEASUREMENTS	THICKNESS MEAN VALUE IN Å	COEFFICIENT OF VARIATION %
1	45	151 ± 2.2	10.2
2	20	145 ± 3.1	9.5
3	20	147 ± 3.4	10.4
4	10	159 ± 6.6	13.0
5	35	139 ± 2.7	11.4
6	15	154 ± 3.3	8.3
7	10	159 ± 5.0	9.9
8	10	153 ± 3.5	7.2
9	10	148 ± 3.4	7.2
10	15	124 ± 2.8	8.7
11	10	122 ± 3.2	8.2
	Mean value	146 ± 4	8.1

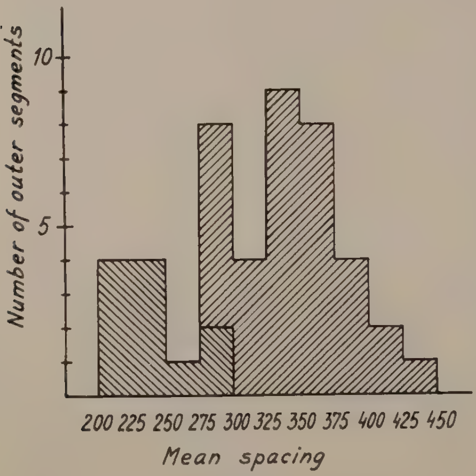

Diagram 1 A

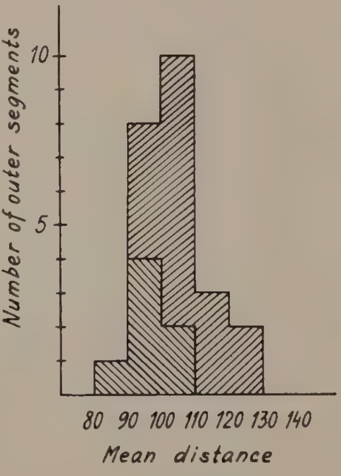

Diagram 1 B

Diagram 1 A The distribution of spacings measured on 45 rod outer segments from the guinea pig eye. The two groups of mean spacings correspond to two different series of specimens treated in a slightly varied way (further data in the text).

Diagram 1 B The distribution of the mean distances between the two membranes of the double membrane discs (measured as the distance between the centers of the single membranes) in 24 rods from the guinea pig eye.

per unit length of the rod outer segments. The estimations have been performed on 45 rods, the mean value obtained representing the average distance between 1600 double membrane discs.

The material is presented in diagram 1 A where the corresponding spacings have been calculated. The material may be divided in two groups characterized by statistically significant differences regarding the spacing between the double membrane discs. In one group there are 30 ± 0.5 double membrane discs per micron, in the second group 41 ± 1.2 per micron. These two groups differ with regard to the fixation and embedding procedure. The retinas of the second group have been fixed in a buffered osmium tetroxide solution where the molar concentration was very carefully adjusted to isotony with respect to guinea pig red blood cells. For washing the retinas of this group after the fixation, a balanced salt solution was used instead of distilled water.

The specimens of the second group show a more regular packing of the double membrane discs with very few spots along the segment where the discs are separated by obvious artificial spaces. These specimens, therefore, have been considered as representing a better preservation of the structure.

The repeating period of the rod outer segment, that is the mean distance between the centers of the double membrane discs, as representing the structural unit, is obtained directly from the number of discs per unit length. The mean value of this period is for the first group 340 ± 2 Å and for the second group 240 ± 8 Å. Diagram 1 A illustrates the distribution of the values and demonstrates the significant difference between the two groups.

Using the value 41 double membrane discs per micron and an average thickness of these discs of 140 Å we obtain 100 Å as the average distance between the double membrane discs. Using the lower value, 30 double membrane discs per micron, will give a mean height of the space in between the double membrane discs of 200 Å.

Diagram 1 B illustrates for comparison the distribution of the values for the distance between the two membranes of the double membrane discs. There is no significant difference between the values from the two groups of specimens. The distance between the membranes of a double membrane disc, therefore, seems to be less affected by osmotic factors than the distance between the double membrane discs.

The total number of membranes in a rod outer segment was calculated from the previous data collected on fragmented material to be about 2000. The thickness of the disk pairs was estimated to 140 Å and the mean length of the rod outer segments was estimated to 17 ± 2.3 μ but it had not been possible to obtain any information regarding the distance between the disc pairs. The figure 2000 was calculated by assuming the disc pairs in direct contact with each other.

The data now obtained from sections secure a more reliable estimation of the total number of membranes as the width of the space between the double membrane discs has been measured. There will be about 1400 membranes in each rod outer segment arranged in about 700 double membrane discs.

The total surface of these membranes is about 4,500 μ^2 per rod, or 45 cm^2 per million rods. The total volume of the membranes would then be about 13 μ^3 and the volume of the compartments surrounded by the two membranes of all double membrane discs would be about 15 μ^3.

Perch rods. The outer segments of the rods from perch eyes (fig. 7) show a striking similarity to the rods of the guinea pig eye. The whole outer segment is uniformly packed with double membrane discs, arranged in a pile and surrounded by a thin outer membrane. There is as sharp a separation between the outer and inner segments as in the guinea pig rods.

The membranes of the double membrane discs are thicker and coarser than the corresponding structure of the guinea pig rods. The average thickness of the single membranes when measured on close-to-focus pictures is 80 ± 2 Å (mean value of 135 measurements).

Fig. 7 Perch rod outer segment. Magnification, × 57,000.

The membranes have a granular appearance with the largest and more distinct granules measuring up to 100 Å in diameter.

The connection between the two membranes of the double membrane disc is continuous all around the edges. In addition to this connection the gap in between the two membranes is bridged by minute dense areas. These connections seem to be especially well developed close to the edges.

The membranes are rather evenly spaced along the segment. The distance between the membranes of a double membrane disc, measured from center to center of the cross cut membranes, is 160 ± 9 Å. The distance between the two adjacent surfaces of the membranes, that is the height of the space in between the membranes of the double membrane discs, therefore, is about 80 Å, and the total thickness of the double membrane discs 240 Å.

There are 31 double membrane discs per micron along the whole length of the rod outer segment or 62 single membranes (estimated on 4 different rods with the following individual spacings 29, 32, 32 and 30 double membrane discs per micron). The estimations represent the average spacing of more than 230 discs. The spacing, with respect to the double membrane discs, therefore, is 320 Å and these discs are separated by an 80 Å wide space.

The length of the rod outer segment is 40.4 ± 0.65 (20 measurements) when measured in the light microscope in sections cut perpendicularly through the retina. Therefore, there are about 1400 double membrane discs in each outer segment and 2800 single discs.

As the diameter of the rods is 1.4 μ the total surface area of the membranes in one rod will be 4,600 μ^2, or 46 cm^2 per million rods.

The discs of the perch rods resemble the discs of the guinea pig rods concerning the incisions. The connections between the double membrane discs along the segment have not yet been studied in detail.

Perch cones. The outer segments of the cones from perch eyes (figs. 8–10) are organized in a different way than the rod

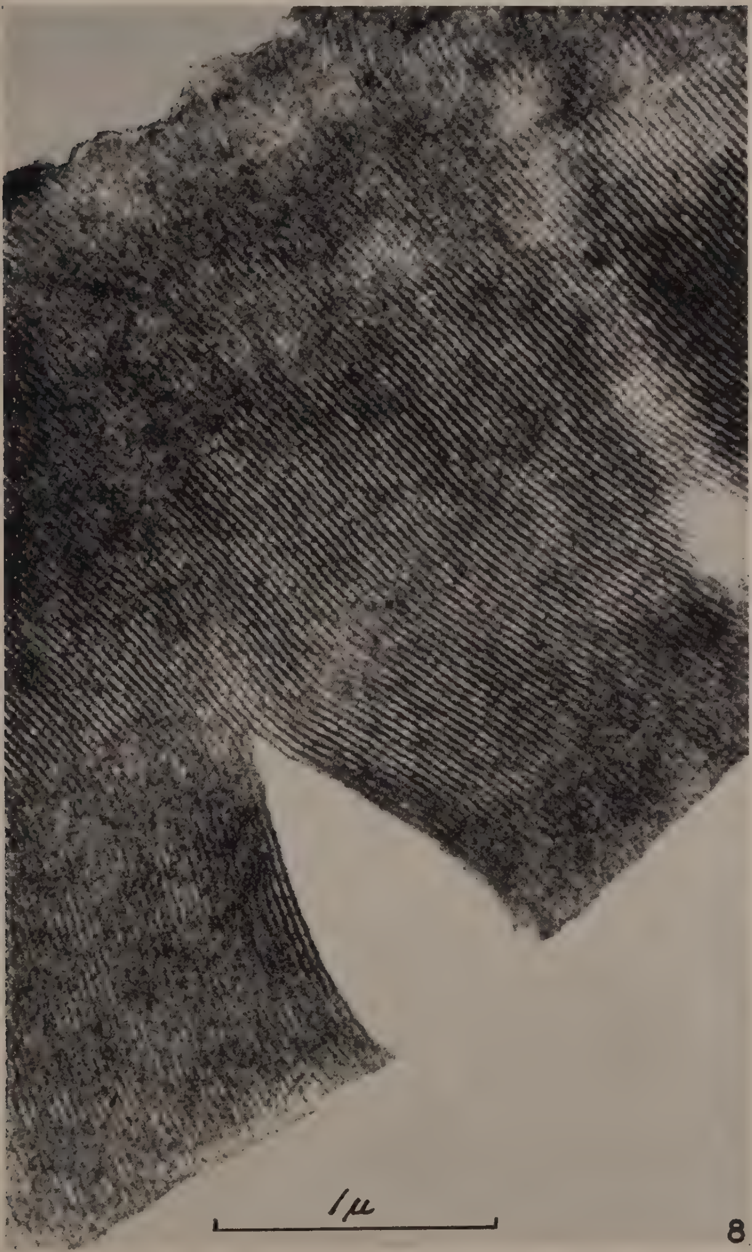

8

Fig. 8 Perch cone outer segment exhibiting a very regular spacing of the single membrane discs. Magnification, × 38,000.

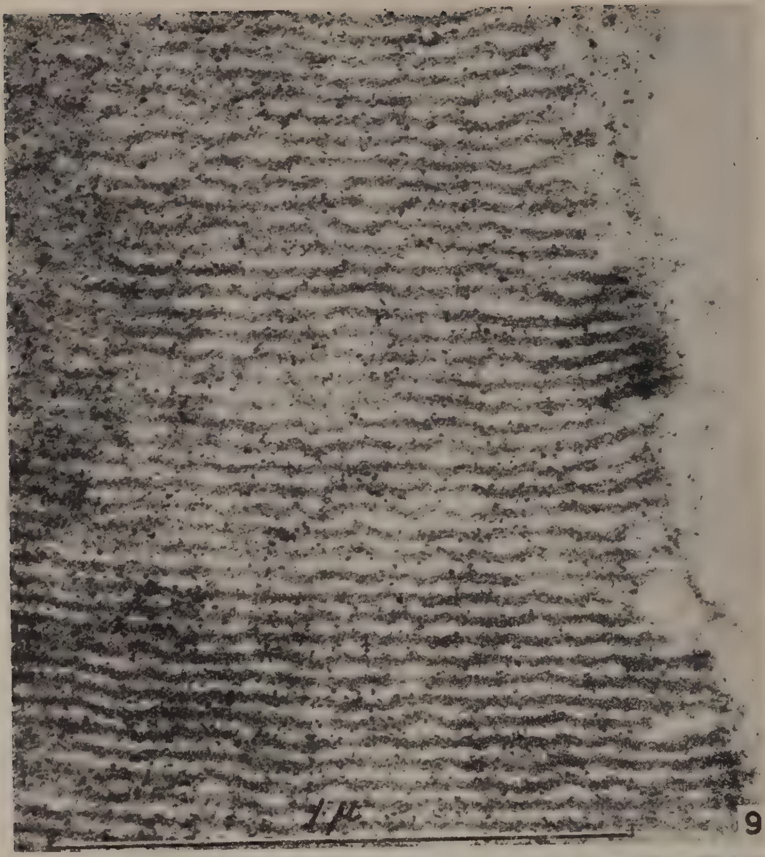

9

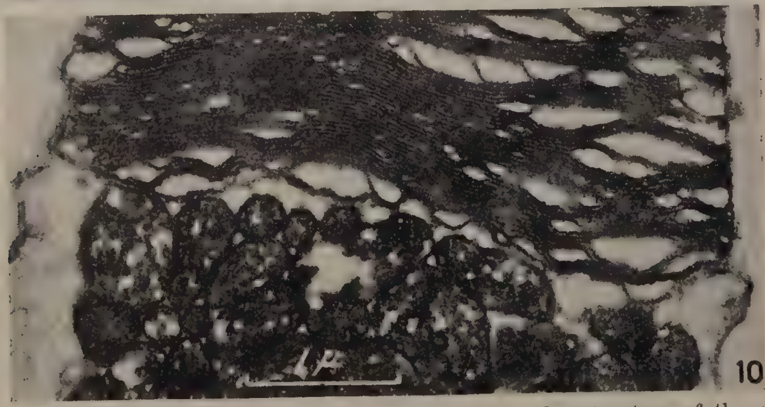

10

Fig. 9 Perch cone outer segment showing the granular structure of the membranes. The black dots are probably osmium deposits. Magnification, × 78.000.

Fig. 10 The border between inner and outer segments of a perch cone. Magnification, × 21,000.

outer segments. We are still dealing with a pile of thin membranes with the same diameter as the diameter of the outer segment and surrounded by a thin outer surface membrane. There is the same sharply marked separation between the inner and outer segments with the pile of membranes wrapped in the outer membrane also along the basal surface (fig. 10).

The differences concern the dimensions of the membranes and their organization. The cone membranes are much thicker than the rod membranes of the same eye and they exhibit a characteristic granular structure when cut tranversely.

The membranes are not associated in pairs but they represent single membranes. This observation does not depend upon lack of resolution of the micrographs as it is possible to observe the internal structure of the membranes without noticing any indications of the individual membranes being split in two closely packed elementary membranes.

TABLE 3

The thickness of the membranes of the perch cones

CONE NO.	NUMBER OF MEASUREMENTS	THICKNESS MEAN VALUE IN Å	COEFFICIENT OF VARIATION %
1	45	182 ± 3.6	13
2	55	185 ± 2.2	9.1
3	25	148 ± 2.6	9
4	25	148 ± 2.5	8

Mean value 166 Å.

The rim around the membranes is slightly thicker than the rest of the membrane. In this thickened part there often is a less dense center presumably indicating an extremely thin duct running along the periphery. In some cases a splitting of the membrane is indicated in connection with this duct but the split does not extend more than a few hundred Ångströms towards the center.

The thickness of the membranes has been measured on 150 membranes from 4 different cone outer segments. The mean thickness is 170 Å (table 3).

The diameter of the granules of these membranes is about 50 Å (mean value of 20 measurements). This measure is bigger than the resolution, 40 Å of the pictures on which the measurements were made and, therefore, does not seem merely to reflect the resolution of the micrographs. Higher resolution has to be gained to justify more extensive measurements. The granular appearance of the cone membranes is shown in figure 9.

The membranes are piled up with 32.9 ± 0.99 membranes per micron along the entire length of the outer segment (table 4).

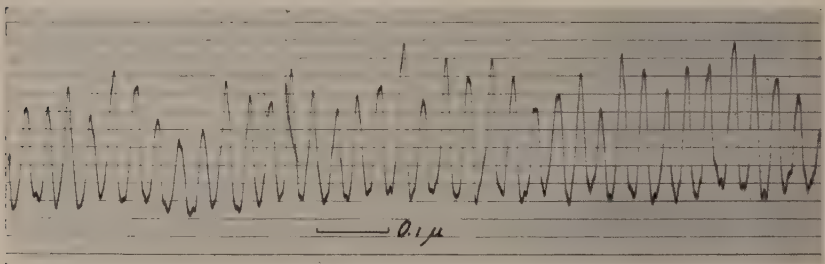

Fig. 11 Photometer tracing across the transverse membranes of a cone outer segment from a perch eye.

The coefficient of variation is 13% for all the estimates on different cones. The coefficient of variation for the estimations on the individual cones varies from 1.1% to 9.6%. The striking regularity of the spacing within each individual cone is illustrated by the photometer tracing, in text figure 11, representing the intensity variation along the long axis of the outer segment.

From table 4 it is obvious that there are great variations regarding the spacing when comparing different cones. The reason for this variation has not yet been analyzed. The cones nos. 2–4 show a striking correspondence regarding the spacing. They all belong to the same retina.

The mean spacing is 300 Å and after subtracting 170 Å as representing the thickness of the membranes the height of the space in between the membranes will be 130 Å.

The total length of the cone outer segment when measured in sections cut thoroughly perpendicularly through the retina is 13.6 ± 0.48 μ (20 measurements). With a spacing of 300 Å there would be 800 membranes in each cone outer segment.

TABLE 4

The number of membranes per unit length (μ) and the corresponding spacing in the perch cones

CONE NO.	NUMBER OF MEMBRANES INCLUDED IN THE ESTIMATE	NUMBER OF MEMBRANES PER μ MEAN VALUES	COEFFICIENT OF VARIATION %	SPACING IN Å
1	167	30.9 ± 0.09	1.1	324
2	205	29.7 ± 0.27	3.6	337
3	215	29.2 ± 0.43	6.0	342
4	257	29.4 ± 0.48	7.1	340
5	200	32.8 ± 0.42	7.0	305
6	158	26.8 ± 0.47	9.4	373
7	50	27.3 ± 0.87	9.6	366
8	205	32.9 ± 0.38	6.7	304
9	158	38.8 ± 0.67	8.1	258
10	139	34.3 ± 0.65	5.7	292
11	36	28.9 ± 1.28	7.7	346
12	186	30.4 ± 0.50	6.2	329
13	277	36.0 ± 0.43	5.0	278
14	90	42.1 ± 1.30	6.8	238
15	69	31.1 ± 0.45	3.2	321
16	110	32.3 ± 0.59	4.8	308
17	114	36.8 ± 0.95	6.8	271
18	90	40.0 ± 1.40	7.9	250
19	314	34.8 ± 0.28	3.5	287
Mean value		32.9 ± 0.99	13	304

The average diameter of the cone outer segment is 2.7 μ. The total surface area of the membranes, therefore, will be 4,700 μ^2 per cone. The total surface per million cones would be about 47 cm^2.

No observations indicating the existence of incisions on these membranes have as yet been made.

DISCUSSION

The observations on sections through the guinea pig retina confirm in several respects the earlier (F. S. Sjöstrand, '48) conclusions regarding the arrangement of the transversely oriented membranes of the rod outer segments. That analysis was based on direct and indirect evidences collected from fragmented material. The conclusions regarding the arrangement of the rod membranes, however, were based mainly on indirect evidences.

The membranes piled up in the outer segment are, as was assumed in the papers just mentioned, organized in pairs and the thickness of such a pair is about 140 Å. The height of the space in between the membranes is 70–80 Å, which is in agreement with the estimate made in the previous papers. The conclusion drawn from the appearance of intermediate stages of fragmentation that the outer segments were uniformly organized along the whole length has also been verified.

Due to the preservation of the arrangement of the membranes in sections it has been possible to add further information regarding the ultrastructure of the rod outer segments.

The two membranes of the double membrane discs are connected all around the edge without any discontinuity and will, therefore, confine a narrow 70–80 Å high and about 2 μ wide compartment, which is completely separated from the interstice between the double membrane discs. These interstices on the other hand seem to communicate all along the outer segment as the outer surface membrane surrounding the disc pile does not seem to be connected to the edges of the double membrane discs. The continuity of the two membranes of the double membrane disc could not be observed in fragmented material. According to the earlier observations it was assumed that the two membranes merely touched each other at the rim. The new observations seem to justify the *definition of the double membrane discs as the structural unit of the rod outer segment.*

The analysis of sections has made it possible to obtain some information regarding the distance between the double membrane discs. This distance varies in specimens prepared in slightly different ways from 100–200 Å. The rather striking constancy of the distance between the two membranes of a double membrane disc contrasts to this variability. The dependence of the former distance on the fixation and embedding procedure make the figure obtained uncertain. As the figure 100 has been derived from specimens prepared with the most elaborate precautions regarding osmotic effects and the outer surface membrane in these preparations has not been broken, not even stretched, but appears wrinkled it seems for the moment reasonable to assume this figure fairly accurate as regards the order of magnitude of the distances discussed.

This would mean that the total number of double membrane discs calculated (700 corresponding to 1400 single membranes for each guinea pig rod outer segment) is of the right order of magnitude.

The independence of the distance between the two membranes of a double membrane disc to different techniques for preparation indicates that the figure obtained, 70–80 Å, is rather reliable.

Text figure 12 represents a schematic presentation of the data collected regarding the ultrastructure of the guinea pig rod outer segments. The upper part represents actual observations and the double membrane disc at the bottom illustrates some additional speculations.

The lipid molecules are, according to the polarization optical data, oriented parallel to the long axis of the outer segments (W. J. Schmidt, '28, '34, '37). Unfortunately no estimations regarding molecular dimensions of the lipids of the visual cells have as yet been published. If we use the figure 63.7 Å obtained for nerve myelin sheath lipids (Bear, Palmer and Schmitt, '41) for a double layer of dried total lipid extract, the distance between the membranes of a double membrane disc would fit best to this dimension.

The existence of oriented lipid molecules between these membranes might explain the constancy of the spacing of these membranes.

Preliminary chemical estimations of the concentration of lipids estimated as the percentage of lipids of the dry weight of isolated guinea pig outer segments have been performed in this laboratory. The isolated rods contain 40% lipids and the relation between lipoid and protein components, therefore, is 2:3.

The calculations of the total volume of the transverse membranes of the rod outer segments relative to the total volume of the narrow double membrane compartments show a relation of approximately 1:1. The interstices between the double membrane discs have not been included in these calculations.

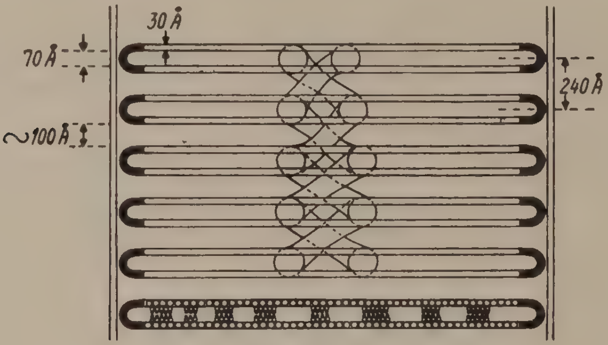

Figure 12 A

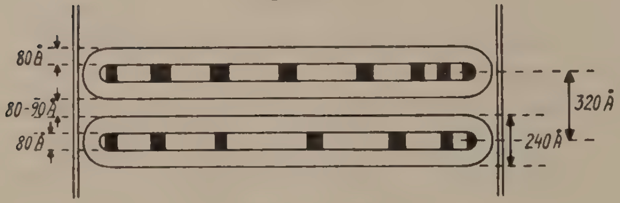

Figure 12 B

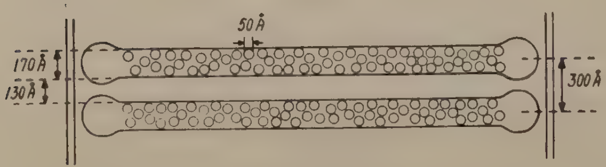

Figure 12 C

Fig. 12 Schematic presentation of the observations and measurements made on the outer segments of rods and cones. The diameters of the discs not drawn in scale.

A Guinea pig rod. In the double membrane disc down at the bottom, the hypothetical arrangement of lipid molecules between the membranes and of the protein molecules in the membranes are included.

B Perch rod.

C Perch cone.

It seems unlikely that the amount of lipids present would suffice to form lipoid layers with the high degree of orientation which is obvious from the polarization optical analysis, between all the single membranes.

From these facts it seems justified tentatively to assume that the lipid molecules are more or less restricted to in the double membrane discs as double layers.

In text figure 12 this double layer has been introduced in the double membrane disc at the bottom. The double layer has been proposed as a discontinuous layer to illustrate the possibility of locally varying concentrations of lipids within the compartment. That arrangement would correspond to the observations made on membranes isolated through fragmentation. The surface of these membranes exhibit a characteristic structure with knobs spread all over the surface. These knobs might well represent fixation artifacts as pointed out in the author's previous papers and it seems unjustified to pay too much attention to them for the moment.

The outer segments of the rods from perch eyes are organized according to the same plan as the guinea pig rods. Text figure 12 B summarizes in a schematic way the observations made. The membranes are coarser (80 Å thick) than the membranes of guinea pig rods (30 Å). But it is striking that the height, 80 Å of the compartment in between the membranes of the double membrane discs of the perch rods is about the same as the corresponding distance in the guinea pig rods, 70–80 Å.

In the double membrane discs from perch rods dense spots, in size corresponding to the knobs observed on isolated membranes, connect the two membranes. This fact indicates a definite difference regarding the material inserted in between the membranes of the double membrane discs and in the interstices between these discs. These spots may well represent those lipids which reduce osmium tetroxide.

Further studies on material fixed with a method that does not affect the solubility of the lipid components, for example freeze-drying, have to be performed before the localization of the lipids in the rod outer segments may be made out.

The observations regarding the behavior of the outer rim of the double membrane discs of the guinea pig rods when distorted through swelling, indicate that the structure of the membranes at the edge differs from the structure of the rest of the membranes. The rim seems to represent a structure which is mechanically more resistant. This observation is in agreement with experiences from fragmented material where the edge represents a slightly thicker part and sometimes occurs preserved even when the membranes are partially broken up. This conclusion has been illustrated by the dark areas of the membranes in figure 12.

The thickness of the single membranes, 30 Å, corresponds to the diameter of a spherical protein molecule. The molecular weight and the arrangement of the protein molecules within these membranes is unknown. The spheres in text figure 12 A indicate the molecular dimension of the membrane but do not represent actual observations. The membranes of the perch rods exhibit a granular appearance but the protein nature of these granules has not yet been demonstrated. No indications of a fibrous protein have, however, as yet been observed.

The double membrane discs are connected in series through thin and short stalks running between the adjacent double membrane discs, at the characteristic incisions of the discs. In the author's previous paper ('48) the possibility was discussed that the characteristic fibrils occurring in fragmented material might constitute a structure running all along the outer segment at the incisions.

The study of sections has shown that there exists no such fiber with that topographic relationship. The fiber observed in fragmented material has been recognized in sections and belongs to a structure presumably related to the transmission of the state of excitation of the outer segment through the inner segment. This structure will be described in a following paper.

It seems obvious that the groove running along the outer segment and formed by the disc incisions and moreover the stalks connecting the double membrane discs may mean different staining properties when using stains for light microscopy. These factors, therefore, seem to constitute the basis for the so-called Kolmer fiber, observed in light microscopy (Kolmer, '04).

The outer segments of perch cones show a marked difference compared to the rods regarding the structure and arrangement of the membranes. The membranes are thick (170 Å) single membranes with a regular spacing of 300 Å. Regarding the cones, therefore, the outer segment is not divided into a large number of narrow and closed compartments as is the rod outer segment. Text figure 12 C presents a scheme showing the quantitative data regarding these membranes.

According to polarization optical data there should exist layers of oriented lipid molecules in between the transversely oriented protein components. The arrangement should be similar to what applies to the rod outer segments with the lipid molecules oriented parallel to the long axis of the outer segment.

There is, in the material presented here, no real indication of the location of the lipids. The distance between the membranes 130 Å would correspond to two double layers of myelin sheath lipids. But the membranes themselves are sufficiently thick to contain oriented lipid molecules.

The difference between rods and cones may mean a pronounced, functional difference, as the conditions for ionic distribution and exchange presumably are quite different.

The isolation of the outer segments from the inner segment through the outer membrane in both rods and cones is rather characteristic. There is only a very delicate connection between these two cell parts. This is, of course, of importance when considering the exchange of metabolites between the inner and outer segments.

The very marked contrast on the micrographs exhibited by the delicate transverse membranes seem to indicate that the osmium tetroxide is reduced at these membranes acting as an electron stain for cellular membranes. This also would explain the fact that osmium fixation affects the birefringence of the outer segments changing the original positive birefringence with respect to the long axis of the rod to a negative birefringence with the optical axis parallel to the long axis of the rod. This effect of the osmium tetroxide is observed also if the lipids have been removed through extraction before the osmium treatment. The negative birefringence produced by the osmium tetroxide might depend upon the accumulation of osmium to the protein membranes and so affecting the refractive index of the part responsible for the negative birefringence. In the case of nerve meylin sheaths the effect is similar, and the positive birefringence with respect to a radial axis, produced by the radially oriented lipid molecules, which is reduced after osmium fixation, recovers if the osmium is removed through treatment with hydrogen peroxide. The organization of the lipid molecules, therefore, does not seem to be destroyed by osmium fixation.

In the case of the outer segments of rods and cones, a control on the extent of fixation artifacts does exist. Analysis of these cell parts by means of polarized light has revealed a basic organization of the rods, indicating the presence of transversely oriented layers, in agreement with electron microscopic observations reported here.

SUMMARY

The outer segments of the rods in the guinea pig and perch eyes and the outer segments of the cones of the perch eye have been analyzed in ultrathin sections by means of high resolution (30 Å) electron microscopy.

1. The outer segments of the guinea pig rods are composed of a pile of 140 Å thick double membrane discs, constituting the structural unit, connected in series by means of short processes or stalks.

The diameter of the discs correspond to the diameter of the rod outer segment, that is, about 2 μ. The double membrane discs are composed of two 30 Å thick membranes connected all around the edge without any indications of a seam or discontinuity. The two membranes, therefore, hem in a narrow, 70–80 Å high compartment completely separated from the interstices in between the double membrane discs.

The incisions of the double membrane discs are superimposed, forming a narrow groove running along the outer segment. The connections between the discs are arranged at the site of these incisions.

The distance between the double membrane discs varies with differences depending upon the fixation and embedding from 100 to 200 Å (mean values).

The oriented lipid molecules are tentatively assumed to be localized to the compartment between the membranes of the double membrane discs.

The whole outer segment is surrounded by a thin membrane, which causes an almost complete separation from the inner segment.

2. The outer segments of the perch rods exhibit a similar organization. The dimensions, however, are different. The thickness of the double membrane discs is 240 Å, the thickness of the membranes 80 Å and the height of the enclosed compartment 80 Å.

The two membranes of the discs are connected within minute areas by means of a material of high electron optical contrast, probably due to staining with osmium.

3. The outer segments of perch cones differ fundamentally from the outer segments of the rods. Each cone outer segment is composed of a pile of 170 Å thick single membrane discs, separated by 130 Å wide spaces. The edges of the discs are slightly thickened, sometimes with a less dense zone in the center of the edge arranged like a duct running all along the rim.

The membranes have a distinct granular structure with a diameter of the granules of about 50 Å.

This investigation has been supported through grants from the following funds: The Knut and Alice Wallenbergs Foundation, The Rockefeller Foundation, The Nobel fund and The Swedish State Medical Research Council.

LITERATURE CITED

BEAR, R. S., K. J. PALMER AND F. O. SCHMITT 1941 X-ray diffraction studies of nerve lipides. J. Cell. and Comp. Physiol., *17:* 355.

GETTNER, M. E., AND J. HILLIER 1950 Serial sections for electron micrography. J. Appl. Phys., *21:* 68.

HILLIER, J., AND M. E. GETTNER 1950 Improved ultra-thin sectioning of tissue for electron microscopy. J. Appl. Phys., *21:* 889.

——— 1950 Sectioning of tissue for electron microscopy. Science, *112:* 520.

KOLMER, R. 1904 Ueber ein Strukturelement der Stäbchen und Zapfen der Froschretina. Anat. Anz., *25:* 102.

NEWMAN, S. B., E. BORYSKO AND M. SWERDLOW 1949 Ultra microtomy by a new method. J. of Research of the National Bureau of Standards, *43:* 183.

SCHMIDT, W. J. 1928 Der submikroskopische Bau der tierischen Gewebe erschlossen aus der Polarisationsoptik. Arch. exp. Zellforsch., *6:* 350.

——— 1934–35 Doppelbrechung, Dichroismus und Feinbau des Aussengliedes der Sehzellen vom Frosch. Zeitschr. für Zellforsch., *22:* 485.

——— 1937 Die Doppelbrechung von Karyoplasma, Zytoplasma und Metaplasma, Berlin.

SJÖSTRAND, F. S. 1948 The ultrastructure of the retinal rods of the guinea pig eye. J. Appl. Phys., *19:* 1188.

——— 1948 An electron microscope study of the retinal rods of the guinea pig eye. J. Cell. and Comp. Physiol., *33:* 383.

——— 1949 On multiple membrane structures in the retinal rods of the guinea pig eye and in nerve tissue. Proceedings of the Conference on Electron Microscopy. Delft 4–8 July, 1949, p. 144.

——— 1951 A method for making ultra-thin tissue sections for electron microscopy at high resolution. Nature, *168:* 646.

THE ULTRASTRUCTURE OF THE INNER SEGMENTS OF THE RETINAL RODS OF THE GUINEA PIG EYE AS REVEALED BY ELECTRON MICROSCOPY [1]

FRITIOF S. SJÖSTRAND
Department of Anatomy, Karolinska Institutet, Stockholm

ELEVEN FIGURES

In earlier papers (F. S. Sjöstrand, '48, '49, '53) the ultrastructure of the outer segments of rods and cones has been analyzed. The present paper gives an account of an analysis of the inner segments of the rods, performed on ultrathin sections of guinea pig retinas.

Previous light microscopic studies on the structure of the inner segments have been reviewed extensively by Kolmer ('36) and by Walls ('42).

The ellipsoid in the distal part of the inner segment has been considered a light concentrating device. The present electron microscopic analysis has presented evidences for this structure constituting a dense aggregation of mitochondria. This assumption was further supported by the fact that these structures may be stained supra-vitally with Janus green B (Elfvin, unpublished).

The outer and inner segments are each covered by a separate outer membrane. Therefore, there is an extensive separation of these cell parts. The only connection between them consists of a bundle of thin fibrils running from the base of the outer segment into the distal end of the inner segment and related to a cross striated inner segment fibril. This structure

---

[1] This paper is based on a report given at the Scandinavian Electron Microscope Society meeting, June 8, 1952 and at the Electron Microscope Society of America meeting, November 1952.

presumably constitutes the structural background for the conduction of the state of excitation from the outer to the inner segments.

MATERIAL AND TECHNIQUES

For the analysis of the structure of the inner segments the same kind of material has been used as for the analysis of the outer segments presented in a previous paper (F. S. Sjöstrand, '53). The preparation technique, the fixation, embedding and sectioning procedures, therefore, have already been described in that paper.

An RCA EMU 2c electron microscope was used with compensated standard objective pole piece and using the standard objective aperture. Three apertures have been used in the projector lens according to Hillier's recommendations and the condensor lens aperture has been reduced.

Regarding magnification calibration see F. S. Sjöstrand ('53). The best resolution of the EMG: s obtained during this study has been 40–50 Å. The limiting factor has mainly been represented by the photographic grain.

RESULTS

The ellipsoid

The inner segment of the guinea pig rods is almost filled with tightly packed, elongated, about 0.25 μ thick rods (figs. 1, 6) oriented parallel to the long axis of the segment. These rod-shaped structures will be called the *inner segment rods* to prevent confusion.

The packing of the inner segment rods is so tight that they will not show up as separate structures in the light microscope. Only a longitudinally oriented striated appearance is indicated. The whole aggregation of inner segment rods represents the ellipsoid.

In very thin sections the inner segment rods show a characteristic internal structure (F. S. Sjöstrand, '53). Each inner segment rod is lined by a double membrane and the interior is filled with densely arranged predominantly transversely oriented double edged structures (figs. 2–3). The two opaque edges of these internal structures are uniformly spaced but

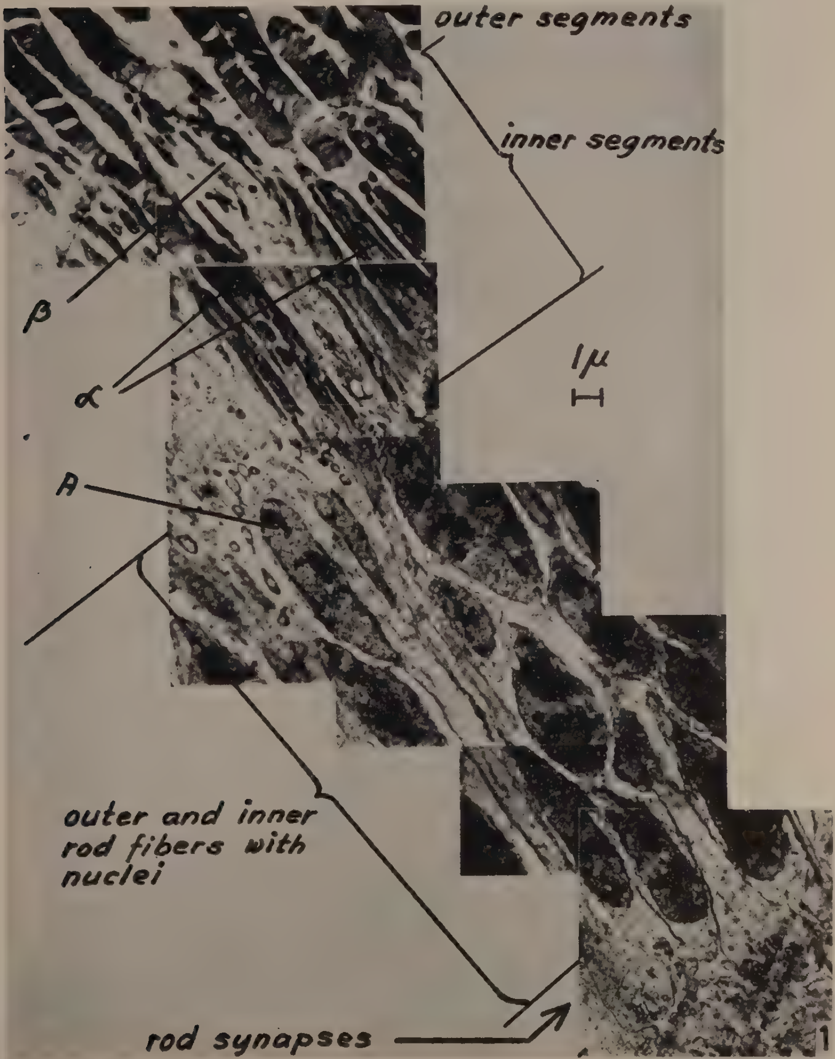

Fig. 1 Montage of pictures of a section of the guinea pig retina showing the different parts of the rod cells. At A a nucleus of a β-cell, perforated by the rod fiber. Magnification, × 3,200.

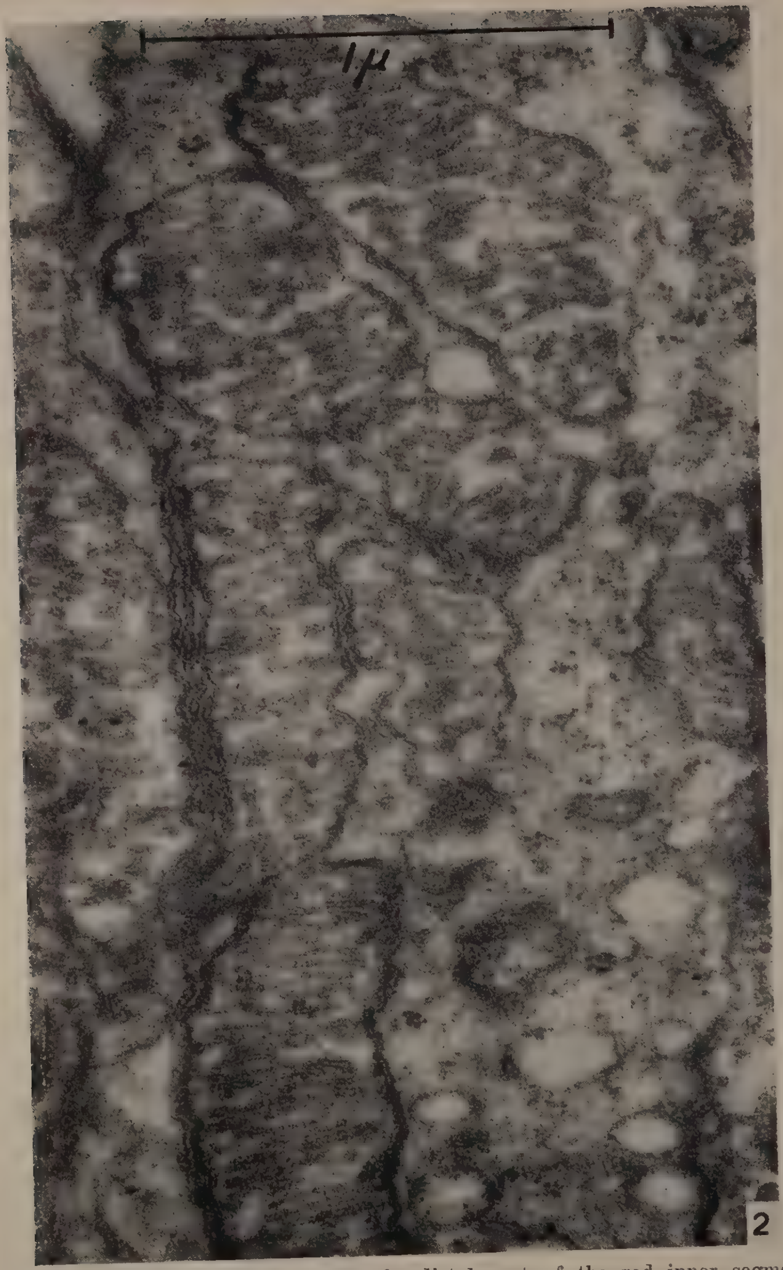

Fig. 2 Ultrathin section through the distal part of the rod inner segment, guinea pig eye. The internal structure and the surface membrane of the mitochondria are seen. The six lines running fairly parallel at the left side represent two outer mitochondria double membranes separated by the two single surface membranes of two adjacent inner segments. To the right, the vacuoles and minute granules of the ground substance are seen. Magnification, × 62,000.

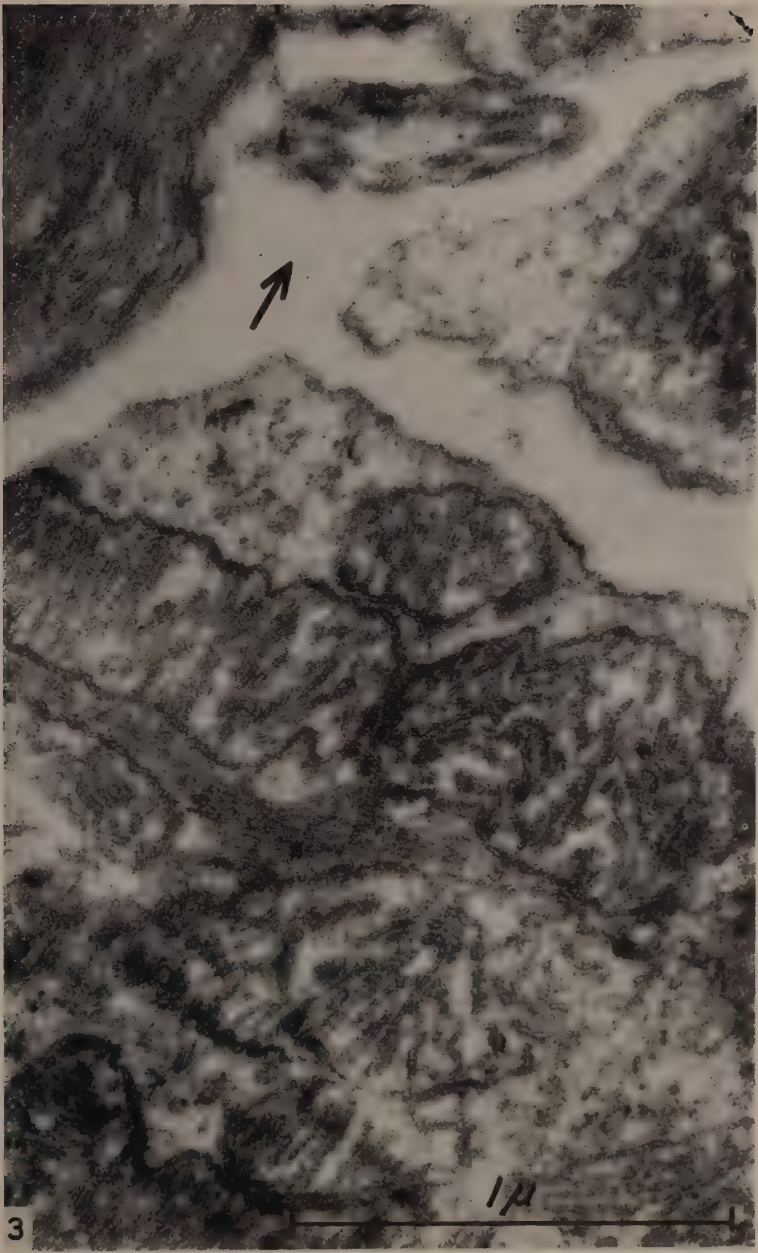

Fig. 3 Ultrathin section through the most distal part of the rod inner segment, guinea pig eye. In the left upper corner a part of an outer segment is visible. The arrow points to a connecting fibril bundle, cut almost transversely. Notice the surrounding membrane of the bundle. In the lower part of the picture the dense aggregation of mitochondria. Magnification, × 59,000.

the length of the structures varies considerably. They may extend across the entire diameter of the inner segment rods or their length may correspond only to a fraction of that distance. They then represent structures with circular or elliptic outlines and with a less opaque center. Sometimes they are oriented parallel or slightly obliquely to the long axis of the inner segment rods and may then show a winded, mutually parallel course.

There are some different possibilities in interpreting this internal structure of the inner segment rods. It may represent a densely edged fibril that runs for instance in a coiled course through the inner segment rod, or we are dealing with double membranes. A third possibility would be that this structure consists of a stack of short, minute rods.

In order to evaluate these possibilities 100 inner segment rods were examined and classified in three categories. The first category represents the inner segment rods which contain predominantly elongated double edged structures, the second those which contain about an equal amount of elongated and circular or oval inner structures and the third category those which contain predominantly circular or oval inner structures.

Assuming that we are dealing with cylindric fibrils the chances for those fibrils appearing as elongated bodies with the length exceeding the diameter 4 times would be about 20% and the chance for shorter bodies would be about 80%. In addition due to the minute dimensions of the assumed fibrils there would be a rather small chance to obtain longitudinal sections through the axis of the fibrils. Therefore, the diameters of the longitudinally cut fibrils would vary considerably.

The proportions between the three categories were: 77% inner segment rods with predominantly elongated double edged structures the length of which corresponds to more than half the diameter of the inner segment rods. Twenty-one per cent of the inner segment rods contain about equal amount of elongated and short inner structures and in only 2% these short structures dominated.

It, therefore, seems justified to assume that these internal double edged structures are not fibrils but flat bodies. This assumption is further supported by the fact that in transverse or nearly transverse sections through the inner segment rods, these internal structures rather frequently do not appear double edged but as irregularly outlined fairly opaque structures similar to pieces of puzzle (fig. 4).

The double edged appearance in sections perpendicular to the large surface of these bodies indicate their consisting of two fairly opaque layers oriented mutually parallel and separated by a less dense space. They will, therefore, be referred to as the *inner double membranes* of the inner segment rods.

When these inner double membranes are oriented transversely and extend across nearly the entire width of the inner segment rods, these rods appear similar to the mitochondria of, for instance, the tubular cells of the mouse kidney and the excretory cells of the pancreas (F. S. Sjöstrand, '53; F. S. Sjöstrand and J. Rhodin, '53).

This structural similarity of the rod-shaped structures of the ellipsoid to the mitochondria indicate that they might represent the mitochondria of the visual cells. This assumption is verified by the observation that they stain supravitally with Janus green B (Elfvin, unpublished).

The total thickness of the outer double membranes of the mitochondria has been measured on 20 mitochondria, the mean value being 150 ± 3 Å. The total amount of measurements is 275 (table 1). The mean distance between the centers of the two perpendicularly cut constituent single membranes of these double membranes is 95 ± 2 Å. The distribution of the values is illustrated in diagram 1. The calculated mean thickness of the single membranes thus will be 55 Å and the mean width of the space in between these single membranes 40 Å.

When measuring the corresponding dimensions of the inner double membranes it was evident that they exhibit a less pronounced contrast than the outer double membranes. The mean total thickness of inner double membranes is 160 ± 3 Å. These measurements were performed on 142 inner double membranes

U. OF I.
LIBRARY

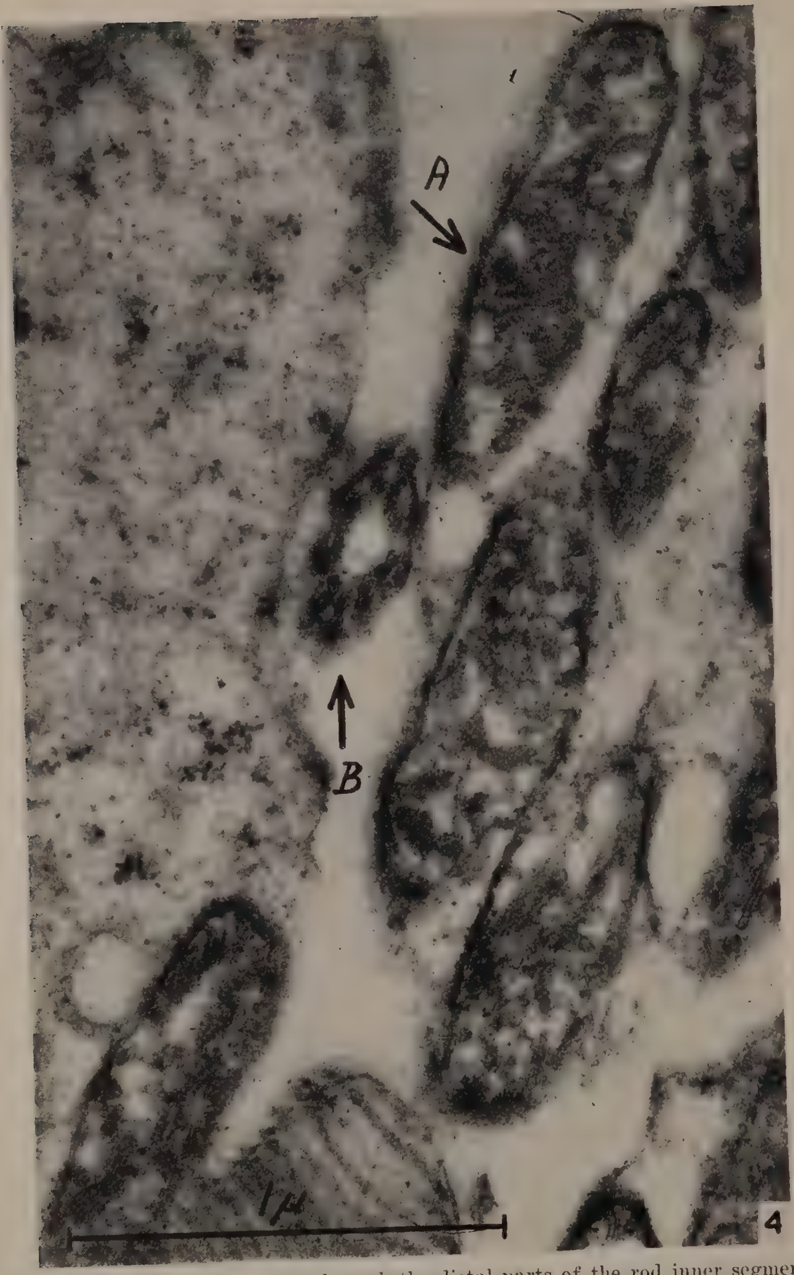

Fig. 4 Thin oblique section through the distal parts of the rod inner segments, guinea pig eye. At A some mitochondria inner membranes oriented parallel to the plane of the section and showing irregular outlines. At B a connecting fibril bundle cut almost transversely. Magnification, × 58,000.

in 15 different mitochondria (table 2). The mean distance between the centers of the constituent single membranes of the double membranes is 100 ± 1 Å. Two hundred and thirteen

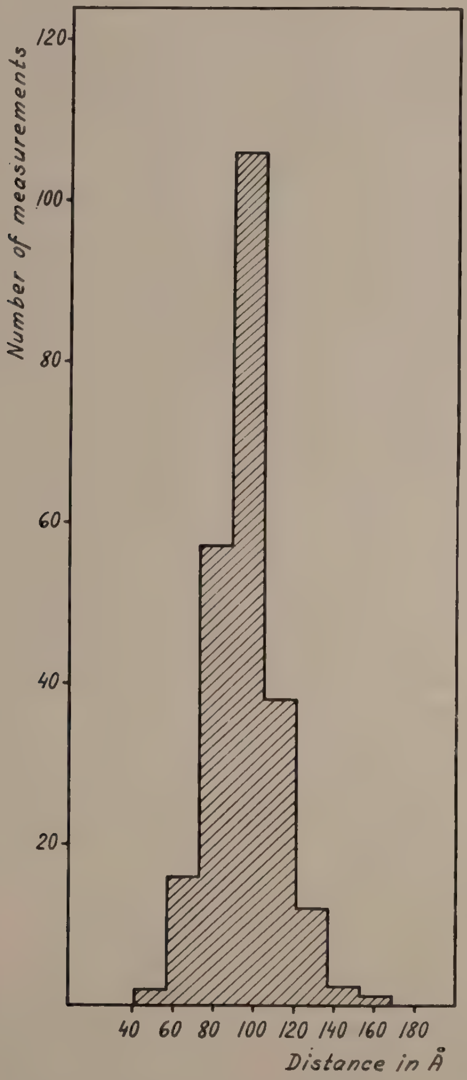

Diagram 1 The mitochondria outer membranes. The distance between the centers of the two constituent single membranes.

TABLE 1

The total thickness of the surface membrane of the rod mitochondria

MITOCHONDRION NO.	NUMBER OF MEASUREMENTS	THICKNESS IN Å	COEFF. OF VARIATION
1	12	169 ± 7	14
2	9	172 ± 8	11
3	10	150 ± 7	15
4	12	142 ± 9	22
5	16	134 ± 5	14
6	10	131 ± 10	24
7	14	143 ± 4	11
8	16	145 ± 1	9
9	18	134 ± 5	16
10	21	169 ± 5	15
11	11	145 ± 10	29
12	24	152 ± 4	13
13	20	143 ± 3	11
14	17	145 ± 6	17
15	10	155 ± 7	15
16	12	126 ± 6	18
17	12	130 ± 11	31
18	16	143 ± 8	24
19	10	156 ± 5	11
20	5	152 ± 1	4
Mean		147 ± 3	

TABLE 2

The total thickness of the inner double membranes of the rod mitochondria

MITOCHONDRION NO.	NUMBER OF MEASUREMENTS	THICKNESS IN Å	COEFF. OF VARIATION
1	18	156 ± 5	15
2	8	169 ± 8	13
3	8	174 ± 9	15
4	13	148 ± 4	9
5	9	171 ± 8	14
6	13	145 ± 6	16
7	9	177 ± 11	21
8	10	165 ± 3	6
9	10	163 ± 11	21
10	6	169 ± 3	4
11	8	168 ± 6	12
12	6	169 ± 9	13
13	10	147 ± 5	10
14	4	134 ± 5	7
15	10	171 ± 7	13
Mean		161 ± 3	

inner membranes in 18 different mitochondria were measured and the distribution of the values is illustrated in diagram 2. The calculated mean thickness of the single membranes is 60 Å and the width of the space in between the two constituent single membranes is 40 Å.

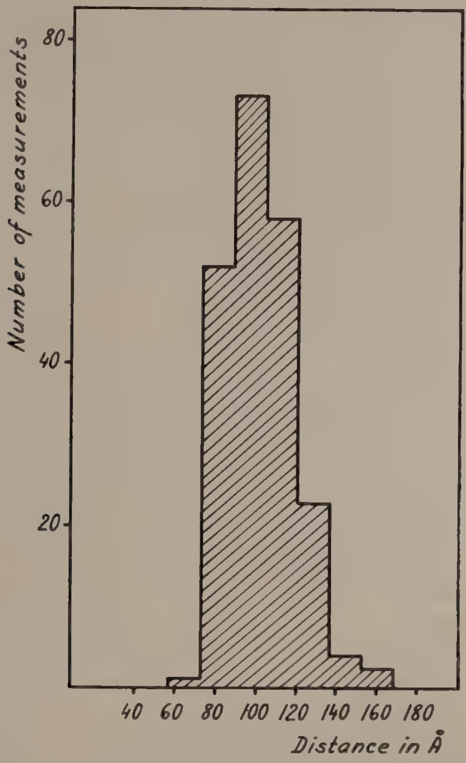

Diagram 2 The mitochondria inner membranes. The distance between the centers of the two constituent single membranes.

These figures correspond well to the mean values obtained for the outer membranes. The differences might well be explained by the differences regarding the contrast of the outer and inner membranes affecting the accuracy of the measurements.

The outer surface membrane of the inner segments

The surface of the inner segment is lined by a thin, single layered membrane. This membrane covers the whole distal end of the inner segment and does not extend to the outer segment (figs. 5, 7), which is completely covered by its own outer surface membrane. There, therefore, exists a discontinuity between these two segments the adjacent surfaces being separated by a minute fissure. A specialized fibril structure which will be described below represents the only connection between the outer and inner segments.

The thickness of the surface membrane of the inner segment appears to be identical to the thickness of each constituent single membrane of the outer mitochondria double membranes (fig. 3), that is about 50 Å. The real thickness might be less as the resolution of the micrographs used for these measurements was not better than 40–50 Å.

The connections between the outer and inner segments

As has been pointed out in a previous paper (F. S. Sjöstrand, '53) it has not been possible to observe any filamentous structure running all along the entire length of the rod outer segment. Only at the base of this segment there are some filaments that bridge the structural discontinuity between outer and inner segments.

At the base of the outer segment the fissure running along the segment and formed by the superposition of all the incisions in the unit discs, broadens somewhat and appears filled with a granular material and a few irregularly curved densely edged fibrils (fig. 7). At the base 16–18 straight fibrils arranged in two concentrical circles emanate and run parallel down to the inner segment (figs. 5–7). The fibrils will here be called *the connecting fibrils.* In the outer ring of connecting fibrils, the fibrils are mutually connected by a thin membrane, the fibrils appearing closely attached to the membrane (fig. 3).

The pencil of connecting fibrils enter the inner segment below its tip, running for some distance along the inner segment

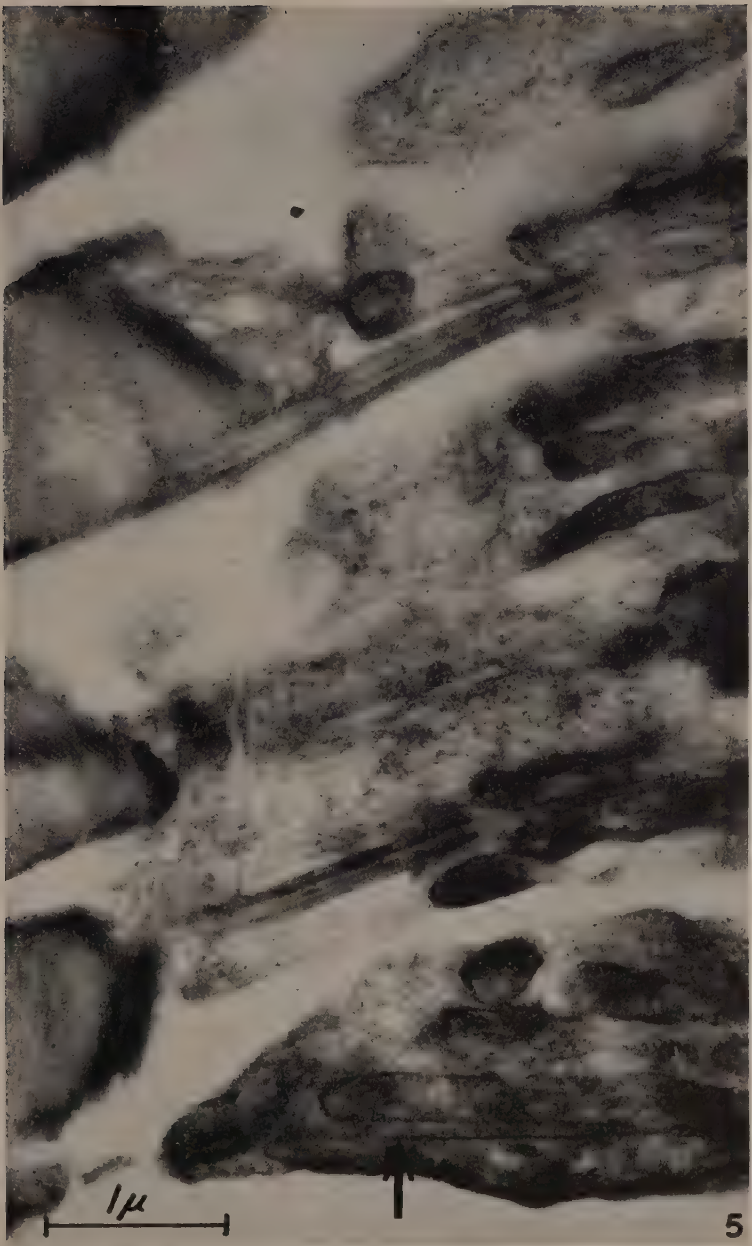

Fig. 5 Longitudinal, thin section across the border between rod inner and outer segments, guinea pig eye. Two connecting fibril bundles are seen penetrating the surface membrane of the inner segments. At the arrow a cross-striated inner segment fibril. Magnification, × 24,000.

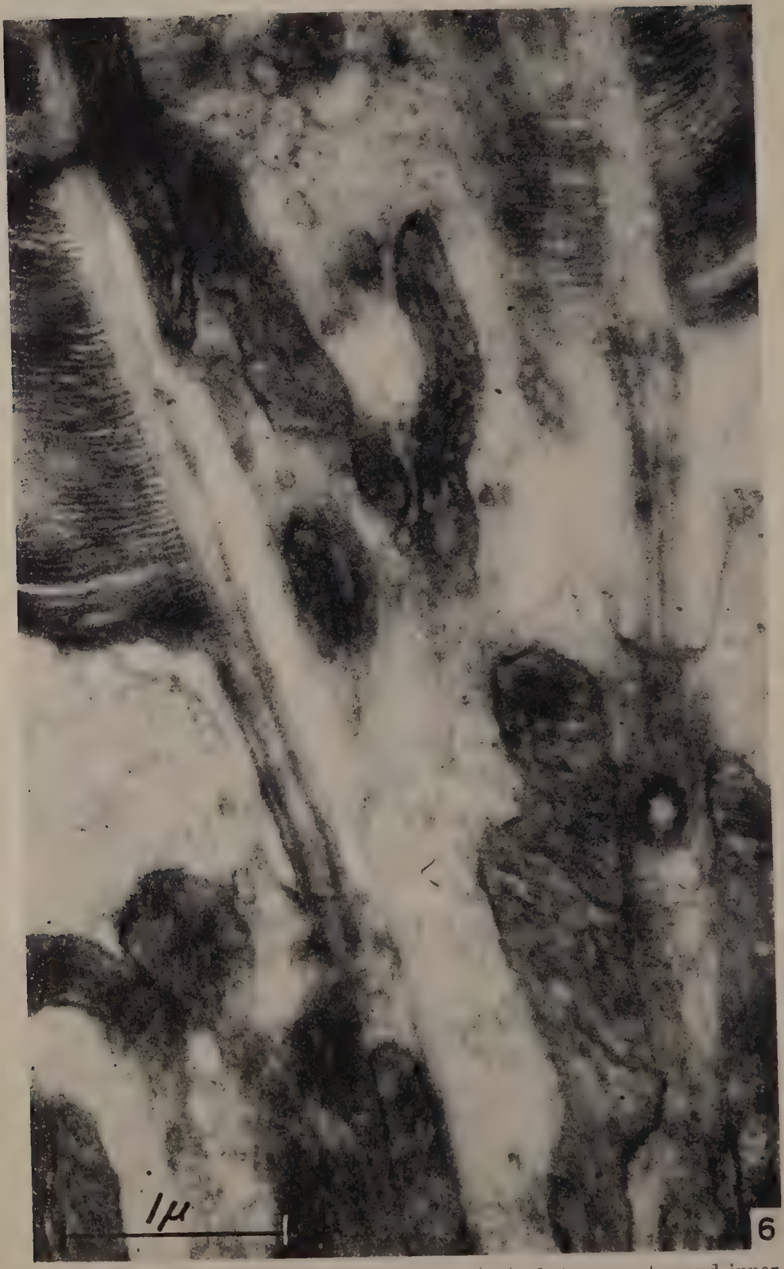

Fig. 6 Longitudinal thin section across the border between outer and inner rod segments. Two connecting fibril bundles are seen running between the outer and inner segment of two rod cells. Magnification, × 29,000.

in a recess-like impression of the surface of the inner segment (fig. 5, 6). The straight fibrils pass almost perpendicularly through the surface membrane of the inner segment. Where the connecting fibrils penetrate, the surface membrane of the inner segment is condensed and thickened.

The length of the fibril bundle when measured from the outer segment to the surface membrane of the inner segment is about 1.5 μ. Its thickness varies somewhat being 0.23 ± 0.007 μ (mean value of measurements on 10 connecting fibril bundles) in its proximal part and becoming slightly thicker about 0.28 μ, towards the outer segment. After entering the inner segment the fibrils pass straight for a distance of about 0.4 μ inside this segment and then end abruptly. The terminal part of the fibrils appear rather opaque and surround a cylindrical space of fairly low opacity. Occasionally (fig. 6) a dense ring may be observed close to the terminal part of the fibrils. The detailed relations of this ring to the fibrils has not as yet been analyzed.

TABLE 3

The spacing of the inner segment fiber

FIBER NO.	SPACING Å
1	615
2	870
3	640
4	725
5	640
Mean	700

The endings of the connecting fibrils show intimate relations to the mitochondria but they do not penetrate into these organelles.

From the endings of the connecting fibrils and presumably as a direct continuation of these fibrils another fibril runs through the major part of the inner segment. This *inner segment fibril* is characterized by a striking cross banding (fig. 5). The spacing of this cross banding is about 700 Å (table 3). It has not been possible to observe this fibril in the most proximal part of the inner segment.

This cross-striated inner segment fibril exhibits very close relation to the mitochondria, running along the sides of and in close contact with the mitochondria.

The ground substance of the inner segment

The ground substance of the inner segment means the part of the cytoplasm of the inner segment that is not organized in mitochondria or the inner segment fibril.

In this ground substance thin fibrils oriented lengthwise, vacuoles and granules of varying size are observed (figs. 2, 7). The structure is especially complicated at the proximal end of the inner segment (fig. 8).

The amount of ground substance seems to vary considerably at the distal end of the inner segment. In some cells it is quite abundant, these inner segments then protruding distally. In the ground substance groups of minute dense granules are constantly observed. The smallest granules measure 40–50 Å in diameter but might well consist of groups of even more minute elements.

The outer limiting membrane and the fiber baskets

The outer limiting membrane of the retina does not appear as a continuous membrane with perforations for the visual cells but appears as some dense material attached to the surface of the inner segment surface membrane at the base of the inner segment (fig. 8). Sometimes a fibrous or lamellated structure within this ''attached'' material is indicated.

These structures might well represent a differentiation of the inner segment surface membrane being restricted to each individual cell. As they form rings or collars around the base of the inner segment they may be referred to as the *basal ring structure* of the inner segment.

The basal ring structures of the neighboring visual cells do not seem to be mutually connected. The narrow spaces that separate them are however of so minute dimensions that this structure will appear as a continuous layer when examined in the light microscope.

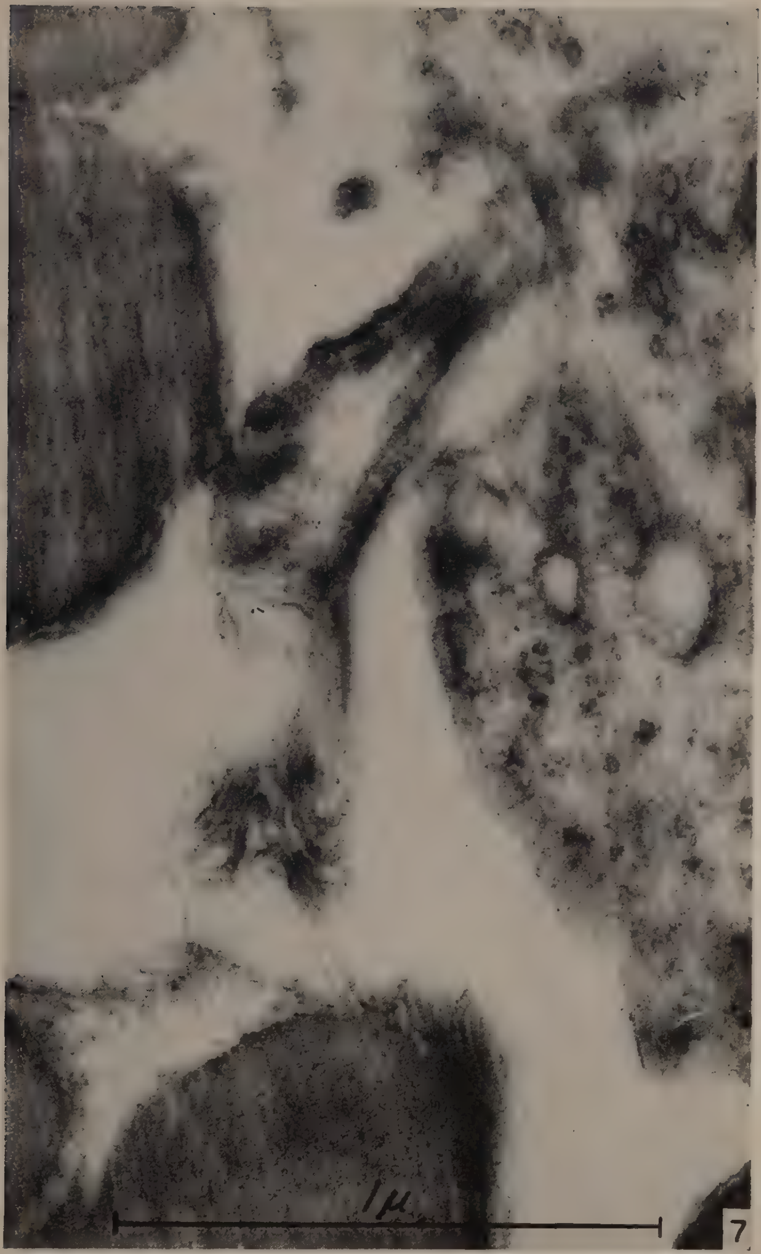

Fig. 7 Ultrathin section through the rod connecting fibril bundle, guinea pig eye. The upper fibrils are the rather straight fibrils bridging the gap between outer and inner segments. The bundle of curved fibrils below are intrasegmental fibrils within the most basal part of the outer segment, partially torn out from the outer segment. Magnification, × 73,000.

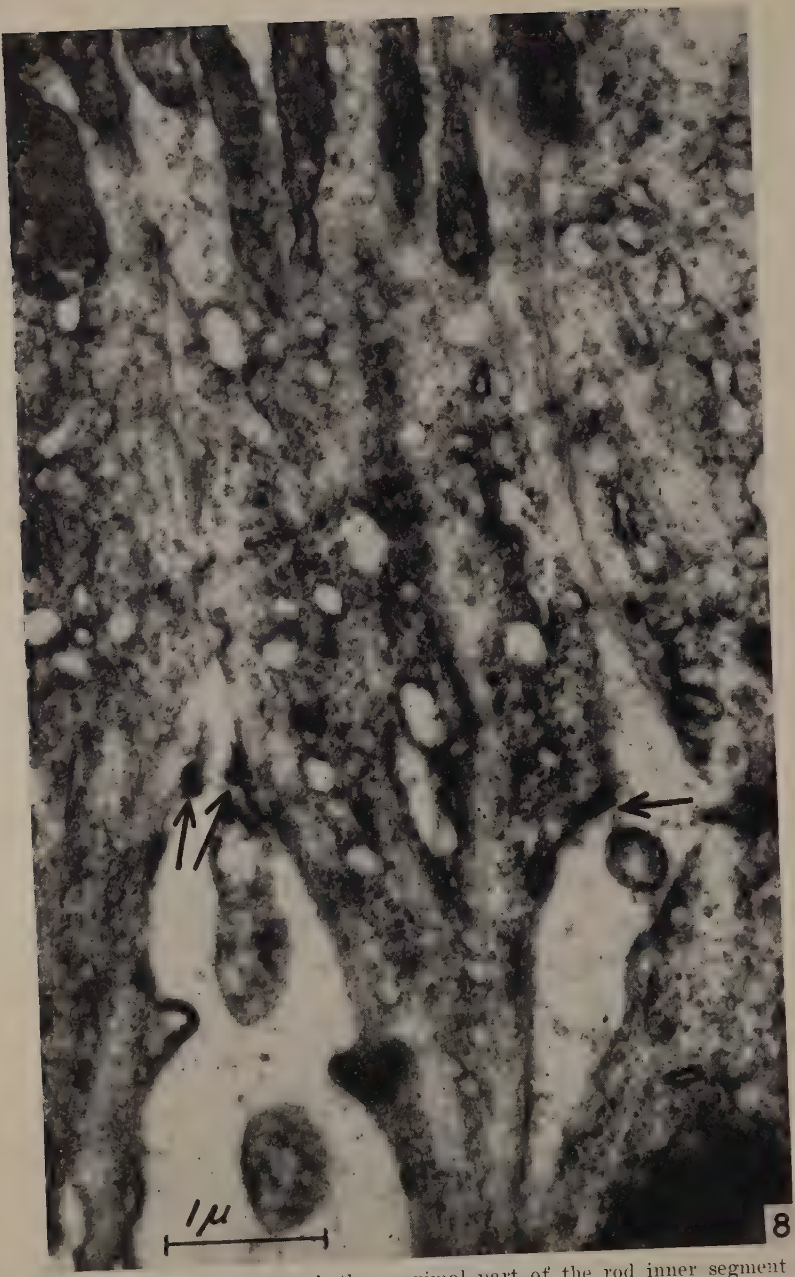

Fig. 8 Thin section through the proximal part of the rod inner segment and the zone of transition into the outer rod fiber. Guinea pig eye. The arrows point to the basal ring structure of the rod inner segment. In the upper part of the picture the proximal ends of the mitochondria. In the cytoplasm irregularly arranged vacuoles and granules. Magnification, × 21,000.

From these basal ring structures long, slender extensions proceed distally all around the basal half of the inner segment. The villiforme extensions appear homogeneous and exhibit an opacity very similar to the opacity of the ground substance of the cytoplam with a slightly more opaque edge. Their distal ends are rounded. They represent the so-called fiber baskets.

Different types of rods

Two different types of rods may be distinguished with respect to the appearance of the inner segment. The one type is characterized by the densely packed mitochondria and the small amount of ground substance. This type will be referred to as the α-cells (fig. 1).

The other type, the β-cells, is defined by its much bigger size due to an abundant amount of ground substance. This difference could depend upon different degrees of swelling during the preparation. But the β-cells also differ with respect to their nuclei, which are located immediately inside the outer limiting membrane. These nuclei also are bigger than the nuclei of the α-cells and are penetrated by the rod fiber (fig. 1), connecting the inner segment and the rod synapse.

DISCUSSION

The chief constituent of the inner segments of guinea pig rods is represented by long slender *mitochondria* especially densely packed or aggregated in its apical part but extending almost all through the inner segment. This aggregation of mitochondria constitutes the so-called ellipsoid.

The inner structure and the surface membrane of the mitochondria exhibit dimensions very similar to those of, for example, mouse kidney mitochondria (F. S. Sjöstrand and J. Rhodin, '53).

The total thickness of the mitochondria double membranes is 150–160 Å, a measure that corresponds well to the thickness of the mouse kidney mitochondria double membranes. The distance between the centers of the two constituent single membranes of these double membranes was measured to only 100 Å which figure is lower than the one obtained for mouse kidney mitochondria. In consequence, the calculated dimensions of the single membranes, 60 Å, and of the height of the separating space, 40 Å, differ from the corresponding figures from mouse kidney mitochondria. It has to be investigated if this difference is a real one or due to differences regarding, for instance, the fixation or the resolution.

It seems reasonable to assume that these double membranes represent protein-lipid structures, the protein constituents presumably localized to the two dense membranes.

The marked aggregation of such a great volume of mitochondria in the inner segment is rather striking. According to our present concept regarding the functional significance of the mitochondria these would represent specialized centers for enzymatic activities. This idea is supported by the demonstration of high concentrations of enzymes in dispersions of isolated mitochondria (literature reviewed by W. C. Schneider and G. H. Hogeboom, '51). The high concentration of bound riboflavin localized to the mitochondria zone of the proximal convoluted tubule cells of mouse kidney (F. S. Sjöstrand, '51) presumably indicates a high concentration of flavoenzymes in the kidney mitochondria.

Considering the probable role of the mitochondria, the apical part of the inner segment might well represent a metabolic center of the retinal rods.

The connection between the outer and inner segments is maintained by the specialized structure, composed of a bundle of fibrils running between the proximal part of the outer segment to the distal part of the inner segment. Except for this connection the two segments are completely separated, each one being bordered by its own surface membrane also along the adjacent surfaces. This arrangement seems to impede to some extent the exchange of metabolites between these two cell parts.

The connecting bundle of fibrils when entering the inner segment immediately establish close connections with the mitochondria. This is also a characteristic of the cross-striated inner segment fibrils. This fibril constitutes a direct continuation of the fibril bundle emanating from the outer segment.

This cross-striated fibril is identical to the fibril which appeared as a contamination in fragmentation preparations of outer segments (F. S. Sjöstrand, '49). When isolating the rod outer segments from the retina by gentle shaking the isolated outer segments, when examined in the light microscope, often exhibit a thin fibril extending from one end like a tail. This "tail" certainly corresponds to the fibril structures observed in the electron microscope. That the cross-striated fibril during the isolation of the outer segments is torn out of the inner segment would indicate that the connection between the outer segment fibril bundle and the inner segment fibril is rather firm. The length of the characteristic "brush" of the isolated fibrils, 1–1.5 μ (F. S. Sjöstrand, '49) corresponds well to the length of the straight connecting fibrils 1.3–1.5 μ. In the isolated fibrils an attached membrane was observed at the spot of transition from the cross-striated fiber to the "brush" fibrils. This membrane certainly corresponds to fragments of the outer surface membrane of the inner segment and indicates the firm connection between the fibrils and this membrane. The cross-striated inner segment fibril may correspond to the inner fiber earlier observed in light microscopic studies (Kolmer, '04). The observations regarding the connecting fibril bundle and the inner segment fibril are presented in a schematic way in figure 9.

Regarding the functional significance of these fibrils it seems justified to assume that they represent a structure for conducting the state of excitation which is caused by the absorption of light energy in the outer segment, from the outer to the inner segment. The excitation would then be conducted down to the aggregation of mitochondria in the distal part of the inner segment.

The cross-striated fibril has not been observed in the proximal part of the inner segment and does not occur further

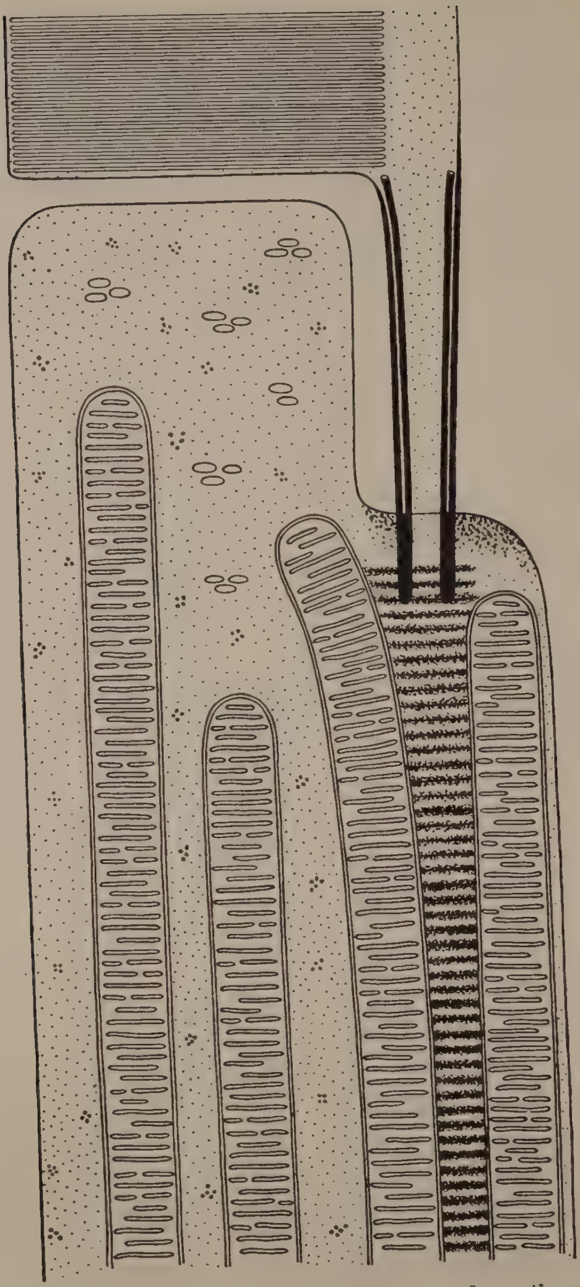

Fig. 9 Schematic presentation of the observations made on the structures connecting the outer and inner segments in the guinea pig retinal rods. Magnification, × 30,000.

down the rod. It, therefore, seems to be restricted to the zone containing the mitochondria.

Accepting as justified to speculate over the functional significance of the morphologic organization observed, the following hypothesis is proposed regarding the course of events taking place in the retinal rod when stimulated through light.

The outer segment functions as the receiver of light energy and is thereby put in an excitatory state. The immense repetition of the structural units within the outer segment increases the probability for the passing photons to hit a reactive center represented by photochemical components and presumably an associated depolarizable membrane structure, represented by the double membrane discs of this segment. The calculations regarding the number of photons necessary for excitation during maximal dark-adaption (Van der Velden, '46) point to the primary process of excitation taking place at a locus of small dimensions in relation to the dimensions of the outer segment. The smallest supramolecular morphologic unit observed is represented by the unit discs. Therefore, it seems justified to assume the primary effect to be restricted to one or two unit discs.

The excitatory state spreads over the outer segment and proceeds down to the inner segment through the connecting fibril bundle surrounded by its membrane.

The topographic relations to the mitochondria and the amount of mitochondria, presumably representing respiratory centers, might indicate that they take part in the process of excitation. Perhaps the excitation of the outer segment acts as a trigger mechanism for the mitochondria to generate or to release the energy necessary for the excitation to be conducted down the rest of the cell.

The parts of the retinal rod situated proximal to the inner segment show a structure very similar to a non myelinated nerve fiber, which might indicate their role as conducting elements connecting the inner segment with the specialized synapse region at the proximal end.

This interpretation would give a sensible role to the inner segment with the elaborate and certainly potent mitochondria apparatus.

The two different types of rods, the α- and β-cells do not differ with respect to the structure of the outer segment. The relations regarding the inner segment and the nuclei of the β-cells are similar to what is characteristic for the cones of mixed retinas. The β-cells do not show, however, the ultrastructural organization of cones.

The outer segments of the β-cells are located farther distally than the α-cell outer segments, due to the longer inner segments of the former cells.

The structural differences of these cells certainly indicate a functional differentiation, the nature of which is not obvious from their morphology. They might represent rods distinguished with respect to their sensitivity to light of different wave lengths. The variance regarding the position of the outer segment represents a fact in harmony with this assumption.

SUMMARY

The inner segment of guinea pig retinal rods has been studied on ultrathin sections at a fairly high resolution (40–50 Å) by means of electron microscopy. The fixation used was 1% osmium tetroxide buffered to pH 7.2 by means of veronal-acetate buffer.

1. The main part of the inner segment consists of long slender mitochondria (confirmed by supra-vital staining with Janus green B) which are densely aggregated, the whole aggregation constituting the so-called ellipsoid.

2. Each mitochondrion is surrounded by a 150 Å thick outer double membrane. Each constituent single membrane of this double membrane measures 55 Å and the width of the separating space in between these membranes 40 Å.

3. The interior of the mitochondria is highly organized with double membranes arranged mutually parallel and mainly perpendicularly to the long axis of the mitochondria. The out-

lines of these double membranes or "plates" are irregular. Their thickness was measured to 160 Å. The thickness of each constituent single membrane of these double membranes is 60 Å and the width of the separating space 40 Å.

4. A specialized structure consisting of a bundle of 16–18 thin fibrils surrounded by a membrane connects the outer and inner segments, which are otherwise completely separated. A cross-striated fibril with a periodicity of about 700 Å forms a direct continuation of this fibril bundle inside the inner segment and proceeds down the apical half of the inner segment in close contact with the mitochondria.

5. The outer limiting membrane does not appear as a membrane but as dense material attached to the inner segment surface membrane forming "rings" around the base of the segment. These "rings" are not mutually connected but are separated by minute spaces.

6. The fiber baskets in the guinea pig retina consists of slender, villiforme extensions from the outer limiting "membrane" substance and run along the sides of the basal half of the inner segment.

7. Two different types of rods, α-cells and β-cells, have been distinguished, differing with respect to the structure of the inner segments, as well as the size, location and structure of the nuclei.

8. A hypothesis regarding the function of the different parts of the visual cells is proposed on the basis of the morphologic organization of these cells.

ACKNOWLEDGMENT

This investigation has been supported by grants from the following funds: The Knut and Alice Wallenberg Foundation, The Rockefeller Foundation, The Nobel Foundation and The Swedish Medical Research Council.

LITERATURE CITED

KOLMER, R. 1904 Ueber ein Strukturelement der Stäbchen und Zapfen der Froschretina. Anat. Anz., *25:* 102.

——— 1936 Die Netzhaut, in von Möllendorff, Handb. der Mikrsk. Anat. des Menschen, *3:* (part 2) 295.

SCHNEIDER, W. C., AND G. H. HOGEBOOM 1951 Cytochemical studies of mammalian tissues: The isolation of cell components by differential centrifugation. A Review. Cancer Research, *11:* 1.

SJÖSTRAND, F. S. 1948 The ultrastructure of the retinal rods of the guinea-pig eye. J. Appl. Phys., *19:* 1188.

——— 1949 An electron microscope study of the retinal rods of the guinea-pig eye. J. Cell. and Comp. Physiol., *33:* 383.

——— 1951 Freeze-drying of tissues for cell analysis by light and electron microscopy. Freezing and drying, report of a symposium, London.

——— 1953 The ultrastructure of the outer segments of rods and cones of the eye as revealed by the electron microscope. J. Cell. and Comp. Physiol., *42:* 1.

——— 1953 The ultrastructure of rod-shaped mitochondria as revealed by electron microscopy. Nature, *171:* 30.

SJÖSTRAND, F. S., AND J. RHODIN 1953 The ultrastructure of the proximal convoluted tubules of the mouse kidney as revealed by high resolution electron microscopy. Exp. Cell Research, *4:* 426.

VAN DER VELDEN, H. A. 1946 Number of quanta necessary for perception of light of human eye. Ophthalmologica, *111:* 321.

THE ACTIVATION BY K^+ AND OCCURRENCE OF PYRUVIC PHOSPHOFERASE IN DIFFERENT SPECIES[1]

P. D. BOYER

Department of Agricultural Biochemistry, University of Minnesota, St. Paul, and the Marine Biological Laboratory, Woods Hole, Mass.

ONE FIGURE

Potassium activation of enzyme reactions was recognized as early as 1937 (Ohlmeyer and Ochoa, '37) and demonstrated for a specific enzyme, pyruvic phosphoferase, in 1942 (Boyer, Lardy and Phillips, '42, '43). Reports on the K^+ or NH_4^+ activation of various enzymes have in most instances been limited to a single tissue and species. The most widely studied K^+ activation has been that of pyruvic phosphoferase, which has been reported for rat muscle (Boyer, Lardy and Phillips, '42, '43), and brain (Utter, '50), rabbit muscle (Kachmar and Boyer, '53) and yeast (Seitz, '49). The studies reported in this paper were undertaken primarily to find if the activation of pyruvic phosphoferase was a fundamental property of the enzyme as found in different tissues and species. In addition the results give information on the occurrence of pyruvic phosphoferase in some marine species and about quantitative differences in the K^+ requirement for maximal activity in the enzyme from different sources.

METHODS

Pyruvic phosphoferase measurements. The assay procedure based on measurement of the amount of pyruvate formed was similar to that previously described (Kachmar and Boyer, '53). For most experiments, measurements were made with an 0.1 ml aliquot of the enzyme preparation in a 1 ml total volume containing 0.005 M $MgSO_4$, 0.002 M sodium adenosine triphosphate (ATP), pH 7.4, 0.1 ml yeast hexokinase in 2% glucose (1/40 dilution of fraction 3-a of Berger et al., '46), 0.02 M sodium phosphate buffer, pH 7.4, 0.001 M sodium phosphopyruvate,[2] pH 7.4, and 0.15 M KCl. The reaction mixture was allowed to incubate for 5–10 minutes at 37° to allow formation of ADP from the ATP before addition of the pyruvic phosphoferase preparation, and then incubated for exactly 10 minutes following addition of the enzyme. Then 1.0 ml of 0.0125% dinitrophenylhydrazine in 1 N HCl was added to stop the enzymic reaction, and the mixture incubated for about 10 minutes at 37°. The tubes were then removed from the bath and 3 ml of 0.5 N NaOH added. After an additional 8–12 minutes the color was read in a photoelectric colorimeter with a green filter. Pyruvate standards contained the same amount of Mg^{++} as the test samples to compensate for the slight turbidity produced by magnesium hydroxide formed. The reaction velocity was linear with time and with enzyme concentration when less than 0.35 μm of pyruvate was formed per milliliter.

---

[1] The experimental work reported herein was done during the tenure of a Lalor Fellowship at the Marine Biological Laboratory. Paper No. 2925, Scientific Journal Series, Minnesota Agricultural Experiment Station. Supported in part by a grant from the Nutrition Foundation, Inc.

Extracts of tissues for assay were prepared by grinding 50–250 mg samples of fresh tissue with 5 ml of 0.02 M sodium phosphate buffer containing 0.001 M sodium ethylenediaminetetraacetate, and filtering in a refrigerator through no. 5 Whatman filter paper. On the basis of preliminary activity tests appropriate dilutions of the filtrate were made with the 0.02 M phosphate, 0.001 M sodium ethylenediaminetetraacetate solution for the enzymic experiments.

RESULTS AND DISCUSSION

Activation by K^+. The results of studies on the occurrence and potassium acitvation of pyruvic phosphoferase are summarized in table 1. The presence of pyruvic phosphoferase was demonstrated by the formation of pyruvate from phosphopyruvate dependent upon the presence of ADP. The assays without ATP additions served as a measure of any

---

[2] I am indebted to Dr. E. Baer of the University of Toronto for a gift of the silver-barium salt of phosphopyruvate.

TABLE 1

The potassium activation of pyruvic phosphoferase in various tissues from different organisms

The assays were conducted as described in the text but without additions of ATP, KCl, or NaCl except as indicated. When added the concentrations of these substances were ATP 0.02 M, KCl 0.15 M, and NaCl 0.15 M. The values for enzyme activity may be taken only as minimum values since tests were not made on the completeness of extraction, possible lowering of substrate concentration by enolase, or possible inactivation before assay in the tissues tested.

ORGANISM	TISSUE	μM PYRUVATE FORMED PER GRAM FRESH TISSUE PER MINUTE			
		$+ K^+$	+ ATP	+ ATP $+ Na^+$	+ ATP $+ K^+$
Rabbit	Heart	0	15	15	100
Rabbit	Liver	0	4	4	18
Rabbit	Kidney	0	1	1	6
Rabbit	Uterus		3	3	18
Rabbit	Brain	4	14	14	70
Dogfish	Skeletal muscle	4	8	11	230
Dogfish	Stomach muscle	0	6		25
Dogfish	Brain stem	0	7	7	110
Skate	Skeletal muscle		5	0	45
Torpedo	Skeletal muscle			0.4	3.6
Fundulus	Skeletal muscle	0	2	2	65
Limulus	Tail muscle		41	45	390
Pecten	Adductor muscle	0	8	7	39
Pecten	Flap muscle	0	0.6	0	6
Thyone	Muscles of Arostotles lantern	0	1	1	6
Phascolosoma	Proboscis retractor muscle	0	0.1	0.1	2.0
Anadonta [1]	Striated adductor muscle	0	26	26	39
	Smooth adductor muscle	0	20	20	36
Tetrahymena [2]	Whole organism	0	23	23	39

[1] The values for anadonta tissues are for extracts dialyzed for two days against 0.02 M sodium phosphate buffer, pH 7.4, 0.001 M sodium versenate.

[2] The tetrahymena extracts were kindly supplied by Dr. Jay Roth. Greater potassium activation was shown with further dilution of the extracts.

pyruvate formation through the action of phosphatases or any other reactions. As can be seen from table 1 formation of pyruvate without ATP present was negligible or very low under the assay conditions used. Comparison of the assays with ATP and ATP $+ K^+$ additions served as a measure of the extent of activation by the added K^+. The assays with added Na^+ in place of K^+ were made to test the specificity of the K^+ activation. The results show that addition of Na^+ under these conditions had little or no effect on the enzyme activity.

The data of table 1 clearly demonstrate a marked activation of the pyruvic phosphoferase reaction by K^+ in all tissues tested. On the basis of studies with rabbit muscle pyruvic phosphoferase (Kachmar and Boyer, '53), it is probable that the activity of the various extracts without added K^+ would have been considerably lower except for extraneous K^+ or NH_4^+ introduced chiefly with the tissue extract. These data, together with previous observations on the K^+ activation of the enzyme from other sources warrant the conclusion that activation by K^+ is probably a general phenomenon. If the activation represented merely an adaptation of the enzyme to the intracellular environment characteristically high in K^+, a generalized activation of pyruvic phosphoferase by K^+ in the absence of similar activation of most intracellular enzymes would not be expected. Thus K^+ appears to have a fundamental but as yet unexplained role in the catalysis by pyruvic phosphoferase.

Occurrence. Pyruvic phosphoferase activity was found to occur in all tissues tested. This suggests that pyruvic phosphoferase and related enzymes of the glycolytic system have a metabolic function in the respective tissues. Very little or no information is available on the occurrence of the usual reactions associated with glycolysis in marine forms and invertebrates other than microorganisms (see von Brand, '45) except for the reports on glycolysis in muscles from oysters and grasshoppers (Humphrey, '50). Of interest is the rather high concentrations of pyruvic phosphoferase in the tail muscle of limulus. This may reflect a high concentration of other glycolytic enzymes and be related to the ability of this organism to survive long periods without oxygen (von Brand, '44).

Quantitative potassium requirement of anadonta and limulus. With extracts from the fresh water species anadonta, only a weak K^+ activation could be demonstrated before dialysis of the extracts. The potassium content of anadonta muscle is approximately 11 mM per kilogram, considerably lower than the values of 100 to 170 mM per kilogram for muscle from marine forms and mammals (Prosser, '50). This suggested the possibility that the pyruvic phosphoferase of anadonta muscle might require K^+ but in a considerably lower concentration than the other forms tested. Substantiation of this suggestion was obtained by measurement of the activity of limulus and of dialyzed anadonta muscle extracts at different K^+ levels as shown in figure 1. From the assumption that the activation of the limulus muscle extract by K^+

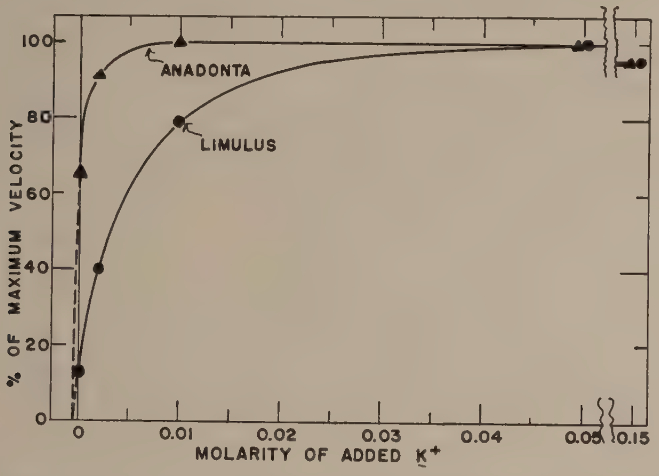

Fig. 1 The activity of pyruvic phosphoferase from anadonta and limulus muscle at different levels of added K^+. The assay conditions were as described in the text. The anadonta muscle extract was dialyzed for two days against 0.02 M sodium phosphate buffer, pH 7.4, 0.001 M sodium ethylenediaminetetraacetate.

conforms to the expected Michaelis relationship, the low activity in the absence of added K^+ can be fairly accurately estimated to be equivalent to that which would be produced by the presence of 5×10^{-4} M K^+. The cations producing this activity came largely from the components of the reaction medium other than the enzyme extract. A plot of 1/v against $1/K^+$ gave a straight line with a calculated K_m (Michaelis constant) for the limulus muscle enzyme of 5×10^{-3} M. On the basis that there was an equivalent of 5×10^{-4} M K^+ in the reaction medium, the value of the K_m for the anadonta muscle enzyme was 3×10^{-4} M. In previous experiments the value of K_m for the rabbit muscle enzyme was found to be 11×10^{-3} M, which is about twice as great as the K_m for the limulus enzyme, and 37 times as great as the K_m for the anadonta enzyme.

SUMMARY

Extracts from 19 different tissues of 11 vertebrate and invertebrate organisms contained pyruvic phosphoferase which was strongly activated by K^+. These results together with previous data lead to the conclusion that activation of pyruvic phosphoferase by K^+ is probably a general phenomenon representing a fundamental property of the enzyme.

The quantitative requirement of K^+ for maximum activity varies. The Michaelis constant for the rabbit muscle enzyme is double and 30 to 40 times greater than the values for the limulus muscle and anadonta muscle enzyme respectively.

LITERATURE CITED

Berger, L., M. W. Slein, S. P. Colowick and C. F. Cori 1946 Isolation of hexokinase from baker's yeast. J. Gen. Physiol., *29:* 379–391.

Boyer, P. D., H. A. Lardy and P. H. Phillips 1942 The role of potassium in muscle phosphorylations. J. Biol. Chem., *146:* 673–682.

——— 1943 Further studies on the role of potassium and other ions in the phosphorylation of the adenylic system. J. Biol. Chem., *149:* 529–541.

Humphrey, G. F. 1950 Glycolysis in oyster muscle. Australian J. Exp. Biol. Med. Sci., *28:* 151–160.

KACHMAR, J. F., AND P. D. BOYER 1953 Kinetic analysis of enzyme reactions. II. The K^+ activation and Ca^{++} inhibition of pyruvic phosphoferase. J. Biol. Chem., *200:* 669–682.

OHLMEYER, P., AND S. OCHOA 1937 Über die Rolle der Cozymase bei der Phosphatübertragung. Biochem. Z., *293:* 338–350.

PROSSER, C. L. 1950 Comparative Animal Physiology. Saunders, Philadelphia.

SEITZ, I. F. 1949 Role of potassium and ammonium ions in the transfer of phosphate from phosphopyruvic acid to the adenylic system. Biokhimiya, *14:* 134–140.

UTTER, M. F. 1950 Mechanism of inhibition of anaerobic glycolysis of brain by sodium ions. J. Biol. Chem., *185:* 499–517.

VON BRAND, T. 1944 Occurrence of anaerobiosis among invertebrates. Biodynamica, *4:* 185–328.

——— 1945 Anaerobic metabolism of invertebrates. Biodynamica, *5:* 165–295.

MEMBRANE POTENTIAL AND THRESHOLD OF SINGLE MUSCLE FIBERS[1]

H. P. JENERICK[2] AND R. W. GERARD[3]
Department of Physiology, University of Chicago

EIGHT FIGURES

There remains little question that propagation involves excitation of successive resting regions by depolarizing eddy currents. The local membrane reaction that leads to the all-or-none response, documented by the action spike, is thus normally associated with depolarization and has often been regarded as a direct consequence of the membrane depolarization. If the response occurs when the membrane potential has fallen to some fixed value, zero or above, then threshold should vary with resting potential. Such a relation has been sought repeatedly in terms of injury potential measurements, but with conflicting results. The impaling technique developed in this laboratory (Graham and Gerard, '46; Ling and Gerard, '49a) permits the precise comparison of membrane potential and current threshold for single muscle fibers as desired conditions are varied. Over an extensive range of many (but not all) variables, threshold for frog sartorius fibers is proportional to the membrane potential excess above 58 mV.

---

[1] Supported by a contract between the Office of Naval Research and the University of Chicago and in part by the Dr. Wallace C. and Clara C. Abbott Fund. A preliminary report appeared in American Journal of Physiology, *163:* 723, 1950; see also H. P. Jenerick.

[2] U. S. Public Health Graduate Fellow 1950–51. Present address: Department of Biology, Massachusetts Institute of Technology.

[3] Present address: Division of Psychiatry, Neuropsychiatric Institute, University of Illnois School of Medicine.

METHOD

The general handling of muscles and measurement of potential followed past practice. For stimulation, a square anodal pulse was passed through the impaling electrode, after recording with it the membrane potential. Periodic measurements of the strength duration curve showed a utilization time of 4 msec, so pulses of 6–10 msec were regularly used. Rheobase was determined in earlier experiments in terms of voltage, later the actual current was measured. Since electrode resistance (20 to 100 megohms) far exceeded that of the membrane and varied with tip diameter, the current and voltage across the membrane were not constant for a given applied voltage. This certainly introduced a spurious variability; but since the conditions prescribed a rather constant electrode — about 5% of those constructed were small enough ($< 1\ \mu$) for proper penetration and large enough to pass adequate current — the results were quite tolerable. More accurate values, 2 to 5% range in threshold for all the fibers in a normal muscle, were obtained by inserting a 0.5 megohm resistor in series with the electrode and amplifying the IR drop produced across it by the stimulus for measurement with an oscilloscope. The exact amount and shape of the current that traversed the fiber membrane was thus obtained. (These fine fluid electrodes change resistance with currents considerably stronger and longer than those used, especially when containing 3 M KCl and dipping in ordinary salt solutions, and they impose irregular oscillations upon a square wave, as discussed in the appendix.)

In some experiments, membrane potential was altered by polarizing currents applied through a second internal electrode, independent of the one for measuring potential and threshold. In others, the membrane state was altered by a change in temperature or salt content or by addition of a drug to the bathing solution, always flowing continuously. Normal conditions were: room temperature 20° except in summer; Ringer solution at pH 7.3–7.4 (1 mM Na phosphate buffer) containing in mM, NaCl, 111; KCl, 1.3; $CaCl_2$, 1.3; $NaHCO_3$, 2.4.

RESULTS

Potassium. Membrane potential was earlier found to vary as the log of the external potassium concentration, the slope being 44 mV for a ten-fold concentration change (Ling and Gerard, '50). Present results (fig. 1) are in agreement, the slope being 43 mV and the correlation coefficient, +.94. A potential of 116 mV is recorded with sufficiently low K, values below 60 mV accompany high K. Threshold likewise is a linear function of [K^+] (fig. 1), with a correlation coefficient of +.95. Threshold as related to membrane potential is plotted in figure 2, for some 500 fibers in 50 muscles of summer frogs, each circle representing 5 to 25 fibers of one muscle. Excluding now the fibers with a potential under 65 mV (largely in a different state, to be discussed) the correlation coefficient of threshold and membrane potential is +.95, and the corresponding prediction index is 68%. This

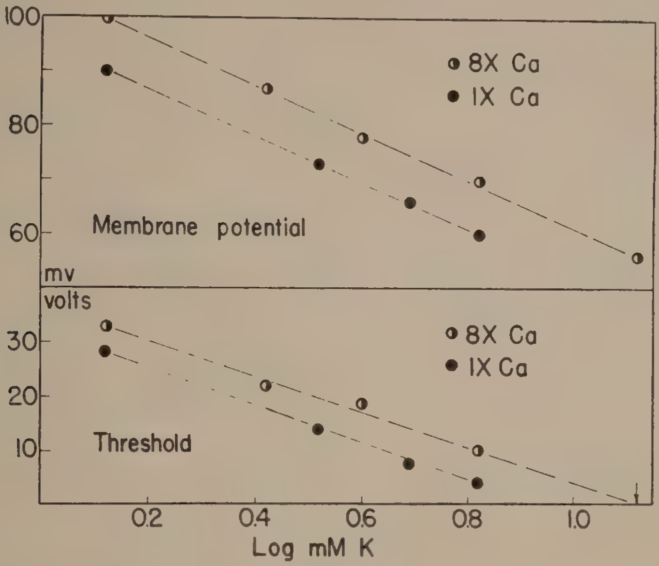

Figure 1

suggests that all factors other than potential contribute only one-third to the determination of threshold — providing that threshold and potential are not both directly determined by [K+]. The standard error of the threshold (Sy, its fluctuation about the regression line) is ± 2.8 volts. The intercept of the plot at zero threshold is at 58 mV membrane potential; a value which occurs in many situations and which seems to separate propagated from local contractions and two parts of the potential.

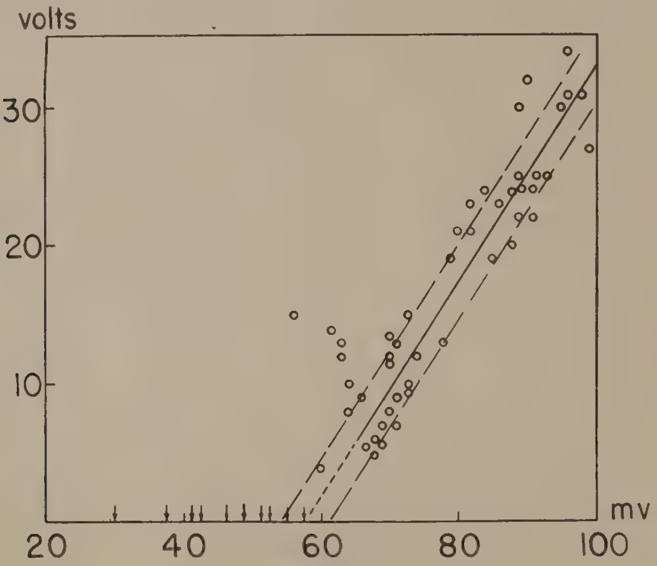

Figure 2

Muscles from winter frogs show the same slope of threshold against membrane potential as do summer muscles, but the absolute position is higher. At a given potential, the winter threshold averages some 4 volts more than the summer one and the zero threshold intercept occurs at 52 mV rather than 58 mV membrane potential. Also, in bull frogs the threshold may be three-fold that of green frogs at like membrane potential. This exemplifies factors, other than absolute potential, that contribute to the determination of threshold. A more extreme instance occurred several times when stale Ringer's solution, over a month old, was used, threshold falling abruptly to about half its normal value in 30 minutes while membrane potential remained unaltered. (This is not related to the depolarization which occurs, reversibly, when a muscle is kept in unstirred solution, more rapidly when the volume is small or the muscle is active. This is presumably due to leakage from the muscle of a depolarizing substance; perhaps K^+, as earlier suggested [Ling and Gerard, '49a] or the nitrogenous material lost at the rate of 25 mg % per hour [Fenn and Cobb, '35]).

Calcium. That potassium is not altering threshold directly but only via changes in membrane potential, is made highly probable by the effects of varying calcium. Calcium acts inversely to potassium on potential and threshold; but five-fold greater concentrations are required, in the case of Ca, to produce comparable shifts of the membrane properties. The concentration of Ca was varied over thirty-fold, from 0.25 to 8 times normal (osmotic balance kept with Na), and the effect of changed K again followed. Membrane potential and threshold showed the same slope against K as before, and threshold remained linked to potential; but the K at which a given threshold and potential appeared was, of course, considerably altered. Results on some 300 fibers in 38 muscles are shown in figure 1 and in figure 3.

The high Ca solutions were of interest in other respects. To avoid possible Ca precipitation, the regular solution was modified by omitting bicarbonate and reducing phosphate to 0.1 mM; this did not alter threshold or potential. But the high Ca (10.4 mM) had a temporary "protecting" action on threshold when membrane potential was lowered, as by high K, below 60 mV. Normally, within a minute of starting the high K solution the potential is down and only local contractions can be obtained; but with high Ca, normal propagated responses can be elicited for some 10 minutes after the potential has dropped. This is another instance of dissociation of potential and threshold, for the latter is higher than the expected value. This type, and the reverse dissociation, were also noted earlier (Gerard and Ling, '48).

pH. It was earlier found (Ling and Gerard, '49a) that membrane potential was independent of pH over a wide range. The present experiments confirm this in the presence of normal or increased calcium. Threshold is also independent of pH, at least over the tested range of 6.2 to 8.8 (60 fibers, not plotted) in normal Ca; but as Ca is increased there develops a progressive dependence of threshold (200 fibers, fig. 4). No such action is seen with K. Since, at high Ca, threshold rises with pH but potential does not, this is another instance of their dissociation.

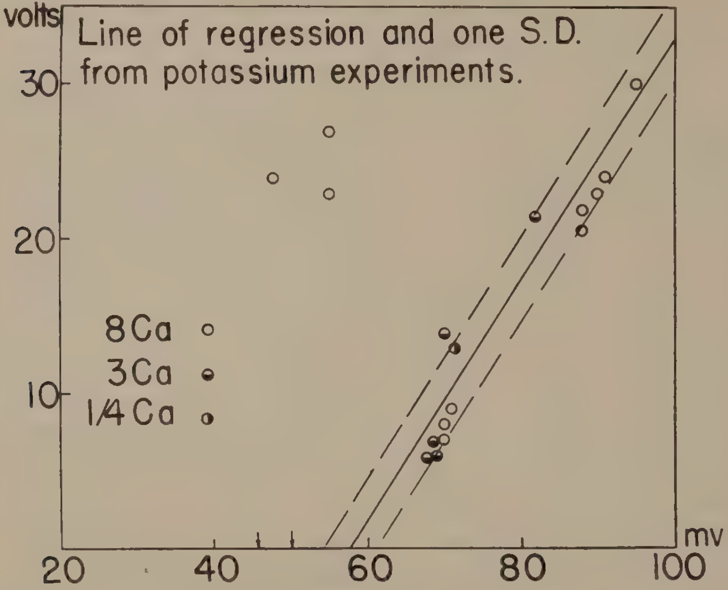

Figure 3

Temperature. The temperature coefficient of the membrane potential was previously found to be the theoretical 1.035 (Ling and Woodbury, '49), under rigorous conditions. In the present series on 250 fibers in 18 muscles the Q_{10}, in the 10°–25°C. range, averaged 1.05 ± .01. It was not altered by K, by the time elapsed since isolation of the muscle (up to 96 hours at 1 to 3°C.), or by the nutritional state of the frog (unfed up to 60 days — at which time the muscle wet weight was 25% below and K 15% above values of control animals; two frogs each). The Q_{10} of the threshold was also 1.05 for fresh muscles from long-enough starved frogs or for long-enough isolated muscles from fed frogs (fig. 5). Fresh muscles from well-nourished animals, however, showed Q_{10} values of 1.8 to 1.9 for threshold, while still having the value of 1.05 for potential; a further dissociation.

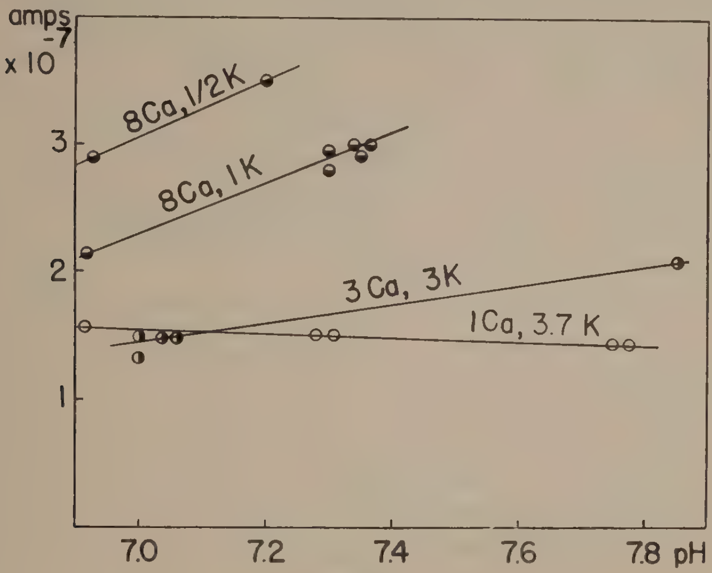

Figure 4

Our preliminary report (Jenerick and Gerard, '50) of a Q_{10} of — 1.7 for threshold, in conflict with the earlier value of + 1.4 (Blair, '35; on muscles isolated for "several days"), was in error. The microelectrode proved to have a Q_{10} of — 1.3 for its resistance; and the utilization time was prolonged at low temperatures beyond the 6 msec duration of the stimulating pulse. The first error was resolved by measuring directly the stimulating current, as described under method;

the second modifying the stimulator to permit pulses up to 60 msec.

Polarization. The membrane potential was raised or lowered by steady polarizing currents passed between internal electrode and ground. From the potential change induced by a given current, the membrane resistance was calculated at 2.5×10^5 ohms (range two to three in three experiments). Assuming that this value remains unaltered during the period of actual stimulation, the threshold stimulating pulse current

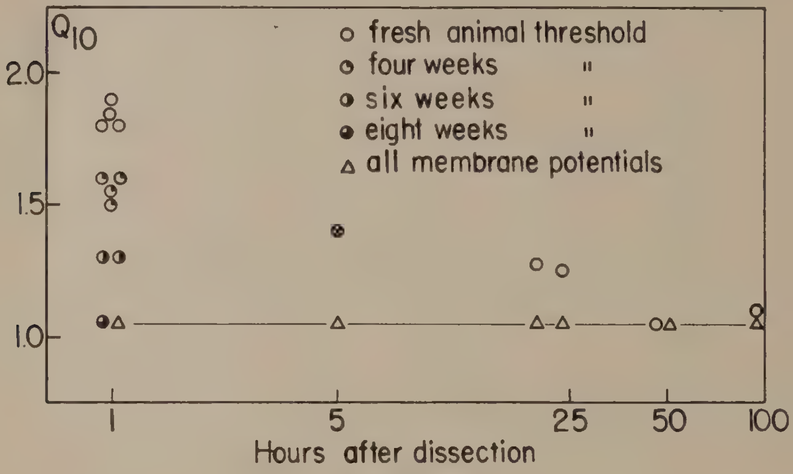

Figure 5

was converted into millivolts of depolarization. In a single experiment, membrane potential was varied by polarization between 63 and 96 mV and the threshold depolarization ranged from 3 to 30 mV; but at each trial response occurred when the preexisting potential was reduced by the stimulus to 57 mV, and the actual points fell in position on the plot of threshold: membrane potential. (The actual range of this critical potential was 54–60 mV, excluding a single value of 66 mV obtained with strong anodal polarization.) When a fiber was progressively depolarized below 55 mV, a localized contracture sometimes appeared about the electrode; and a stimulus also gave only a local response and at a low threshold. These exploratory observations are extended in the following paper.

Drugs. A number of substances was used to alter membrane potential; mostly these results are of a preliminary character.

Eserine. In 2×10^{-5} M concentration in Ringer, eserine sulfate did not alter potential or threshold over an hour's exposure. This concentration alters end plate potential in a few minutes (Eccles and McFarland, '49); and a ten-fold weaker solution is reported (Chang, '49) to lower muscle rheobase — but this may have been due to depolarization by standing in a small volume. Frog brain EEG or Q_{O_2} is not affected (Brooks, Ransmeier and Gerard, '49).

Acetylcholine. This was explored as the chloride in Ringer, at concentrations from 10^{-6} to 10^{-5} M. Responses varied from none to violent twitching, even as between paired muscles, and with little relation to drug strength — as reported by Blair ('38). Perhaps the specific end plate sensitivity to ACh (Kuffler, '43; Bartels, '48) is involved in these erratic responses. In some 100 fibers in 8 muscles, potential tended to rise in the middle concentration range; in one case a fall occurred, but usually twitching set in before any depolarization was seen. In all cases, threshold changed in parallel with potential. It seems clear, from the feebleness of the eserine and ACh effects, that the main relations reported in this paper are not due to inadvertent measurements of end plate properties.

Azide. As earlier noted (Ling and Gerard, '49b), azide gives a rapid depolarization to about 60 mV, followed by a much slower fall. (The facts, that azide inhibits ATP-ase [Meyerhof and Wilson, '49] and that this enzyme is at the surface of neurones [Libet, '48] are of interest in this connection.) This has been fully explored with 1 or 2 mM sodium azide in Ringer. The rapid fall, within 10 minutes, is exponential with time; and the curve breaks sharply at 60 mV. On return to Ringer, recovery towards normal potential also starts within 10 minutes; and a distinct toughening of the cell surface in azide, shown by difficulty in inserting the microelectrode, is also reversed.

The rapid depolarization tends to be to a given level rather than by a given amount. Thus, initial potential values varied by 26 mV in 4 experiments (85 fibers) in 1 mM azide but the levels of depolarization reached varied by only 6 mV. In all cases (170 fibers), when the potential of a given fiber was below 57 to 60 mV it gave only local contractions, when above this level — either during "spontaneous" fluctuation or during the quick fall on exposure to or the rise after removal from azide — full propagated twitches were obtained. In several instances, adjacent fibers in a muscle varied by one or two millivolts in potential, at the critical level of 57 mV, and that with the higher potential gave a normal twitch, the other a local response. Above this critical potential, threshold again varied strictly in parallel with potential.

Ryanodine. This alkaloid was tested in Ringer at concentrations from 0.1 to 1 mg %. It does depolarize (5 mV in one hour at 0.2 mg %; 10 mV, at 0.4 mg %; 8 mV after 10 sec. tetanus in 0.4 mg %); but it also produces contracture even with no significant potential fall (1 to 2 mV). Rigor is complete in 20 minutes at 1 mg %, in 180 minutes at 0.1 mg %. The depolarization and rigor development are independent (compare Taylor, '52) and threshold-potential relations are often not measurable because of contracture; indeed, some fibers gave 10 to 20 twitches after a single shock of normal strength, depolarized below 60 mV, and then gave only local responses. But in three of 6 muscles (125 fibers), the fall of threshold with potential could be followed to a reasonable extent. The two properties again changed in parallel, as in the other types of experiment.

Choline chloride. A 2.5% solution of choline chloride in water is presumably isotonic (Lorente de Nó, '47). In it, membrane potentials fell and held at 65–75 mV (20 fibers) unless flow was stopped, when the potential fell 20 mV in 20 minutes; presumably due to rapid accumulation of ions, leaking from the muscle. In flowing solution, contractions became abortive, spreading only 4 or 5 mm from the point of stimulation, and by 10 minutes only typical local contractions appeared. At any potential, the threshold was at the value expected for normal muscles; but it fell with time, as the abortive twitch became shorter, until the low-threshold local response remained.

Procaine. A 0.3% solution of procaine (HCl) in Ringer depolarized a normal muscle, by 10 to 20 mV; and raised the potential of muscle from a frog starved for 60 days, by 8 mV. In the latter case, threshold was tripled. Even in normal muscle, separation of potential and response occurred; for, at potentials as high as 85 mV, only local responses were obtained, within one minute of adding the drug. The local contractions were obtained at thresholds that were normal for propagated twitches and that varied with membrane potential (over 70 to 85 mV) in the normal manner.

Local responses. Below a critical membrane potential (58 mV in summer frogs, 52 mV in winter ones), which is the same when produced by any one of many agents (salts, drugs, currents), a stimulus produces no propagated twitch but only a local shortening. This has some of the attributes of a contracture, persisting, for example, for the duration of a constant current; but it is reversible and repeatable. Observation under the microscope indicates that gradation of response occurs, both in the length of the contracting segment (which may be only 50 μ) and in the degree of shortening of each unit length; but these are only impressions. Surely the response is graded with stimulus strength; so the determination of true threshold becomes slightly subjective, as the feeblest visible flicker is noted or overlooked. Nevertheless, there is no uncertainty about this fact: a good-sized local response is produced by a stimulus to a fiber with a membrane potential of, say, 56 mV, even though that same stimulus applied a few minutes earlier or later, to the same fiber, with a membrane potential of, say, 58 mV, produces neither propagated nor local response and a stronger stimulus produces only the propagated twitch. Nor is there any uncertainty, in those special cases where local responses are obtained at high membrane potentials (choline Cl, procaine), that the threshold for these, as for propagated twitches, varies with the potential. Only in two or three instances has an increase in stimulus strength converted a local response to a propagated one, and these could be observational errors. At a membrane potential around 50 mV, threshold for local responses is probably minimal. As the potential becomes less, the threshold becomes greater, until, at 20–30 mV, the full output of the stimulator (100 volts) does not excite.

DISCUSSION

Above a critical level of membrane potential, threshold varies with potential under a considerable range of, but not all, conditions and the current required to stimulate is just sufficient to lower the potential across the membrane to this critical level. Below the critical potential, propagated all-or-none responses vanish and a local contracture appears. This is obtained with feebler currents than are required for the propagated response, the threshold decreasing with membrane potential to a minimum and then rising to inexcitability at lower potentials, and its size is graded with stimulus strength above threshold. These local responses of the contractile apparatus, separated from the normally antecedent propagation along the membrane, are thus still not independent of membrane state. It will be convenient to leave their discussion to the following paper, concerned with the link between membrane and contractile units, and to consider here the normal twitch response obtained when the membrane potential is above the critical value.

The threshold is plotted against membrane potential, in figure 6, for nearly 500 single muscle fibers under the whole gamut of our experimental conditions. Although the cor relation is less sharp than when only one variable is considered, correlation coefficient 0.82 (for potentials above 62 mV) as compared with 0.95 for the potassium experiments alone, it is still impressive. And the prediction index (43%

as compared with 68% in the potassium series) indicates that, despite all deliberately introduced variables and the unknown ones of sampling, season, and what not, the membrane potential contributes over two-fifths of the total control of threshold. At the 60–65 mV level, the linear relation between these variables starts to break down, presumably a transition zone as the non-propagated response, clearly present at 58 mV, begins to become quantitatively significant.

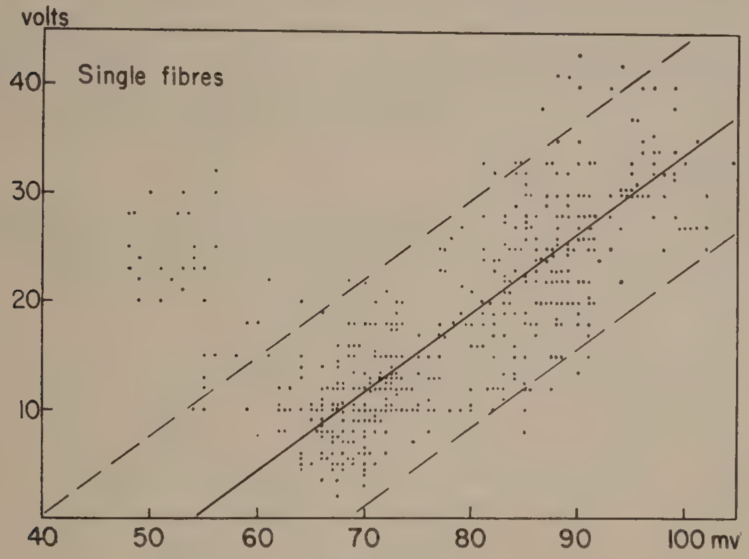

Figure 6

Earlier reports on the relation of membrane polarization level to threshold have been analyzed elsewhere (Jenerick, '51). Some workers found the reverse relation to that here reported (e.g., Okabe, '33) or obtained more complex variations (Hoeber and Waldenberg, '09; Voelkel, '21). Since the demarcation potential of a whole muscle was measured in all previous experiments and since twitches and contractures were often not distinguished, discrepant findings could be expected. On the other hand, a lowering of threshold with increasing potassium (Toman and Woodbury, '47; Walker and LaPorte, '47; Roeder, '48; Rivkine, '50) or decreasing calcium (Brink, Bronk and Larrabee, '46) has been reported regularly and for a great variety of tissues and conditions, as has also lowering with cathodal currents (Katz, '39; Lorente de Nó, '47) and with drugs (Kuffler, '48; Welsh and Gordon, '47) that decrease polarization, and an increase with hyperpolarizing drugs (Shanes, '48; Blavier et al., '50). Thresholds and potentials vary together in time and space after subthreshold stimuli, e.g., an inadequate end plate potential (Katz, '47) or applied current can sum with chemicals to excite or block (Kuffler, '46; Audiat, '34). Still it remains true that some agents, as narcotics (Guttman, '38) or MFA (Boyarsky et al., '48), alter threshold without changing the membrane polarization.

Following Blair ('41) but relating excitation (X) to stimulating current (I) rather than voltage and accepting accommodation as negligible for brief shocks to muscle (Blair, '41),

$$\frac{dX}{dt} = -MI + m\,(X_o - X) \qquad (1)$$

where M and m are constants. The time constant (T) is 1/m and, in a simple membrane model with a battery driving current across a resistance and capacitance in parallel,[4] $M = 1/C$ and $m = 1/RC$. Integrating (1) and rearranging,

$$I = \frac{X_o - X}{M/m} \cdot \frac{1}{1 - e^{-mt}}$$

For large t, I becomes the rheobase (I_r) and

$$I_r = \frac{m}{M}\,(X_o - X_t) = \frac{X_o - X_t}{TM} = \frac{X_o - X_t}{R}$$

The rheobase is thus proportional to $X_o - X_t$ and, for $X_t \geqq 0$ (and M and m true constants), its graph resembles that of rheobase against membrane potential. If X_o is the

---

[4] For the model 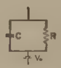

the total voltage across the membrane is $V = Vo - Vc$ and the total current is

$$I = Ic + Ir = C\,\frac{d(Vc)}{dt} + \frac{Vc}{R} = -C\,\frac{dV}{dt} + \frac{Vo - V}{R}\,.$$

Thus $\frac{dV}{dt} = \frac{-I}{C} + \frac{Vo - V}{RC}$ and, if $V = X$, $M = \frac{1}{C}$ and $m = \frac{1}{RC}$ from (1).

initial membrane potential and X_t the intercept of the line extrapolated to zero rheobase at 57 mV, the plots are identical. Neglecting such facts as the change of resistance with the current and the production of local responses, the rheobase depends only on membrane potential and resistance. It is of interest that membrane capacitance, which drops out of the equation, is not altered during excitation (Cole and Curtis, '38).

The rheobase of a variety of tissues is increased by agents which raise membrane potential or lower resistance — as Ca + Ba (Guttman, '38), veratrine (Guttman and Cole, '41), cocaine (Guttman and Cole, '41; Hou, '30), anelectrotonus (Cole and Curtis, '40), or deterioration (Guttman and Cole, '41) — and decreased by the reverse group — cooling (Hou, '30), catelectrotonus (Curtis and Cole, '40), or acetylcholine (Rössel, '48). When both potential and resistance change in the same direction, as under electrotonus or K (Carleton, et al., '38), the rheobase shift is with that showing the greater change. (Resistance change, if not measured, was inferred from chronaxie change on the evidence [Blair, '41] that chronaxie is proportional to T and so to RC, C remaining unchanged.)

Considering more particularly the dependence of threshold on membrane potential, only the potential above some critical value ($X_o - X_t$) is involved. A response occurs when the membrane is depolarized to the critical level, rather than to zero, and the current required to stimulate is just that which, with a given membrane resistance, produces an IR drop sufficient to give this depolarization. Besides the present experiments, many on nerve have shown that a partial depolarization could excite, that any form of threshold current generates a constant negative prepotential (Schoepfle, '43; Schoepfle and Susman, '50), that the time-duration curve for producing a given subthreshold electrotonic potential follows the curve for excitation (Harris and Rosenberg, '35), and that the values of these various parameters vary in the expected direction with polarization (Cole, '41) or salts (Harris and Rosenberg, '35).

For frog sartorius, with a normal membrane potential of 90 mV and a critical potential of about 55 mV (52 to 58 winter to summer), the depolarization required, 35 mV, is about 30% of the total spike potential, 120 mV (Nastuk and Hodgkin, '50). Just such a percentage depolarization by the normal end plate potential or by drugs or cathodal currents is required to initiate a muscle response (Kuffler, '42; '43; '45a), and this has now been demonstrated (Nastuk, '51) with an impaling electrode in a fiber near an end plate treated with ACh — discharge occurs when the potential has fallen to 50–60 mV. Recent independent microelectrode studies of frog sartorius (Fatt and Katz, '51) show that the muscle fiber responds to excitation via the end plate when the initial membrane potential has been diminished by a "step" potential to a critical value of 50 mV. A critical value of 45 mV (range 40 to 48; table 11) was found for applied electrical stimuli. It is doubtful that these values differ significantly from each other or, allowing for different species, etc., from our value of 55 mV. (In nerve, Rosenblueth and Luco, '50, find that the cathodal local response needed to produce a spike is greater for short than for long stimuli. Since the local response as measured is not the same as depolarization, these results do not conflict with those on muscle. Depolarization may [Marmont, '49] or may not [Rosenblueth and Luco, '50] increase during the shock-spike interval.)

All these findings are in harmony with the present evidence: when a lower potential is recorded on partially withdrawing a blunt needle, the threshold is correspondingly low; in general, any change induced in the potential is associated with a corresponding change in threshold; the threshold extrapolates to zero at 57 mV membrane potential; the threshold current does in fact depolarize to this value; when the potential is lowered to this level by a variety of agents (KCl, caffeine, ryanodine, azide, currents, depolarizing substances from muscle), local responses or contractures replace the all-or-none twitches.

It would be tempting to relate the excitation fraction of the membrane potential to the A fraction described for muscle (Ling and Gerard, '49b), as to the L fraction of nerve (Lorente de Nó, '47), but this appears unsound. The A fraction is that part of the total potential related to CrP concentration, and when total potential is decreased by high external potassium, for example, the A fraction is decreased only in proportion (Ling and Gerard, unpublished). Thus, nearly two-thirds of the A potential is presumably still present when K has lowered the membrane potential from 90 to 58 mV, yet the excitation potential fraction is zero. Also indicating that the excitation fraction base is not altered by K, as is the base of the A fraction, azide drops the membrane potential to the same level, whether in 1.3 or 4.8 mM potassium solutions, and this is not related to CrP concentration (Ling and Gerard, '49a, table VII-C). The basis for the actual value of the critical potential is speculative. In terms of the sodium hypothesis, it would be the potential at which altered membrane permeability leads to a greater inward current (Na) than outward current (K minus Cl) and thus to further depolarization (Hodgkin, '51).

The rise of threshold at high K, which lowers membrane potential below 60 mV and so has presumably dropped the excitation fraction to zero, requires some explanation. High K does lead to increased Q_{O_2} and CrP (Tipton, '36), perhaps related to increased accommodation and lowering of X_t; and certainly it lowers membrane resistance (Hodgkin, '51), which should raise the rheobase. Only with high Ca also present, which might counteract the lowered resistance more fully than the lowered potential (although current experiments do not support this), have propagated responses been obtained at potentials below 50 mV. The actual threshold for these was also minimal.

Yet other factors are involved. Responses in high K, high Ca survive only for 10 minutes; the ability of a weak stimulus to give a local contraction when the membrane potential is just below 57 mV, while a considerably stronger one gives neither local nor propagated response when the potential is a trifle higher, is quite unexplained; and the Q_{10} of the threshold of fresh muscle is 1.9 while that of stale or starved muscle is 1.05. The latter value agrees with the Q_{10} of the membrane potential and also with low values for nerve-rheobase (1.1, Schaefer, '40) and time constants for electrotonus and excitation (Schoepfle, '50), these latter also on starved animals (personal communication). The high Q_{10} of normal muscle suggests a strong temperature dependence of m in equation 1, or of R, actually seen even after a period of isolation (Blair, '35), which is lost with deterioration. It may not be concluded, therefore, that rheobase is a simple function of membrane potential and resistance alone; but such a relation is a rather powerful first approximation.

SUMMARY

The rheobase and the membrane potential were measured on the same sartorius muscle fiber with an impaling microelectrode. Over a wide range of values, induced by salts, drugs, temperature, and polarizing currents, the two vary in parallel.

At membrane potentials between 116 and 65 mV, as controlled by external potassium, rheobase is directly proportional to potential; between 65 and 57 mV rheobase is inversely related to potential; between 57 and 30 mV only local graded contractions can be elicited; and below 30 mV no response occurs. The correlation of threshold is with potential rather than with potassium concentration; for it remains through varying concentrations of calcium, which antagonizes the potassium.

A critical potential, 57 mV in summer to 52 mV in winter frogs, exists for initiating a propagated response. The stimulating current required at threshold is just sufficient, for the given membrane resistance, to reduce the pre-existing potential to this value. An equation relates rheobase to this excitation fraction of the membrane potential and to the membrane resistance.

This is a good first approximation to the experimental facts, but a number of special situations exist. In high Ca solutions, threshold increases with pH but potential is unaffected — as is true for both in normal salt solutions. In high K-high Ca, propagated responses may be obtained for 10 minutes at potentials below 50 mV. The Q_{10} of potential and of rheobase is the same (1.05) in stale or starved muscles, but that of rheobase is higher (1.9) in fresh muscles from well-fed animals. The changes in potential, threshold, or contracture induced by procaine, azide or ryanodine have peculiar features. The relation of local contractions to membrane potential, especially their suppression by a slight potential increase, remains unexplained. Despite all these variables, the over-all correlation of rheobase and potential is 0.82 for nearly 500 fibers (0.95 with K as the only variable) and over 40% of the threshold variance (nearly 70% for K) depends on the potential.

We are indebted to Dr. R. E. Taylor for the appendix and for critical discussion throughout.

APPENDIX

Effect of current flow on microelectrode resistance

Several workers (personal communications) have observed the resistance of a Ling-Gerard type electrode to vary as a result of carrying current. This is a result of altered electrolyte concentration in the needle tip due to electro-osmotic flow, the glass being charged negatively with respect to the solution.

Resistances of microelectrodes, dipping into solutions of various salts, were calculated from applied constant voltages and measured currents. A calomel cell-KCl agar bridge of negligible resistance (ca. 3000 ohms) served as indifferent electrode.

Figure 7 shows typical curves of current flow at 50 volts, through an electrode filled with 1 M KCl. The ordinate scale unit is a millimicroohm, the reciprocal of a thousand megohms. Following a preliminary period with current flowing out through the tip (electrode as anode), the current was reversed for two minutes (cathode) and then the electrode again made anodal. The voltage was adjusted to give a current of 0.5 microampere at zero time, approximately the rheobase of a muscle fiber with an internal anode. With the tip cathode, resistance increases when the outside solution is less concentrated than that in the tip and decreases when the outside solution is more concentrated; and in either case returns to normal for the electrode in a few minutes with the tip anode. pH changes over a wide range (1 N HCl to 1 N NaOH), or the substitution of Na for K, did not alter these relations.

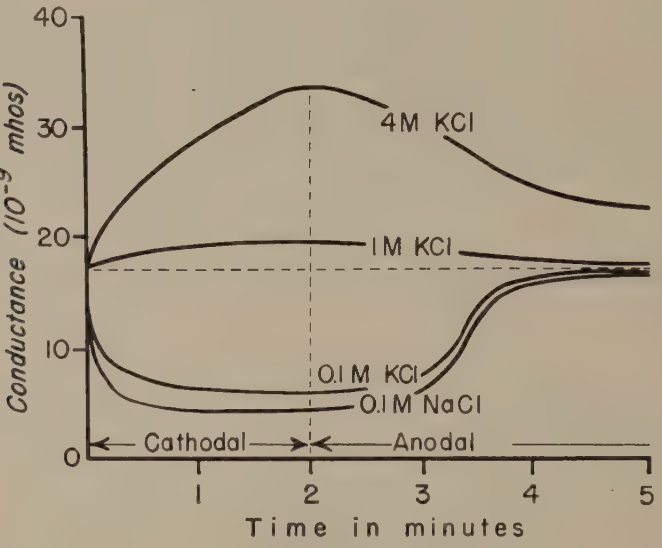

Figure 7

The results are in the direction and of the magnitude to be expected for electro-osmotic flow. The zeta potential should make the solution positive with respect to the glass and the solution should thus move in the direction of the current, but available data do not permit exact calculation. The electrode was left open at the butt end to eliminate any hydrostatic effects, and resistance produced during 20 minutes of free diffusion between tip and solution could be wiped out by one microampere flowing from the tip for about two minutes. Flow can be seen when a solution has been allowed to become dusty. Clear oscillations of the fluid then appear under the microscope in the immediate vicinity of a needle carrying an alternating current.

Two other observations of interest may be related to this flow. Occasionally a constant voltage pulse applied to a microelectrode produces a non-constant current flow. This is not a recording artifact. The variations in flow during a short pulse form a family of curves, represented somewhat schematically in figure 8, consisting of damped oscillations whose frequency and initial amplitude increase with the voltage applied. The oscillations may begin in any phase, from needle to needle; but the initial phase is relatively constant for a given needle. No similar oscillations occur following the applied pulse. Probably the oscillations are associated with small bits of sediment, salt crystals or bubbles and can sometimes be eliminated by applying sweeping fluid from the tip with a large anodal pulse.

The last observation is associated with such large "anodal" current pulses. Some needles may show a very large, and sometimes unstable resistance, say 100 megohms. Following a series of large voltage pulses, this may fall to a much lower, say 5 megohms, an always stable value. Has a particle been dislodged from a bad needle, or a good needle been ruined? We discard needles which have a high resistance and will not tolerate large applied voltages.

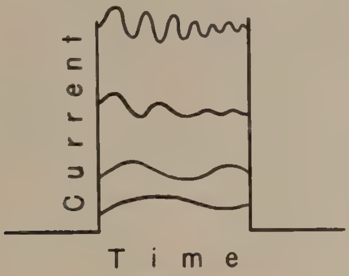

Figure 8

LITERATURE CITED

AUDIAT, J. 1934 Retablissement par anélectrotonus de la conduction du nerf supprimée par divers agents. Compt. rend. Soc. biol., *117:* 1042–1044.

BARTELS, H. 1948 Influence of acetylcholine on the resting potential of striated frog muscle. Pflüg. Arch. ges. Physiol., *250:* 277–294.

BLAIR, H. A. 1935 Temperature coefficients in electrical excitation. J. Cell. and Comp. Physiol., *6:* 291–316.

——— 1938 The effect of acetylcholine on the excitability of the frog's sartorius muscle. Am. J. Physiol., *124:* 372–378.

——— 1941 Muscle excitability. Biol. Symp., *3:* 51–93.

BLAVIER, J., J. LECOMTE, P. OSTERRIETH AND E. VANREMOORTERE 1950 Desensibilation au potassium par les anesthesiques locaux. Arch. internat. physiol., *57:* 393–398.

BOYARSKY, L. L., A. ROSENBLATT, S. POSTEL AND R. W. GERARD 1949 Action of methyl fluoroacetate on respiration and potential of nerve. Am. J. Physiol., *157:* 291–298.

BRINK, F., JR., D. W. BRONK AND M. G. LARRABEE 1946 Chemical excitation of nerve. Ann. N. Y. Acad. Sci., *47:* 457–486.

BROOKS, V. B., R. E. RANSMEIER AND R. W. GERARD 1949 Action of anticholinesterases, drugs, and intermediates on respiration and electrical activity of the isolated frog brain. Am. J. Physiol., *157:* 299–316.

CARLETON, B. H., H. A. BLAIR AND W. B. LATCHFORD 1938 The effects of the chlorides of potassium, calcium, and sodium on the alpha excitability of muscle. J. Cell. and Comp. Physiol., *12:* 223–236.

CHANG, P. T. S. 1949 Change of muscle excitability by eserine, acetone, and methyl alcohol. Proc. Soc. Exp. Biol. and Med., *72:* 17–18.

COLE, K. S. 1941 Rectification and inductance in the squid giant axon. J. Gen. Physiol., *25:* 29–51.

COLE, K. S., AND H. J. CURTIS 1938 Electric impedance of the squid giant axon during activity. J. Gen. Physiol., *22:* 649–670.

———— 1940 Membrane potential of the giant squid axon during current flow. J. Gen. Physiol., *24:* 551–563.

ECCLES, J. C., AND W. V. MACFARLANE 1949 Actions of anticholinesterases on end plate potential of frog muscle. J. Neurophysiol., *12:* 59–80.

FATT, P., AND B. KATZ 1951 An analysis of the end plate potential recorded with an intracellular electrode. J. Physiol., *111:* 320–370.

FENN, W. O., AND D. M. COBB 1935 The diffusion of nitrogenous compounds from frog muscle in Ringer's solution. J. Cell. and Comp. Physiol., *6:* 469–485.

GERARD, R. W., AND G. LING 1948 Membrane potential of single muscle fibers. Am. J. Physiol., *155:* 437–438.

GRAHAM, J., AND R. W. GERARD 1946 Membrane potentials and excitation of impaled single muscle fibers. J. Cell. and Comp. Physiol., *28:* 99–117.

GUTTMAN, R. 1938–1939 The electrical impedance of muscle during the action of narcotics and other agents. J. Gen. Physiol., *22:* 567–591.

GUTTMAN, R., AND K. S. COLE 1941 Electrical rectification in single muscle fibers. Proc. Soc. Exp. Biol. and Med., *48:* 293–297.

HARRIS, D. T., AND H. ROSENBERG 1935 The strength duration curve for constant electrotonic potential in nerve. J. Physiol., *84:* 11–12P.

HÖBER, R., AND H. WALDENBERG 1909 Über den Einfluss von Salzen starker organischer Basen auf den Ruheström und die Erregbarkeit von Froschmuskeln. Pflüg. Arch. ges. Physiol., *126:* 331–350.

HODGKIN, A. L. 1951 Ionic basis of electrical activity in nerve and muscle. Biol. Rev., *26:* 339–409.

HOU, C. L. 1930–1931 Über die Veranderungen der Reizzeitspannungs Kurve durch Narkose, Kalte and Veratrin. Pflüg. Arch. ges. Physiol., *226:* 676–688.

JENERICK, H. P. 1951 The membrane potential as a contributing factor to the rheobasic threshold of muscle. Doctoral dissertation, University of Chicago.

KATZ, B. 1939 The "anti-curare" action of a sub-threshold catelectrotonus. J. Physiol., *95:* 286–304.

——— 1947 Sub-threshold potentials in medullated nerve. J. Physiol., *106:* 66–79.

KUFFLER, S. W. 1942 Electric potential changes at an isolated neuromuscular junction. J. Neurophysiol., *5:* 18–26.

——— 1943 Specific excitability of the end plate region in normal and denervated muscle. J. Neurophysiol., *6:* 99–110.

——— 1945 Electric excitability of nerve-muscle fiber preparations. J. Neurophysiol., *8:* 75–87.

——— 1946 The relation of electric potential changes to contracture in skeletal muscle. J. Neurophysiol., *9:* 367–377.

——— 1948 Physiology of the neuromuscular junction: electrical aspects. Fed. Proc., *7:* 437–446.

LIBET, B. 1948 Adenosinetriphosphatase (ATP-ase) in nerve. Fed. Proc., *7:* 72.

LING, G., AND R. W. GERARD 1949a The normal membrane potential of frog sartorius fibers. J. Cell. and Comp. Physiol., *34:* 383–396.

——— 1949b The membrane potential and metabolism of muscle fibers. J. Cell. and Comp. Physiol., *34:* 413–438.

——— 1950 External potassium and the membrane potential of single muscle fibers. Nature, *165:* 113–114.

LING, G., AND J. W. WOODBURY 1949 Effect of temperature on the membrane potential of frog muscle fibers. J. Cell. and Comp. Physiol., *34:* 407–412.

LORENTE DE NÓ, R. 1947 A study of nerve physiology. Studies from the Rockefeller Institute, Vols. 131–132, New York.

MARMONT, G. 1949 Studies on the axon membrane. I. A new method. J. Cell. and Comp. Physiol., *34:* 351–382.

MEYERHOF, O., AND J. R. WILSON 1949 Studies on the enzymatic system of tumor glycolysis. I. Glycolysis of free sugar in homogenates and extracts of transplanted rat sarcoma. Arch. Biochem., *21:* 1–21.

NASTUK, W. L. 1951 Personal communication.

NASTUK, W. L., AND A. L. HODGKIN 1950 The electrical activity of single muscle fibers. J. Cell. and Comp. Physiol., *35:* 39–73.

OKABE, S. 1933 Membrane potential of the muscle as a determining factor in excitability. Jap. J. Med. Sci., Part III, Biophysics, *3:* 1–53.

RIVKINE, A. 1950 Action d'une variation de potassium ou de calcium sur l'électrocérébrogramme de la grenouille perfusée. Arch. internat. physiol., *57:* 245–266.

ROEDER, K. D. 1948 The effects of potassium and calcium on the nervous system of the cockroach Periplaneta americana. J. Cell. and Comp. Physiol., *31:* 327–338.

ROSENBLUETH, A., AND J. V. LUCO 1950 The local response of myelinated mammalian axons. J. Cell. and Comp. Physiol., *36:* 289–332.

RÖSSEL, W. 1948 Influence of acetylcholine on the polarizability (impedance) of poikilothermic heart and muscle. Pflüg. Arch. ges. Physiol., *250:* 200–222.

SCHAEFER, H. 1940 Elektrophysiologie, I Band. F. Deuticke, Wien.

SCHOEPFLE, G. M. 1943 The role of polarization in electrical excitation of nerve. J. Cell. and Comp. Physiol., *22:* 199–204.

——— 1950 Electrotonic potentials elicited by threshold stimuli from sheath-free nerve at different temperatures. Am. J. Physiol., *163:* 229–293.

SCHOEPFLE, G. M., AND N. SUSMAN 1950 Physical significance of strength-duration curve for excitation of nerve. J. Neurophysiol., *13:* 289–293.

SHANES, A. M. 1948 The effect of stabilizing and unstabilizing agents in relation to the metabolic mechanism supporting the resting potential of nerve. Biol. Bull., *95:* 245.

TAYLOR, R. E. 1952 The following paper.

TIPTON, S. R. 1936 Phosphocreatine and lactic acid changes in potassium chloride contracture of frog muscles in acid solutions. J. Cell. and Comp. Physiol., *7:* 433–443.

TOMAN, J. E. P., J. W. WOODBURY AND L. A. WOODBURY 1947 Mechanism of nerve conduction block produced by anticholinesterases. J. Neurophysiol., *10:* 429–441.

VOELKEL, H. 1921 Die Beziehungen des Ruheströmes zur Erregbarkeit. Pflüg. Arch. ges. Physiol., *191:* 200–210.

WALKER, S. M., AND Y. LAPORTE 1947 Effects of potassium on the endplate potential and neuromuscular transmission in the curarized semitendinosus of the frog. J. Neurophysiol., *10:* 79–85.

WELSH, J. H., AND H. T. GORDON 1947 The mode of action of certain insecticides on the arthropod nerve axon. J. Cell. and Comp. Physiol., *30:* 147–171.

THE CONTRACTILE PROCESS IS NOT ASSOCIATED WITH POTENTIAL CHANGES[1]

ROBERT E. TAYLOR[2]
Department of Physiology, University of Chicago

SEVEN FIGURES

Considerable evidence was presented at an early date, much of it reviewed by Schütz ('36) and Bogue and Mendez ('30), that the electrical and mechanical events in heart muscle are largely independent with regard to duration and size. Perhaps the idea that an electrical sign is associated with the operation of the contractile mechanism arose because normally the action potential and the contraction of heart muscle have about the same duration.

The action potential, as recorded with external electrodes, is very similar for skeletal muscle and for nerve, but many have suggested that part of the muscle action potential is associated with the contraction per se (e.g., Lee 1887; Schenk, 1895; and with oscillographic recording, Bishop and Gilson, '27; Rosenblueth, '44). Gelfan and Bishop ('32) questioned the general validity of a potential-contraction relation, since they could find no potential changes during submaximal contractions or certain mechanically-induced contractures in the retro-lingual membrane of the frog.

The potential changes seen in the frog gastrocnemius (Bremer, '32) during normal twitch and neuro-muscular contracture are difficult to interpret because of the complex geometry of this muscle and the use of external electrodes. The view (Arbeiter, '21; Einthoven, '24) that all potential changes associated with a twitch, both in heart and skeletal muscle, are due to the contraction is unacceptable because the spike potential can easily be blocked without interfering with the contractile ability of the muscle (see Gasser,'30).

---

[1] Preliminary report, Am. J. Physiol., *9:* 124 (1950). These studies were supported by a contract between the Office of Naval Research, Department of the Navy and the University of Chicago and by a grant from the Dr. Wallace G. and Clara A. Abbott Memorial Fund of the University of Chicago.

[2] Merck Fellow, 1951; Public Health Fellow, 1952. Present address: Neuropsychiatric Institute, University of Illinois College of Medicine.

An extensive literature concerning electrical changes during chemically-induced contractures (see esp. Beritoff and Woronzow, '26) is difficult to interpret because of the recording methods used; while the problem of potentials during and after electrically-induced contractures has received little attention, presumably because of the small region of muscle to which these are ordinarily limited. A method for producing cathodal contractures in a large region of muscle will be presented and these questions reopened in the discussion.

It has been suggested (Ling and Gerard, '49) that the post-tetanic membrane potential fall (the *innere Wirkung* of du Bois Reymond, see Burdon-Sanderson, 1895, and Beritoff and Woronzow, '26, and probably identical with the *Kontraktions-Potential* of Buchthal and Peterfi, '34) is caused by the lowered creatine phosphate attendant upon contraction. This, in terms of the theory of Boyle and Conway ('41), might provide a mechanism for potential changes during the mechanical portion of the twitch. While the experimental results to be presented create certain difficulties for this hypothesis, the situation is by no means simple.

The principal impression gained from the literature on electrical changes during muscular contraction is that artifact-free recording probably cannot be achieved with external electrodes. The major source of artifact seems to be movement (see Fulton, '26, p. 204) possibly supplemented by distortion potentials (de Meyer, '21). Diphasic recording does not show slow changes, and tissue destruction to obtain monophasic recording releases harmful substances and also introduces new sources of movement artifact. Monophasic recording, moreover, would record changes in internal resistance of contracting fibers as apparent membrane potential changes. All these errors are augmented by the necessity of maintaining the muscle in air or oil, which favors an increased extracellular concentration of potassium, by leakage, and an attendant depression.

Most of these difficulties have been overcome by the technique, introduced by Graham and Gerard ('46) and improved by Ling and Gerard ('49), of impaling single muscle fibers with microelectrodes. Truly monophasic recording is possible without injury, the full membrane potential is obtained independently of the resistance of cell membrane and interior, and the muscle may be immersed in fresh Ringer.

METHODS

Membrane resting and action potentials were measured by impaling single (undissected) fibers of the excised frog sartorius with Ling-Gerard micro-pipettes, filled with 3 molar KCl, and drawn with a long taper, to a tip diameter less than one micron, so that they were not broken or expelled by contraction.

For measurement of membrane potential alone, the recording system was a simple cathode follower-galvanometer based on an electrometer tube (Victoreen 5803). Calomel cells were used throughout for fluid metal coupling. For measurements of action potentials, and of membrane potentials with less accuracy, a single cathode follower, designed by M. Davis and similar in principle to that used by Nastuk and Hodgkin ('50), fed directly into the input of a DuMont 304H Oscilloscope. The sensitivity was 15 mv/inch, input impedance was 200 megohms, and response was flat from D.C. to 10 kilocycles. The input capacity was sufficiently reduced by a cathode-coupled input shield so that the high resistance of the microelectrodes caused no significant distortion. Action potentials were recorded on 35 mm film with a Fairchild oscilloscope camera.

Flowing Ringer solution of the following composition was commonly employed: 111.3 mM NaCl; 2.5 mM KCl; 1.3 mM $CaCl_2$; 1.0 mM phosphate buffer adjusted to pH 7.3.

The first technique used to produce the usual twitch and to give continuous current contractures without twitch, employed two microelectrodes inserted into a single fiber. Current was passed through one and membrane potential recorded with the other, with respect to an indifferent electrode in the surrounding fluid. This procedure, however, has three drawbacks. First, a detailed investigation (Jenerick and Gerard, '53) has shown that considerable change in the resistance of the microelectrode occurs with current flow, due to the electro-osmotic movement of fluid in the tip. The solution is positive with respect to the glass and, since excitation occurs only if the impaling electrode is anode, stimulation pumps 3 M KCl into the cell — apparently sufficient to raise the membrane potential near the electrode several millivolts, following the application of threshold currents for 10–20 seconds. Second, the contractures produced in this way occupy only about 1 mm length of fiber. If, following the contracture, the membrane potential is changed, the measured change will differ from the actual one by the amount of IR drop of local currents through the resistance in series with the membrane "battery." This effect has been calculated, assuming that the simple core conductor model is valid and that any residual membrane potential change, being proportional to the current applied, will have an exponentially decaying spatial distribution. The measured potential change would be decreased by the flow of local currents within one space constant to either side of the original polarizing electrode, and increased beyond this region. At this electrode, the measured change would be one-half of the actual change. These effects of current depend upon the membrane resistance only as it affects the space constant, which is here assumed to be short compared to fiber length. The third difficulty is that contracture occurs over a small region of only one fiber, and chemical investigation is precluded.

To circumvent these difficulties, two types of large fluid electrodes, based upon one earlier developed for nerve (Taylor, '52), were used to produce local contractures in much of the length of the muscle. The electrode is so shaped that the total applied longitudinal current density increases linearly with distance over that length in which the contracture is desired. The frog sartorius is only a moderately good simple core conductor (Katz, '48), as theoretically required, but in practice the method works.

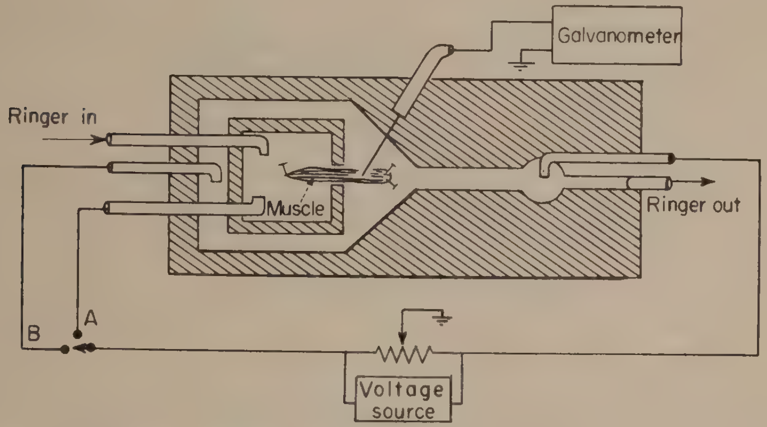

Fig. 1 Horizontal triangle polarizing chamber. Shaded area, wax; unshaded area, flowing Ringer solution.

The first electrode used is diagrammed in figure 1. The shaded area represents wax, molded into a trough of the shape indicated. The muscle was fastened through its tendons to cork on the bottom of the trough and with a small opening to allow transillumination for microscopic observation. If current is applied through electrode B as cathode and the right hand electrode as anode, muscle in the triangular part of the chamber contracts while the remainder does not. In the fresh muscle, a twitch results if the current is increased with sufficient rapidity, otherwise not (see Lucas, '07).

The second chamber used, figure 2, employs the same principle but the triangle is vertically oriented and filled with Ringer-agar. The muscle is held as indicated immersed in a thin film of flowing Ringer that covers the agar. With the electrode at the lower corner of the triangle as cathode, current will enter the muscle fibers near the anodal corner and leave more or less uniformly from the rest of the fiber. With a space constant for electrotonic spread of 2–2.5 mm (frog sartorius in Ringer, 2.2 to 2.6, Fatt and Katz, '51; or 2.0, one experiment under present conditions), a constant current contracture should, and does, occur in all but about 3 mm of the "anodal" end of the muscle. Contracture appears where current is flowing outward through the membrane, and is apparently not related to the density of the longitudinal current inside the fiber. With a reversed current, contracture occurs only in a region about 2 mm long near the now "cathodal" end of the muscle. Voltage measurements along the surface of a muscle placed in this chamber are shown in figure

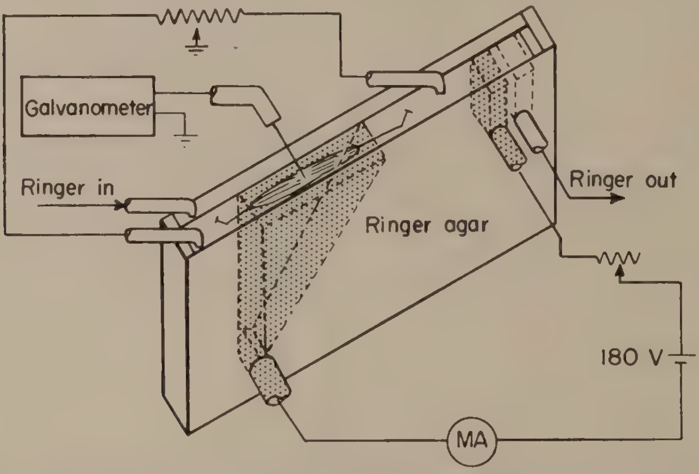

Fig. 2 Vertical triangle polarizing chamber. With electrode in lower corner as cathode, contracture occurs in all except 2–3 mm of muscle held as indicated.

3, a double logarithmic plot of voltage versus distance from the right angle corner. If current density increases linearly from this corner, voltage should have the form $V = ax^2$ and the log-log representation should be a straight line of slope 2. This is very nearly the case. The solid line is drawn with slope 2 through the point $x = 3$ cm.

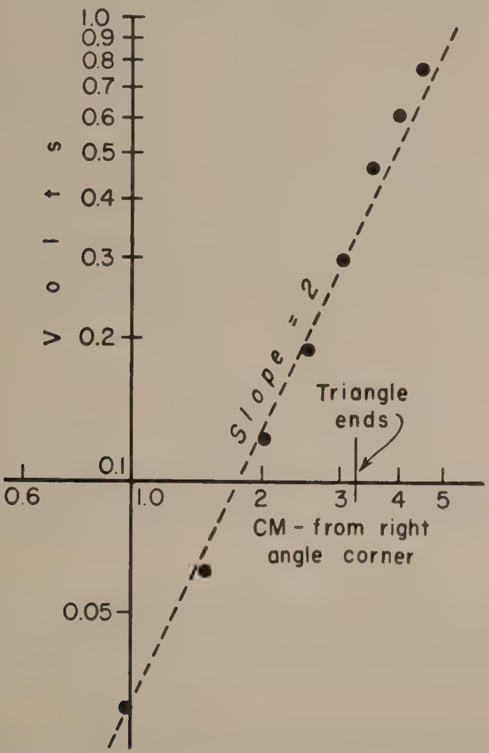

Fig. 3 Log-log plot of voltage along surface of muscle as in figure 2, against distance from right angle corner. Line drawn through point $x = 3$ cm with the theoretically desirable slope of two.

The theoretical membrane current distribution of a core conductor of finite length in a region of longitudinal linearly-increasing current density is of sufficient interest to justify some statement of an extension of that applicable to a core conductor of infinite length (Taylor, '52). Consider an infinite cylinder (fig. 4) in which the longitudinal current has the form $I = ax,\ x \geqq 0;\ I = 0,\ x \leqq 0$. Extending from the point $x = x_o$ to $x = x_1$ is a smaller concentric cylinder whose internal resistance per cm length in ohm/cm is r_2, and this is surrounded by a membrane whose resistance per cm length in ohm · cm is r_m. Call the resistance per cm length outside the inner cylinder in ohm/cm, r_1. Then the current flowing inward through the membrane, i_m, in amperes per cm length is given by

$$i_m(X) = \frac{r_1 a}{r_1 + r_2}\left[1 + \frac{X_1 \cosh(X - X_o) - X_o \cosh(X_1 - X)}{\sinh(X_1 - X_o)}\right]$$

where $X = x/\lambda$ and $\lambda^2 = r_m/(r_1 + r_2)$. λ is the usual space constant of electrotonic spread.

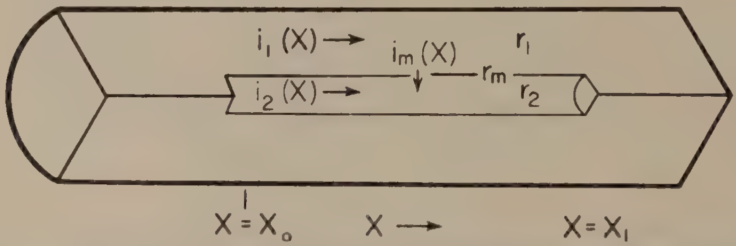

Fig. 4 Geometry of system considered for membrane current distribution in idealized muscle fiber of finite length in region of applied longitudinal current density. $I = ax$.

A graph of the theoretical distribution of membrane current in such a system, for a fiber length of 30 λ, is shown in figure 5 for two cases: the fiber extends from $X = 0$ to $X = 30$ and from $X = 10$ to $X = 40$. The coordinates of the graph are $I_m(X) = i_m(X)\ \frac{(r_1 + r_2)}{r_1 a}$ (normalized so that $I = 1$ in the plateau region) and $(X - X_o)$. When $X_o = 0$, the membrane current is essentially constant from $X = 0$ to $X = 25$. If the fiber does not extend to the point where the longitudinal current begins to increase, the current density near this point is larger than in the plateau region.

Deviation of the structure of the muscle from that assumed in the simple core conductor model causes deviation of the applied membrane current from its calculated form. An experimental check requires maintaining an accurate virtual ground in the chamber, which is difficult, but actual use of the chamber demonstrates that most of the muscle is, in fact, subjected to uniform membrane polarization.

As indicated in figure 2, neither electrode used for supplying current can be at ground potential, since this would put several volts across the recording electrodes. Such a steady voltage could not be circumvented by shunting the polarization electrodes with resistance with variable center tap to ground, because currents, up to 100 ma, polarized the electrodes. To maintain some point in the chamber at ground potential, two additional electrodes were used with such a shunt potentiometer (fig. 2), but then any movement of the recording electrode entailed resetting of the ground connection. For many purposes this arrangement was satisfactory,

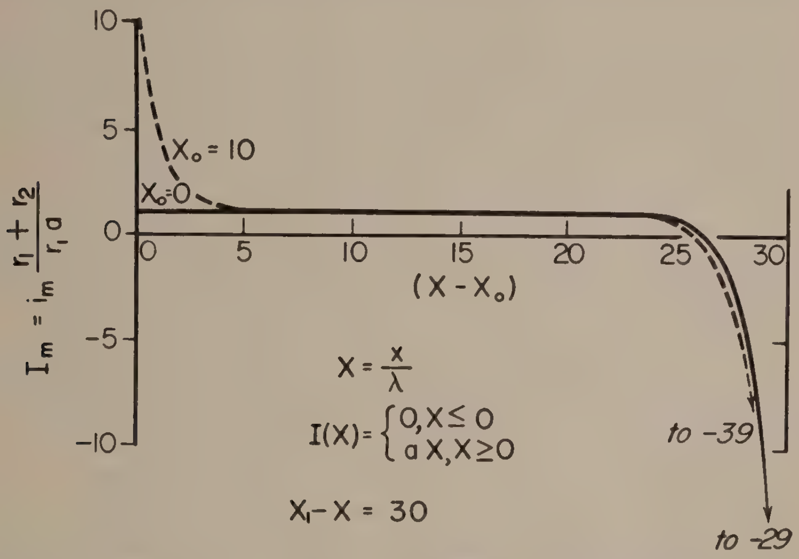

Fig. 5 Membrane current density distribution in fiber of length 30 λ for the idealized case shown in figure 4. Membrane current density normalized so that magnitude is unity in plateau region. Solid line: case where fiber begins at point $x = 0$. Dotted: case where fiber begins at point $x = 10\lambda$, i.e., $X_o = 10$. $\lambda^2 = r_m/(r_1 + r_2)$.

but precise measurements of the membrane potential during current flow were obscured by changes in the recorded potential, due to slight variations in the fluid depth or small movements of the recording electrode. Quantitative measurements are, therefore, reported only before or after passing currents.

For study of the relation between isotonic shortening and membrane potential during caffeine action, the muscle was mounted in a simple chamber with provision for flowing Ringer. A string tied to one end of the muscle passed around a glass rod as pulley, rose from the chamber and was held taut with a 2-gm weight. The position of the weight was read on an attached scale to about one-tenth of a millimeter, a sufficiently accurate measure of muscle length.

RESULTS

Simple twitch. Action potentials associated with the simple twitch have the form shown in figure 6, in agreement with Nastuk and Hodgkin ('50). The spike is followed by a negative after potential which lasts into the period of contraction, the point of interest here. There is nothing to suggest that this after potential is associated with the contraction per se; it presumably has the same significance as for nerve.

The action potentials shown in figure 6 are, except for amplitudes, typical of hundreds, observed in fresh muscle with large membrane potentials and in muscles in stagnant Ringer with low membrane potentials. Any potentials seen during the period of actual movement (fig. 6, B) were variable from twitch to twitch and occurred when the microelectrode was too large — as indicated by variability in repeated measurements of the membrane potential. Occasionally, potential changes were seen during movement even with a "good" needle (fig. 6, B), but these were non-reproducible and were clearly artifacts. The important point regarding the consistent records is that artifacts are excluded; whereas with external electrodes, even when comparable records are obtained, this is not the case. It is concluded that, in the normal twitch of the frog sartorius muscle, all the observed potential changes are associated with the conduction of excitation in the membrane and none with the operation of the contractile mechanism. Whether the after potential is associated in any way with the operation of the excitation-contraction coupling process remains to be investigated.

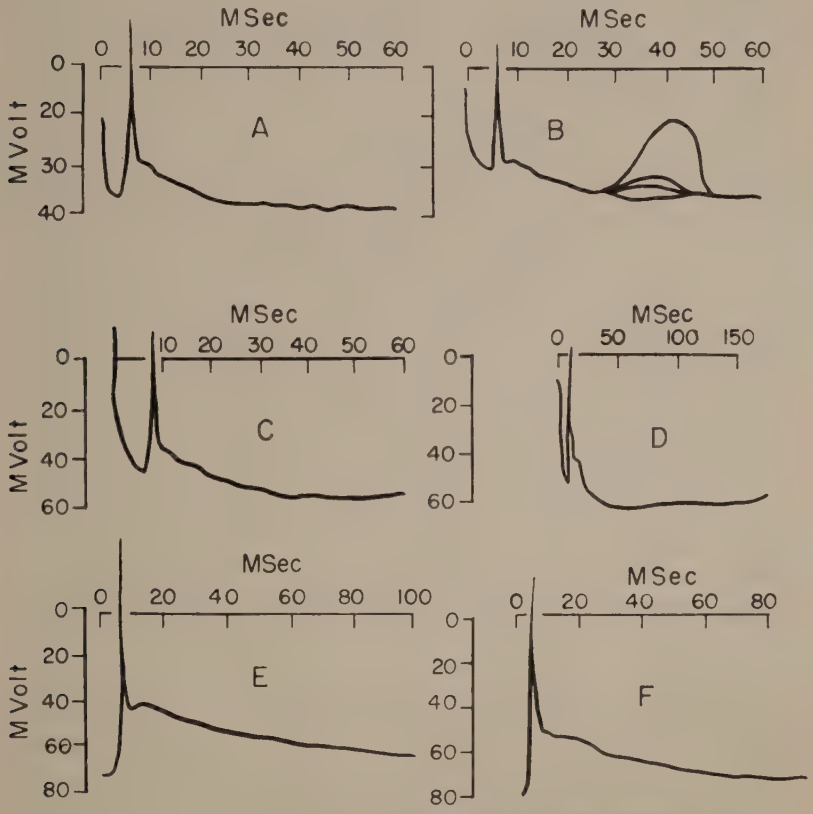

Fig. 6 Representative action potentials, normal twitch.

Constant current contracture. Contracture can appear in the region where an applied constant current leaves a muscle fiber. The production of constant current contractures (Wundt, 1859) as well as of non-propagated anodal break contractures, was demonstrated in situ in the frog by Biedermann (1895, p. 270). Lucas ('07) showed that increasing the current gradually would avoid the initial twitch. Later workers investigated certain aspects of these contractures, principally in the retro-lingual membrane of the frog (Gelfan and Gerard, '30; Gelfan, '33), but the technical difficulties discussed above rendered electrical measurements difficult.

A fresh muscle in the vertical chamber (fig. 2) exhibits a contracture on application of a constant current only slightly above the twitch rheobase. It relaxes in a few seconds, although current continues, and can be re-established if the current is sufficiently increased. The following points on threshold changes deserve note here. The muscle rapidly accommodates to the constant current; within 15 seconds its contracture threshold may rise ten- to twenty-fold, and after one minute of cathodal polarization, with a current of 2.5 times the initial twitch threshold, it will no longer respond with a conducted action potential or produce a normal twitch. At this time the membrane potential is normal. Following a short (one to two minutes) period of this amount of polarization, the contracture threshold returns smoothly to its original value within a minute or two, but the twitch threshold, if it reappears at all, does so suddenly, at its original value. Anodal polarization restores both thresholds under many conditions, but the twitch and local contractures do not seem to be related in any definite way. The former is tremendously more labile.

Currents up to 10 times those required to give an initial contracture have been applied repeatedly, for periods up to three minutes. No change in membrane potential has been observed after termination of the current in some 20 muscles under various conditions — fresh, depressed in stagnant Ringer or by subcontracture concentrations of caffeine or KCl, curarized or not. Sufficiently strong or more enduring currents would be expected to produce post-polarization changes.

The membrane potential is not easily measured during current flow, for the reasons mentioned above, but no sharp break in the magnitude of the passive potential changes produced by a gradually increasing applied current occurs when contractures appear. Also, while a constant current is flowing, the membrane potential does not change by more than a millivolt or two when an initial contracture relaxes, apparently completely. Individual measurements are not accurate under these conditions but any consistent membrane potential change associated with the relaxation during constant current flow would surely have been detected in the many observations.

Post-anodal contracture. With anodal constant currents (anode at the lower corner of the triangle in fig. 2), current flows inward through most of the membrane of each fiber. At break, threshold falls abruptly — the change fades out with a time constant of about 15 seconds (followed in two experiments) — and, if the initial current has been of great enough magnitude and duration, the threshold becomes negative and a post-anodal contracture results.

The membrane potential can be measured accurately during the post-anodal period. A transient discharge of the membrane capacity occurs at break, of course, with a time constant in the order of 10 milliseconds; but, following this, the membrane potential is constant and at the prepolarization value. Not only the equilibrium levels but the transients are independent of the appearance of a contracture, identical ones, within the 1–3 mV accuracy of the measurements, appearing after a given current whether post-anodal contracture is present after a long passage or absent after a short passage. It is thus fairly certain that post-anodal contracture in the frog sartorius is not associated with any active potential change nor with any considerable change in the membrane time constant. Observed under the microscope, all the fibers appeared to participate in the post-anodal contracture, but conceivably just those in which the membrane potential was measured were not contracting. Such an error is unlikely, since measurements were made on many fibers across the surface of a muscle and on several muscles, with uniform results.

Caffeine contracture. Muscles soaked in caffeine shorten and lose potential, but the two changes are independent. The time course of the membrane potential change of three sartorii, in three different concentrations of caffeine in flowing Ringer solution, is shown in figure 7. Each point on a curve is the average of measurements on 4 to 8 surface fibers; and each number gives the per cent of the final isotonic shortening

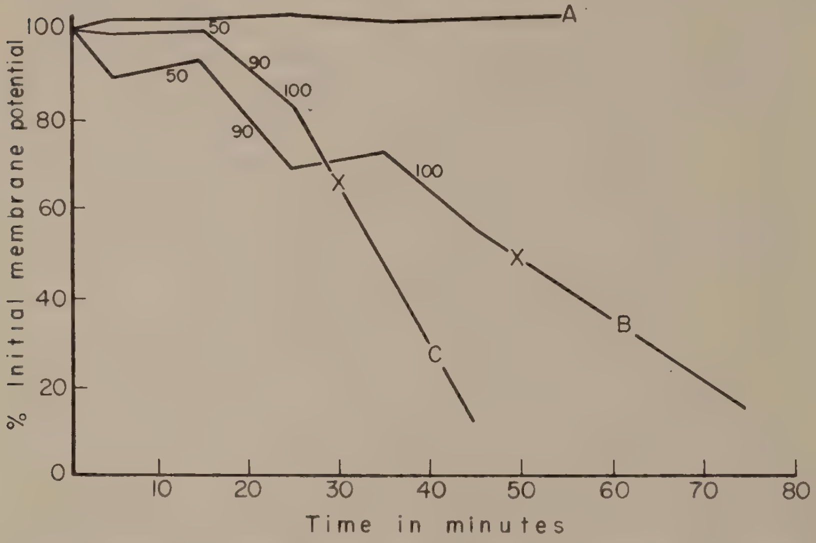

Fig. 7 Membrane potential versus time for various concentrations of caffeine. Curve A, 0.05%; B, 0.08%; C, 0.1%, in Ringer. Numbers indicate per cent of final isotonic shortening with 2 gm load. Cross indicates muscle completely inexcitable electrically. Each point average of 4 to 8 fibers across surface of single sartorius.

(2-gm load) that had been reached at the time indicated. The time of onset of caffeine contracture is notoriously variable, so that the earlier shortening in the 0.08% than the 0.1% caffeine is not significant. The important point is that the muscle had completed 50% of its shortening at a time when the membrane potential was unchanged (0.1% caffeine) or only 5% lowered (0.08% caffeine). Moreover, neither at the onset nor at the completion of shortening was there any indication of a break in the time course of the membrane potential curves.

Local contractures can still be elicited by electric currents up to about 5 minutes after the caffeine shortening has reached its full size (fig. 7).

DISCUSSION

Action potentials of the frog sartorius, when measured with an internal electrode and minimal artifact, have a form similar to those of nerve. Any potential changes, at most a few millivolts, seen during the mechanical part of the twitch are not reproducible and appear to be artifacts associated with improper needles. Capillaries used regularly in the present investigation, with a taper over about one inch, usually yielded no contraction potentials. That the normal large negative after potential, while perhaps associated with the coupling of excitation-contraction, is not caused by any operation of the contractile mechanism is further shown by the absence of potential changes during other types of contraction activation. Aside from the capacitative transients and conducted activity, the membrane potential remains unchanged during cathodal or anodal polarization or post-polarization periods, whether contractures are evoked or not and whether they persist or not.

Potential changes during chemically-induced contractures show no relation to the extent of shortening. The present results with caffeine are similar to those with IAA (Lui, '48) and with potassium and other ions (E. Fischer, '24). (For discussion of earlier results see Beritoff and Woronzow, '26; Riesser, '36.) No potential change has been seen with water rigor (Biedermann, 1897; Tobias, '50), $CaCl_2$ contracture (Gerard and Ling, '48) or ryanodine contracture (Jenerick and Gerard, '53). Unfortunately, no simple criterion, other than reversibility, exists for deciding in each case whether the shortening is of the same type as normal contraction. There is little doubt that it is so for KCl and caffeine (Gasser, '30), while it probably is not so for the muscle "clotting" produced by injected calcium ions (Woodward, '48) or by strong electrical stimulation (Speidel, '39).

In a twitch or tetanus of normal muscle, the conducted activity in the membrane somehow activates the contractile system. Whether this is accomplished by the eddy currents which result from membrane activity or by the activity per se is not established, but several lines of evidence militate against a local current mechanism. Kuffler ('46) pointed out that since contracture-producing substances depolarize all points almost simultaneously, no local currents should flow. Moreover, depolarization as such need not occur, since, as mentioned, contracture can occur without depolarization. High potassium (23 mg % in Ringer) initially increases and then depresses the peak twitch tension but progressively decreases the action potential height (Sandow, '50). This dissociation also speaks against local currents as the effective agent in contraction activation; but there is no a priori reason for the action potential height to correlate with the magnitude of the local current (the magnitude of the first derivative, at the first inflection, of the monophasic action potential should correlate) and, according to Hill ('51) the peak twitch tension should change with twitch duration even with unaltered contractile activation. A final indication that local currents do not activate contraction is the observation (Jenerick and Gerard, '53) that excitation of the membrane, by square pulses between inside and outside electrodes, occurs in fresh muscle with normal membrane potential at strengths well below those that produce local contraction. If the exponentially rising current in the normal action potential behaves like a constant current pulse, the threshold for propagation would be reached before the local current could activate the contractile mechanism, and in the excited region the local current through the membrane is inwardly directed, which usually causes relaxation.

The suggestion of Bay and Szent-Györgyi ('51), that the longitudinal potential fields inside the fiber during the action potential are directly coupled to the contractile process, is untenable. As Graham and Gerard ('46) showed, and as now confirmed with the finer electrodes, no excitation occurs with the internal electrode as cathode, with respect to an outer diffuse electrode, at currents 200 times the threshold value for an internal anode. The longitudinal currents have approximately the same distribution in the two cases, while being in opposite directions. The rectifying properties of the membrane cannot overcome this difficulty, since calculation shows that the maximum longitudinal potential gradient in the vicinity of an internal electrode is independent of the membrane properties. This longitudinal gradient will fall off more rapidly with distance from the electrode if the membrane resistance is small (cathodal polarization) than if it is large (anodal polarization); so if longitudinal potential fields produce contraction, the anodal (internal cathodal) situation should be optimal, which is just the reverse of the facts. A further, very simple, experiment demonstrates the same thing. If current is passed between two external electrodes widely separated on a muscle, near either electrode the current through the membrane of a fiber would be quite symmetrical around the electrode. The internal longitudinal fields of potential, on the contrary, far from being symmetrical, would have the maximal gradient between, not near, the electrodes. Yet the local contracture occurs in the vicinity of the cathode and is reasonably symmetrical. The situation is comparable for anodal contracture following the cessation of current, as in the present experiments and others (Katz, '49). Any theory of contraction activation which assigns longitudinal potential fields or currents a major role is thus excluded. It would appear, then, that the normal contraction activating link is the membrane excitation as such, not the depolarization or the local currents associated with it.

Electrically induced contractures occur only in relation to a membrane region through which current is flowing out or has been flowing in. An apparent exception in the retrolingual membrane, an external microelectrode exciting when anode (Gelfan, '39), is probably due to nearby virtual cathodes. The membrane may be unexcited, or inexcitable, in the usual sense and still be an integral part of the mechanism of contraction activation. The electrically-induced contractures, under such conditions, are not examples of direct stimulation of the contractile system, as often supposed, but still involve membrane action. Some chemicals may act through this same step, others on a step still further along in the chain of events. Identification of such separate points of action by various agents would contribute greatly to an understanding of the mechanism coupling excitation to contraction.

It is generally accepted that ordinary tetanic fatigue results from membrane inexcitability rather than from exhaustion of energy reserves (Gasser, '30). This membrane inexcitability is readily accounted for by the post-tetanic membrane potential fall (Jenerick and Gerard, '53), which is proportional to and presumed a consequence of, the concurrent breakdown of CrP (Ling and Gerard, '49). Superficially, the present finding, of no post-electrical contracture membrane potential changes, seems to be in conflict, as is the further finding that cathodal polarization, continued beyond the time of visible contracture, results in a progressive breakdown of CrP (Taylor and Abood, '52). CrP breakdown per se, however, might result in a membrane potential change or not, depending upon whether the phosphate released remained in free solution or was reesterified. Since it is hardly likely that the system would be in equilibrium if free phosphate accumulated, the amount of membrane potential change would depend upon the permeability of the muscle membrane to the ions involved and no conclusion is possible at present.

SUMMARY

The action potential spike of the frog sartorius muscle was measured with an intracellular electrode. This must be sufficiently fine and flexible to avoid displacement during the twitch, else electrical artifacts accompany movement.

A large negative after potential is present, but no true potential changes appear with the mechanical part of the twitch. Post-anodal contractures and cathodal contractures, measured when the accommodating muscle had relaxed during the maintained flow of current, showed no potential concomitant, nor is there a break in the time course of membrane potential change due to caffeine when contracture occurs or when it becomes maximal.

It is concluded that no potential change is associated with the operation of the contractile mechanism.

No change occurs in potential following a cathodal contracture induced by applied currents even ten-fold those initially producing contracture and even lasting three minutes.

A chamber is described, in which the above observations on polarization were made, whereby a trans-membrane current may be applied in a relatively uniform manner over about 90% of the frog sartorius. In such experiments it is clear that a constant current contracture occurs only in that region of a muscle fiber where the applied current is flowing outward through the surface membrane. The contracture is not related to the magnitude of the longitudinal currents, or fields, inside the fiber. It follows that the applied current does not act on the contractile substances directly, but via the membrane.

The relation of these findings to the mechanism coupling excitation and contraction is discussed. Present evidence indicates that neither the local currents nor the depolarization as such links the action potential to the contraction.

The membrane potential falls after a tetanus but not after an electrical contracture. Consideration shows no necessary conflict between these results and the suggestion of Ling and Gerard ('49) that the post-tetanic creatine phosphate breakdown is the cause of the potential fall.

ACKNOWLEDGMENT

The author is happy to express his indebtedness to Prof. R. W. Gerard for his advice and encouragement during the course of this work.

LITERATURE CITED

ARBEITER, W. C. A. 1920 Phenomènes méchaniques et électriques dans le coeur de la grenouille après soustraction de Calcium. Arch. Néer. de Physiol., *5:* 185.

BAY, Z., AND A. SZENT-GYÖRGYI 1951 "Window fields" in muscle. Nature, *167:* 482.

BERITOFF, J. S., AND D. WORONZOW 1926 Die elektrische Reaktion des Muskels bei Kontraktur. Zeit. Biol., *84:* 417.

BIEDERMANN, W. 1896 Electrophysiology, Vol. 1. Transl. by F. A. Welby, Macmillan, New York.

BISHOP, G. H., AND A. S. GILSON, JR. 1927 Action potentials accompanying the contractile process in skeletal muscle. Am. J. Physiol., *82:* 478.

BOGUE, J. YULE, AND RAFAEL MENDEZ 1930 The relation between the mechanical and electrical response of the frog's heart. J. Physiol., *69:* 316.

BOYLE, P. J., AND E. J. CONWAY 1941 Potassium accumulation in muscle and associated changes. J. Physiol., *100:* 1.

BUCHTHAL, FR., AND T. PETERFI 1934 Die Potentialdifferenzen einzelner lebender Muskelfasern im Ruhezustand und während der Kontraktion. Pflüg. Arch. ges. Physiol., *234:* 527.

BREMER, F. 1932 Researches on the contracture of skeletal muscle. J. Physiol., *76:* 65.

BURDON-SANDERSON, J. 1895 The electrical response to stimulation of muscle and its relation to the mechanical response. J. Physiol., *18:* 117.

EINTHOVEN, W. 1924 The relation of mechanical and eletrical phenomena of muscular contraction with special reference to the cardiac muscle. Harv. Lect., *20:* 111.

ENGLEMAN, T. W. 1870 Beiträge zur allgemeinen Muskel- und Nervenphysiologie. Pflüg. Arch. ges. Physiol., *3:* 247.

FATT, P., AND B. KATZ 1951 An analysis of the end-plate potential recorded with an intracellular electrode. J. Physiol., *115:* 320.

FISCHER, E. 1924 Die elektrischen Erscheinnungen des quergestreiften Muskels während der Einwirkung von contracturezeugenden Substanzen. Pflüg. Arch. ges. Physiol., *203:* 580.

FULTON, J. F. 1926 Muscular contraction and reflex control of movement. The Williams and Wilkins Co., Baltimore.

VON FREY, M. 1909 Allgemeine Physiologie der quergestreiften Muskeln. Nagel's Handbuch d. Physiol. d. Menschen, Bd. 4, 427.

GASSER, H. S. 1930 Contractures of skeletal muscle. Physiol. Rev., *10:* 35.

GELFAN, S. 1933 The submaximal response of the single muscle fiber. J. Physiol., *80:* 285.

GELFAN, S., AND G. H. BISHOP 1932 Action potentials from single muscle fibers. Am. J. Physiol., *101:* 678.

GELFAN, S., AND R. W. GERARD 1930 Studies of single muscle fibers. II. A further analysis of the grading mechanism. Am. J. Physiol., *95:* 412.

GERARD, R. W., AND G. LING 1948 The membrane potential of single muscle fibers. (Abstract) Am. J. Physiol., *155:* 437.

GRAHAM, J., AND R. W. GERARD 1946 Membrane potentials and excitation of impaled single muscle fibers. J. Cell. and Comp. Physiol., *28:* 99.

HILL, A. V. 1951 The transition from rest to full activity in muscle: the velocity of shortening. Proc. Roy. Soc. Lond. (B), *138:* 329.

JENERICK, H. J., AND R. W. GERARD Preceding paper.

KATZ, B. 1948 The electrical properties of the muscle fiber membrane. Proc. Roy. Soc. Lond. (B), *135:* 506.

——— 1949 Les constants électriques de la membrane du muscle. Arch. Sci. Physiol., *3:* 285.

KUFFLER, S. W. 1946 The relation of electric potential changes to contracture in skeletal muscle. J. Neurophysiol., *9:* 367.

LEE, F. S. 1887 Ueber die elektrischen Erscheinungen, welche die Muskelzukung begleiten. Arch. f. Physiol. (du Bois Reymond): 204.

LING, G., AND R. W. GERARD 1949 The membrane potential and metabolism of muscle fibers. J. Cell. and Comp. Physiol., *34:* 413.

LIU, Y. M., C. H. HSU AND T. P. FENG 1948 Electric potential change accompanying the development of rigor in IAA poisoned muscle. Nature, *162:* 962.

LUCAS, K. 1907 On the rate of variation of the exciting current as a factor in electrical stimulation. J. Physiol., *36:* 253.

DE MEYER, J. 1921 Sur les courants de deformation des muscles. Arch int. Physiol., *16:* 64.

NASTUK, W. L., AND A. L. HODGKIN 1950 The electrical activity in single muscle fibers. J. Cell. and Comp. Physiol., *35:* 39.

RIESSER, O. 1936 Vergleichende Muskelphysiologie. Ergebn. Physiol., *38:* 133.

ROSENBLUETH, A., AND J. G. RAMO 1944 Electrogramas del Nervio y de los Musculos. Arch. Inst. Cardiol. (Mexico), *14:* 12.

SANDOW, A. 1950 The latent period of muscular contraction. Arch. Phys. Med., *31:* 367.

SCHAEFER, H. 1940 Electrophysiologie. Wien: F. Deuticke.

SCHÜTZ, E. 1936 Elektrophysiologie des Herzens bei einphasischer Ableitung. Ergebn. Physiol., *38:* 493.

SCHENK, F. 1895 Untersuchungen über die Natur einiger Dauercontractionen des Muskels. Pflüg. Arch. ges. Physiol., *61:* 494.

SPEIDEL, C. C. 1939 Studies of living muscles. II. Histological changes in single fibers of striated muscle during coagulation and clotting. Am. J. Anat., *65:* 471.

TAYLOR, R. E. 1952 The distribution of membrane current in nerve with longitudinal linearly increasing applied current. Bull. Math. Biophys., *14:* 265.

TOBIAS, J. M. 1950 Injury and membrane potentials in frog muscle after depleting potassium and producing other changes by soaking in potassium free salt solution or distilled water. J. Cell. and Comp. Physiol., *36:* 1.

WOODWARD, A. A., JR. 1948 Protoplasmic clotting in isolated muscle fibers. J. Cell. and Comp. Physiol., *31:* 359.

WUNDT, W. 1859 Ueber den Verlauf der Muskelzusammenziehung bei directer Muskelreizung. Arch. f. Anat. Physiol. u. Wiss. Med., p. 549.

THE ORIGIN AND NATURE OF GRANULES FOUND IN MACROPHAGES OF THE WHITE MOUSE FOLLOWING INTRAVENOUS INJECTION OF THOROTRAST[1, 2]

EUGENE BELL
Arnold Biological Laboratory, Brown University, Providence, R. I.

FOUR FIGURES

INTRODUCTION

Thorium dioxide, when injected intravenously in the form of Thorotrast into the mouse, is eventually stored in the macrophages as visible granules. The present report is concerned with processes involved in the formation of these granules.

After injection Thorotrast remains only briefly in the circulation. Maxfield and Mortensen ('41) made determinations on the rate of removal of the radioactive material from the blood of the white rat and found no trace of ThO_2 after 8 hours. Recent studies (Easton, '52; Wilson and Leduc, '50) have considered Thorotrast distribution and related macrophage movements, indicating that small amounts may be redistributed or eliminated as macrophages laden with granules move about.

Observations on the granules themselves were made by Hugenin et al. ('31) who noticed that Thorotrast was de-

---

[1] I gratefully acknowledge the help of Dr. J. Walter Wilson, Chairman of the Department of Biology, Brown University, whose suggestions and counsel throughout the course of this investigation have been invaluable. Dextrin and Thorotrast were obtained through the kindness of the Heyden Chemical Corporation of New York.

[2] This work was supported in part by a grant from the National Cancer Institute, U. S. Public Health Service administered by Dr. J. Walter Wilson.

posited in reticulo-endothelial cells in the form of fine granules, and that when treated with the aniline dye the granules stain a bright blue. It was observed in our laboratory that the granules exhibited variable staining reactions in liver sections routinely treated with Bouin's and PAS depending upon the time lapse between injection of Thorotrast and fixation. This variation in staining capacity suggested that the granules were invested with an organic matrix possibly acquired in the blood stream.

Considering modifications which a foreign material may undergo in the circulation, Tait and Elvidge ('26) suggested that fibrinogen is transformed to fibrin as a result of injecting quartz suspension. Knisely et al. ('48), discussing foreign particles in general, propose that most particles will not be phagocytized unless they are previously coated, and that the coating may in some way be related to fibrin. They also report that although heparin will not prevent macrophages from ingesting foreign particles, it will slow down the rate of blood clearance. By the technique of quartz rod illumination this group observed *in vivo* that heparin inhibits or retards but does not prevent the formation of the coating around the foreign material. Biozzi et al. ('51) suggest that fibrin is the protein which becomes associated with carbon particles after injection of India ink. They found that as they increased the dosage of India ink, blood fibrinogen and the number of platelets decreased proportionately.

In a previous study (Bell, '52) Thorotrast granules from mouse liver and spleen were separated from a homogenate by differential centrifugation.

The results of the present investigation indicate that the isolated granule (Thorotrast which has undergone modification in the circulation and probably in the macrophages as well), is rich in protein and polysaccharide. It has also been found that dextrin, present in Thorotrast as a protective colloid, is in part removed by a blood amylase and that a protein, apparently fibrin, becomes associated with thorium dioxide.

MATERIALS AND METHODS

An inbred strain of albino mice (BUC) kept at Brown University Biology department was used throughout the experiments.

A micro-adaptation of the Somogyi-Nelson blood sugar technique developed by Bloom (personal communication) was used for sugar determinations. Animals were fasted for 18 hours prior to tests. Blood samples were taken with a micropipette after snipping off the end of the tail of an animal warmed under a lamp for about a minute. After the fasting blood was taken, 0.2 cm^3 of Thorotrast was injected into the tail vein. The same quantities of dextrin, physiological saline, and India ink were injected into control animals. Dextrin was made up in sterile saline in the same concentration as it occurs in Thorotrast.[3] A filtered 25% solution of Higgins India ink in saline was also prepared.

Whole blood, for amylase activity determinations, was withdrawn by heart puncture and treated with 100 units of heparin (Roche, Organon). Thorotrast was used as a substrate in approximately the same proportion to blood as the amounts injected, i.e., 0.2 cm^3 Thorotrast in 2.0 cm^3 of blood. Reactions were carried out at 37.4°C. Samples were withdrawn at intervals shown in figure 2 and analyzed for sugar content in the same manner as blood taken from the tail vein. Assuming that the dextrin present in Thorotrast is hydrolyzed by the action of a blood amylase, the activity of the amylase was calculated in mg % of reducing sugar produced. Reducing values for Thorotrast and dextrin were also expressed in mg % so that convenient comparison could be made with the data for actual blood sugars.

The amount of ThO_2 remaining in the blood after injecting 0.2 cm^3 of Thorotrast was determined by measuring the degree of radioactivity of blood samples taken at successive intervals following injection. Where the interval was two minutes or less, the animal was sacrificed by injecting 0.2–0.4 cm^3 of air through the same needle used for injecting Thorotrast. Where the interval was longer than two minutes, the animal was etherized. Blood was withdrawn by heart puncture after cutting a window in the thorax. Two samples of 0.25 cm^3 each were taken from each animal and ashed in metal planchettes. Since maximum radioactivity could be measured after partially ashing blood samples for one hour on a hot plate, this procedure was adopted in preference to prolonged ashing in a muffle furnace. Radioactivity was measured with a Tracerlab SC 1-b Autoscaler and Geiger tube of 1.6 mg/cm^2 window thickness. The degree of phagocytosis is expressed in terms of the radioactivity of the blood at a given time after injection of Thorotrast (counts per minute less background).

---

[3] The following analysis for Thorotrast is given in the American Medical Association's Council on Pharmacy Report ('32): ThO_2, 25% by volume, 19–20% by weight; dextrin, 16–19% by weight of whole; methyl p-hydroxy benzoate, 0.15% added as a preservative; the colloid is made up in an aqueous medium.

The ThO_2 content of granules was determined as follows: Thorotrast was oven dried for 15 hours at 110°C., then ashed in a muffle furnace at 500°C. Samples were permitted to cool in a dessicator, weighed, and their radioactivity determined with the counter. A standard relationship between radioactivity and weight was established for ashed Thorotrast. The same procedure was followed for the granules which were washed 4 times in distilled water after initial separation and cleaning.

RESULTS

Modification of Thorotrast in vitro by liver homogenate, blood serum, blood plasma and enzymes

A thick whitish suspension of particulate material was observed after about 30 minutes when Thorotrast was incubated in equal amounts with liver homogenate, blood serum or plasma. After several hours a small test tube containing the mixture could be inverted without disturbing the gel which had formed. If the tube was tapped sharply a few times the gel became a sol, but if again left undisturbed for a few hours the mixture gelled. The process could be repeated over a period of several days, after which the precipitate settled out and the thixotropy was apparently lost.

By placing a drop of Thorotrast under a cover slip and a drop of blood fraction or enzyme at the edge of the slip and observing the interface of the fluids as they met, broad streams of precipitate were seen to form. If the enzymes (10% solutions of filtered pangestin and a-amylase) were inactivated by boiling, no precipitate was ever observed.

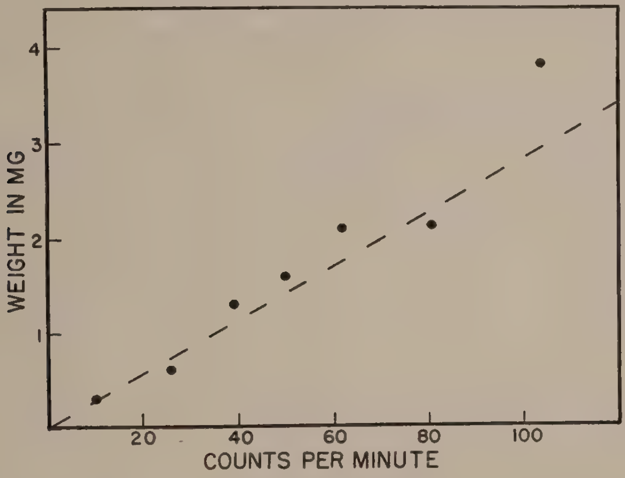

Fig. 1 The weight of ashed granules is plotted against their radioactivity. The points show deviation from the radioactivity-weight curve for ashed Thorotrast which is represented by the broken line.

Analysis of granules

To show that the radioactivity of the granules could be used as an index of their ThO_2 content, a standard curve (fig. 1) of weight in milligrams vs. radioactivity was set up for ashed Thorotrast and found to be linear in the appropriate weight range. Values for all but one of the 7 samples of ashed granules lay close to the standard curve. Upon comparing the dried and ashed weights of the granules (table 1) it was found that the weight loss averaged 23% or that approximately 77% of the granules by dry weight was thorium dioxide.

If the particle is 23% organic, then the protein nitrogen, determined by the Leitch method (Leitch, '48), which amounted to 1.1% of the granule by dry weight, represents 4.8% of the organic material. Thus approximately one-fourth of the organic portion of the dried granules would be composed of protein.

Since fibrin is soluble in sodium sulfide, granules carefully washed in sucrose and distilled water were treated with 10% Na_2S for 24 hours. After centrifugation the addition of trichloracetic acid (10%) to the supernatant resulted in the formation of a precipitate which gave a positive biuret test. Na_2S alone was not precipitated by trichloracetic acid. Although the test is not specific for fibrin, it did confirm the presence of protein in the granules.

TABLE 1

The weight loss of dried granules after ashing at 500°C.

WEIGHT OF DRY GRANULES (IN MG)	WEIGHT OF ASHED GRANULES (IN MG)	% WEIGHT LOSS
3.0	2.1	30.0
0.8	0.6	25.0
2.6	2.1	19.2
4.7	3.8	19.0
2.0	1.6	20.0
1.7	1.3	23.5
0.4	0.3	25.0

Acid hydrolysis, followed by analysis for reducing sugar, further established the presence of a polysaccharide which was already indicated by a strong PAS reaction both on the slide and in the test tube. However, it has not been determined whether the polysaccharide is dextrin.

Hydrolysis of the dextrin component of Thorotrast by blood amylase

Dextrin, present in Thorotrast as a protective colloid, is rapidly hydrolyzed (fig. 2) by a blood amylase. *In vitro* the reducing value of the blood rises sharply after a few minutes of incubation and remains above 200 mg %. The reducing value of untreated Thorotrast is extremely low (about 20 mg %) and cannot be held responsible for the four- to five-fold rise in reducing sugar.

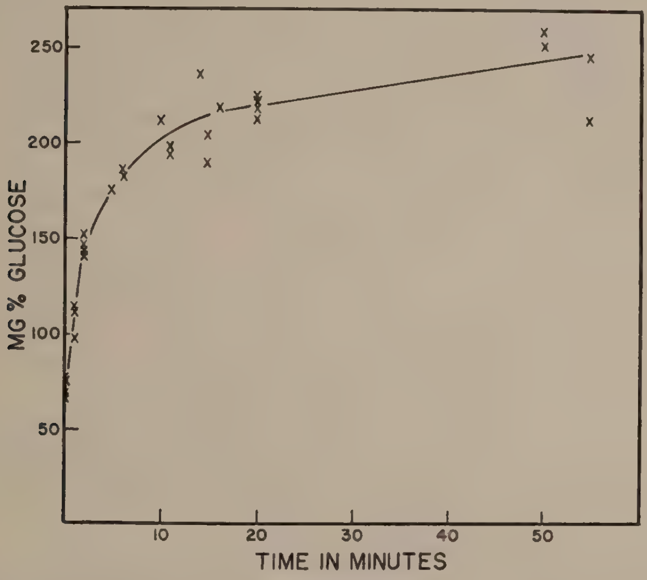

Fig. 2 The hydrolytic action of blood amylase on the dextrin component of Thorotrast is plotted against time. Enzyme activity is calculated as mg % of reducing substance (glucose) produced by the hydrolysis.

In the animal the same effect is apparent (fig. 3); by comparison with fasting blood sugar the rise is nearly four-fold after injection of Thorotrast. To insure that the effect was not a stress reaction to Thorotrast or to the act of injection itself, dextrin, India ink and saline were injected as well. The blood sugar curve for dextrin, closely paralleled the curve for Thorotrast, indicating that the response was due to dextrin and not ThO_2. The values for saline were scattered within the range of normal variations for fasting blood, while blood taken after the injection of India ink showed a decrease in sugar content.

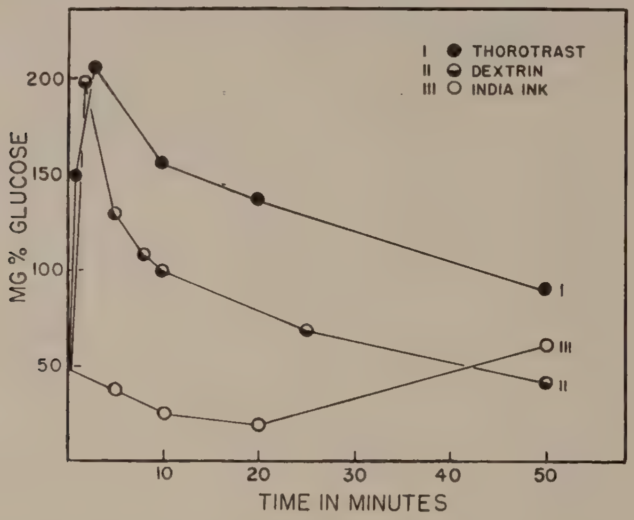

Fig. 3 The change of blood sugar values with time is shown following injection of Thorotrast into experimental animals. Blood sugar curves for control animals injected with dextrin and India ink are also shown.

The effect of heparin on the rate of phagocytosis of Thorotrast

In an initial period of about 10 minutes less than 20% of the injected Thorotrast is cleared from the circulation (fig. 4). This is followed by a very short period of intense phagocytic activity during which approximately 50% of the Thorotrast remaining in the blood is removed. The rate of clearance after about 15 minutes decreases sharply. The injection of 100 units of heparin (0.1 cm^3 Roche Organon) before administration of Thorotrast had no appreciable effect on the rate of blood clearance. However, the histological appearance of the macrophages in the liver was altered in the case of the heparin-injected animal. Normally in Thorotrast-injected animals, the ingested material will appear in the macrophages either in granular form or in the form of plaques. The plaques are homogeneous in appearance and are sometimes as large as nuclei of liver paraenchymal cells. However, in the heparinized animals these plaques appear to be completely absent, the foreign material being exclusively ingested in the form of fine granules.

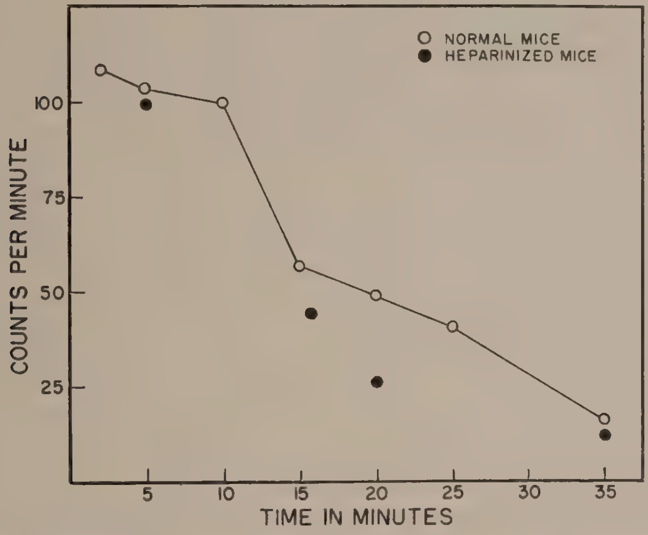

Fig. 4 Phagocytosis of Thorotrast in normal and heparinized animals is represented by the radioactivity of blood samples withdrawn at successive intervals.

DISCUSSION

Our evidence indicates that before protein becomes associated with Thorium dioxide, some part of the dextrin contained in Thorotrast as a protective colloid is "digested" off by a blood amylase. The 400% rise in blood sugar immediately following the injection of Thorotrast is a clear indication that the dextrin, which itself has a low reducing value, undergoes hydrolysis. The reduction of the protective action of dextrin leads to the liberation of ThO_2 from its stabilizing element and results in a precipitation. It is apparently at this point that the plasma proteins are brought into association with ThO_2 and that the coating which may be necessary for selective phagocytosis is formed.

Although the above events occur as soon as Thorotrast is injected, the rate of the process responsible for altering the foreign material and bringing it into association with blood elements, has a noticeable effect on the rapidity with which the particles are phagocytized. As the results indicate, during the first 10 minutes less than one-fifth of the injected material is cleared from the circulation, while in a much shorter time following this, the bulk of the ThO_2 is removed. The process by which foreign particles are coated in the circulation, probably a prerequisite for ingestion, might account for the initial delay in phagocytosis.

The absence of ThO_2 plaques in macrophages of heparinized animals can be looked upon as an effect resulting from the inhibition of fibrin formation around the colloidal masses. Knisely reports, in connection with colloidal mercuric sulphide injected into frogs, that he observed thin coatings and strands forming around masses of the injected material and that these masses are instantly engulfed by Kupffer cells when they touch the sinusoid walls of the liver. In the present instance, it is apparent from the plaque-like appearance of the foreign material in some of the macrophages of non-heparinized animals that large masses of Thorotrast are frequently captured. When this occurs, it is possible that only a surface layer of dextrin has undergone complete modification. Consequently, protein is deposited around a core of partially unaffected Thorotrast. This would account for the polysaccharide content of the granules.

Although the overall rate of phagocytosis is unaffected by heparin, the formation of a thin coating around a large mass of colloidal material is not only slowed, but probably interfered with, since the thickness of film necessary to support a heavy mass cannot be built up before the mass disperses. This would result in the formation of aggregates of small size, which in fact is the condition observed in the macrophages of the heparinized animal. Fibrin, then, may be one of the proteins found in the granule complex.

There is evidence, however, that more than one protein is involved in the granule which is ultimately found in the macrophage. Davis ('46) points out that Bennhold found Thorotrast to migrate electrophoretically with globulin and suggests that globulin may play a part in transporting the colloid to the reticulo-endothelial cells. The fact that thixotropy results from the incubation of Thorotrast with either plasma or liver homogenate may be an indication that different proteins are affected in each case. Further indication of the non-specificity of the reaction is the precipitation which is brought about by addition of Thorotrast to enzymatic proteins.

SUMMARY

1. Granules found in macrophages of the white mouse following intravenous injection of Thorotrast are shown to consist of about 77% ThO_2 and 23% organic material by dry weight. Of the 23% approximately one-fourth is protein. The granules are found to be rich in polysaccharide.

2. The first event which follows administration of Thorotrast is the hydrolysis of its dextrin component by a blood amylase. By comparison with fasting blood the rise in blood sugar is nearly four-fold a few minutes after injection. It is shown that the effect is not a stress reaction.

3. The loss of colloidal stability following the hydrolysis of dextrin incubated *in vitro* with several protein systems results in a precipitation reaction in the presence of amylase. It is suggested that when this occurs in the circulation, plasma proteins are brought into association with ThO_2 and that the coating which may be necessary for phagocytosis is formed. Evidence indicates that the protein reaction is non-specific.

4. Although the rate of phagocytosis is unaffected by heparinizing animals prior to injection of thorotrast, the histological appearance of the ingested material in the macrophages of these animals differs from that of normal indi-

viduals in that the particle size is always small. It is suggested that the absence of large masses of Thorotrast in macrophages of heparinized mice indicates that fibrin is involved in the formation of the granule in the circulation.

LITERATURE CITED

Bell, E. 1952 Enzyme activity of granules elaborated in mouse liver and spleen following intravenous injection of ThO_2. J. Nat. Canc. Inst., *13:* 240–241.

Bloom, R. A. Personal communication (thesis in preparation; Brown University).

Biozzi, G., B. Benacerraf, G. Mene and B. N. Halperin 1951 Étude Quantitative de l'Activite Gramulopexique du système Réticulo-Endothélial par l'Injection Intraveineuse d'Encre de Chine Chez les Diversas Espèces animales. Annales de l'institute Pasteur, *81:* 164–172.

Council on Pharmacy and Chemistry Report 1932 Thorotrast. J. Am. Med. Assn., *99:* 2183–2185.

Davis, B. D. 1946 Physiological significance of the binding of molecules by plasma proteins. American Scientist, *34:* 611–618.

Easton, T. W. 1952 The role of macrophage movements in the transport and elimination of intravenous thorium dioxide in mice. Am. J. Anat., *90:* 1–34.

Huguenin, R., A. Nemours and G. Albot 1931 Les hepatites et les cirrhoses experimentales au bioxyde de thorium. C.R. de la Soc. de biol., *108:* 879–881.

Knisely, M. H., E. H. Bloch and L. Warner 1948 Selective Phagocytosis I. Det Kgl. Danske Vidensk. Selskab, Biol. Skrifter, *4:* 1–93.

Leitch, V. C. 1948 Nessler method of nitrogen determination. Franklin Institute Journal, *245:* 355–359.

Maxfield, F. A., and O. A. Mortensen 1941 Use of the radioactive properties of thorium for a quantitative study of phagocytosis. J. App. Physics, *12:* 197–202.

Tait, J., and A. R. Elvidge 1926 Effect upon platelets and on blood coagulation of injecting foreign particles into the blood stream. J. Physiol., *62:* 129–144.

Wilson, J. W., and E. H. Leduc 1950 Movements of macrophages studied with the use of Thorotrast. J. Nat. Canc. Inst., *10:* 1348–1349.

THE EFFECT OF OXYGEN UPON THE IMMOBILIZATION REACTION IN FIREFLY LUMINESCENCE[1]

J. WOODLAND HASTINGS,[2] WILLIAM D. McELROY
AND JANE COULOMBRE
*McCollum-Pratt Institute and Department of Biology,
The Johns Hopkins University, Baltimore, Maryland*

FIVE FIGURES

INTRODUCTION

Light production in firefly extracts depends upon luciferin, luciferase, an inorganic ion (Mg^{++} or Mn^{++}), adenosine triphosphate and oxygen (McElroy, '51a, b; McElroy and Strehler, '49a). When these components are mixed in optimum concentrations, an initial flash of light occurs which decays in about one minute to a low "basal" level at 5 to 15% of the initial flash intensity. Various factors which cannot be discussed here affect the rate at which the decay occurs and the basal intensity level which is reached. It has been demonstrated, however, that no measurable quantity of any of the reactants is utilized during this decay period (McElroy, '51b). If an additional quantity of enzyme is added to the system following the decay, a second response, similar to the first, is obtained, indicating that adequate concentrations of ATP, luciferin and ions are still present and are available for light production (McElroy, Coulombre and Hastings, unpublished). On the basis of this and other data, it has been proposed that the enzyme forms an intermediate complex with ATP, luciferin and Mg^{++} which reacts with molecular oxygen to form an excited state that subsequently decomposes to emit a quantum of light. A schematic representation of this idea is presented in figure 1.

---

[1] Contribution no. 39 of the McCollum-Pratt Institute.

[2] Post-Doctoral Fellow, Atomic Energy Commission.

The fact that the light intensity declines to such a low level during the first two minutes is attributed to the formation of an inactive intermediate which immobilizes the enzyme. Present indications are that the inactive complex differs from the active intermediate by an increased number of inorganic ions and protein molecules in the complex. Thus, when all the reactants required for light emission are mixed, the velocity of the reaction rapidly drops to a fraction of its initial rate without any appreciable utilization of the reactants.

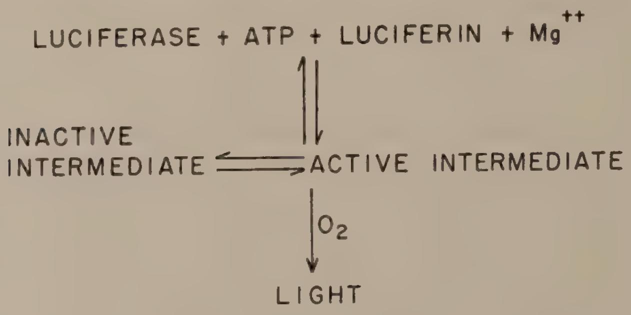

Figure 1

Since previous studies (McElroy, '51b) have shown that the formation of the inactive intermediate requires luciferin, ATP, luciferase, and Mg^{++}, it was of interest to determine whether or not, in the absence of oxygen, the inactive intermediate would be formed. Secondly, since previous studies indicate that it is the oxidative process which leads to the activation and subsequent light emission, a study of the effect of oxygen on a chemiluminescent reaction which requires ATP would be of particular interest. Previous studies on bioluminescent reactions where it has not been possible to show the participation of ATP have indicated that this oxidative reaction occurs following the formation of an intermediate enzyme-substrate-oxygen complex (Hastings, '52a, '52b). Apparently in the firefly ATP is required for the complex formation before the oxidative reaction takes place. While luminescence still persists at very low oxygen concentrations (5% of steady state intensity at 3×10^{-6} Atm. oxygen), there is no evidence for light production under conditions where oxygen is rigorously excluded.

MATERIALS AND METHODS

The luciferin and luciferase were purified from dried, frozen lanterns of the firefly, *Photinus pyralis*, by slight modifications of methods previously published (McElroy and Coulombre, '52). A crude extract of luciferase was prepared by extracting 13 gm of acetone powder of lanterns three times with cold water. The luciferase was partially purified by adsorption upon calcium phosphate gel. Several water washings of the gel removed the luciferin. The luciferase was subsequently eluted with 7% $(NH_4)_2SO_4$, precipitated with 60% $(NH_4)_2SO_4$, and finally redissolved in 150 ml of water. The luciferin was purified from the gel washings by prolonged dialysis and subsequent concentration by distillation. Additional purification of the luciferin was achieved by extraction with ethyl acetate and finally concentrating in water. The reaction mixture for light production consisted of 0.1 ml luciferase, 1 ml luciferin, 1 ml of 0.01 M $MgSO_4$ and 1 ml of 0.004 M ATP, made up to a volume of 20 ml with 0.05 M glycine buffer, pH 8.

The techniques for controlling oxygen concentration were essentially those described earlier (Hastings, '52a). Gas mixtures containing known oxygen concentrations were prepared by mixing hydrogen, rigorously purified over hot platinized asbestos, with small quantities of electrolytically produced oxygen. The various gas mixtures were continuously bubbled through the reaction mixture by means of a sintered glass disc so that the water phase was in equilibrium with the gas phase. Light intensity was measured by means of a newly designed and constructed multiplier phototube apparatus which has a sensitivity range of 10^6 and is accurate to better than 0.5%. The readings were recorded on moving paper by means of an Esterline Angus Graphic recorder which is accurate to within 2%. Rapid flashes were observed on a cathode ray oscilloscope and photographed for permanent records.

RESULTS

When a reaction mixture which has reached the basal steady state intensity is deaerated with purified hydrogen, the light goes out within a minute or two after deaeration is begun. When air or oxygen is readmitted to this solution, an extremely bright flash of light appears with a maximum intensity between 50 and 75 times the steady state level. The flash is very brief, of about one second duration, and quickly returns to the steady state level. Figure 2 shows an oscilloscope photograph of such a flash. In some cases the curve is symmetrical; in others the rise is somewhat steeper than the fall. The latter cases are attributed to experimental conditions where the oxygen was admitted particularly rapidly. The flash, as observed in these experiments, had a duration of the order of from one to three seconds. The above procedure may be repeated as often as is desired using the same reaction mixture and the same qualitative result is obtained. In practice the luminescence becomes very dim after 10 to 20 minutes, as a result of surface denaturation of the enzyme through bubbling. The flash phenomenon is interpreted as

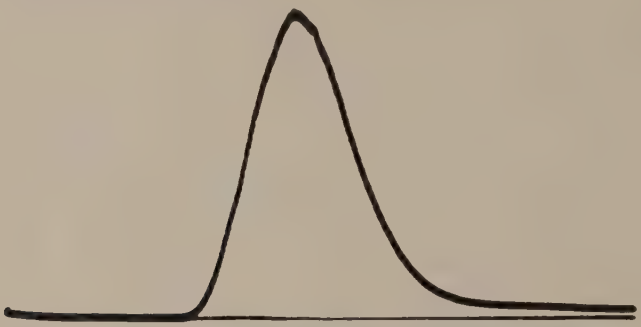

Fig. 2 Photograph of oscilloscope screen. Ordinate light intensity, abscissa time. Total time of sweep, 7 seconds. Oxygen added to reaction mixture to start reaction. See text for details.

being due to the accumulation of an active intermediate which, during the steady state condition under aerobic conditions, is present in only relatively low concentrations. The reaction of the active intermediate with oxygen is an extremely fast reaction for upon the admission of oxygen to such a system this active intermediate is rapidly utilized and gives rise to the flash.

If the reaction mixture is deaerated with gas mixtures of lowered oxygen concentration instead of pure hydrogen, it can be observed that the height of the flash increases with lower oxygen concentrations. Table 1 gives typical results from such an experiment where all factors except the oxygen concentration are identical. From this type of experiment it appears that the flash intensity is maximum at or below 0.001% oxygen.

TABLE 1

Intensity of the flash which occurs when air is admitted to a luminescent solution which has been maintained under different oxygen concentrations. Intensity is given in light units. Control level of luminescence in this case was 1.6 light units.

PER CENT OXYGEN	FLASH INTENSITY
0.00028	87
0.00071	102
0.0016	75
0.0049	40
0.0097	52
0.024	30
0.052	16
0.12	9.2
0.25	4.6
0.53	3.2
1.8	1.7

Two methods were used in order to get quantitative data on the relation between steady state light intensity and the oxygen concentration in solution. The first was done by taking a reaction mixture which had reached the basal light intensity level and deaerating with a lowered oxygen concentration (instead of pure hydrogen) as shown in figure 3. As the gas stream containing 0.024% oxygen is bubbled through the solution, the light intensity decreases and goes through a minimum before leveling off at a steady state level for that oxygen concentration. The increase following the minimum is interpreted as being the result of an increased accumulation of the active intermediate under low oxygen concentration. The time for the re-establishment of steady state conditions is of the order of one minute, approximately the same time as is required for the system to come into the steady state condition when the reactants are initially mixed. When

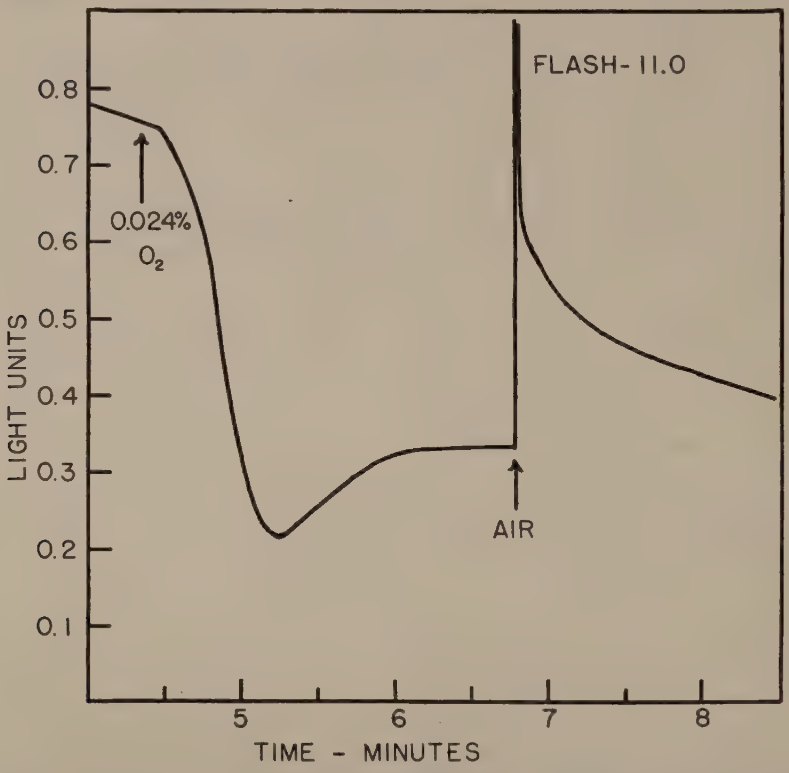

Fig. 3 Effect of changing oxygen concentration in reaction mixture upon light intensity. Ordinate light, abscissa time from start of reaction when reactants were mixed. See text for details.

air is subsequently admitted, a flash is obtained which is about 15 times as bright as the steady state intensity, not so bright as would be expected if the system had been under strict anaerobic conditions. By extrapolation an estimation may be made of the amount by which the intensity is decreased during the steady state conditions under this particular oxygen concentration.

The second method for obtaining data concerning the relation between oxygen concentration and light intensity is as follows. Instead of deaerating the system after the steady state period had been reached, the system was equilibrated with various lowered oxygen concentrations before initiating the reaction with the enzyme (luciferase). The particular gas mixture was bubbled continuously, and the light intensity was measured continuously after the luciferase was added to start the reaction. Under control conditions, i.e., when air is used for the equilibrating gas, the complexing is considered complete within two and one-half minutes from the start of the reaction. In figure 4, the intensities observed at this time have been plotted with respect to the oxygen concentrations under which the reaction had been proceeding. When these data are compared to data obtained by the first method described above, very good agreement is obtained. This fact is regarded as good evidence that the complexing reactions do in fact proceed independently of the oxygen concentration involved. Had the lowered oxygen affected the binding of the enzyme in one way or another, it would be surprising if the two methods for obtaining the relation between oxygen concentration and light intensity would give the same results.

Two additional observations support this conclusion. First, in the above series of experiments air is admitted to the various reaction mixtures following the reading at two and one-half minutes. The typical flash is observed, after which the intensity returns to the low steady state level. In all cases, irrespective of the oxygen concentration used, the intensity in air returns to a level which corresponds to the intensity of the control reaction in air at the same time after the start of the reaction. Second, if all the components of the reaction are mixed under strictly oxygen-free conditions and air admitted at various time intervals after mixing, the intensity to which the reaction mixture returns after the flash again corresponds to the intensity level which the control reaction had arrived at in the same time (fig. 5). If the reactions which lead to the formation of the inactive intermediate did not occur under oxygen-free conditions, one would expect that the reaction would proceed as the control from the time air is first admitted.

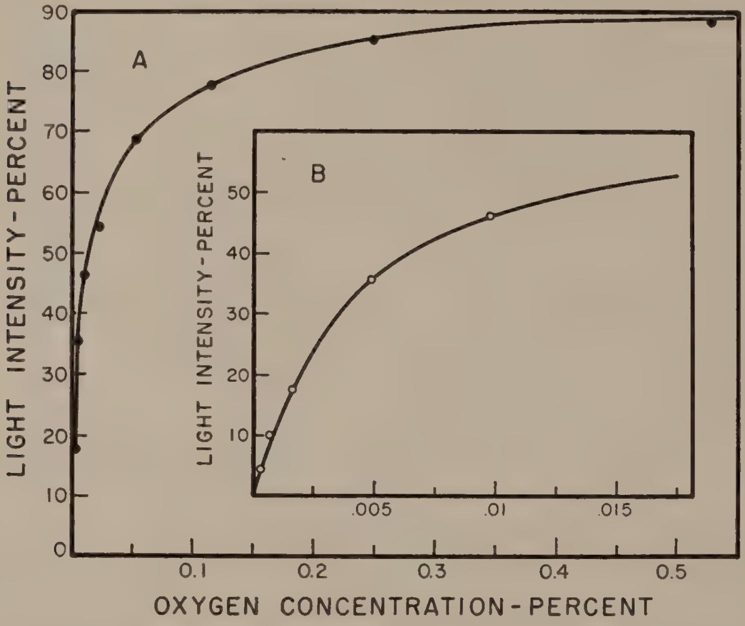

Fig. 4 Plot of light intensity against oxygen concentration. Light intensity is given as per cent of control intensity (in air), all measurements made two and one-half minutes after mixing reactants. A: over range to 0.6% oxygen, B: expansion of lower part of scale to show curve relationship at low oxygen concentrations.

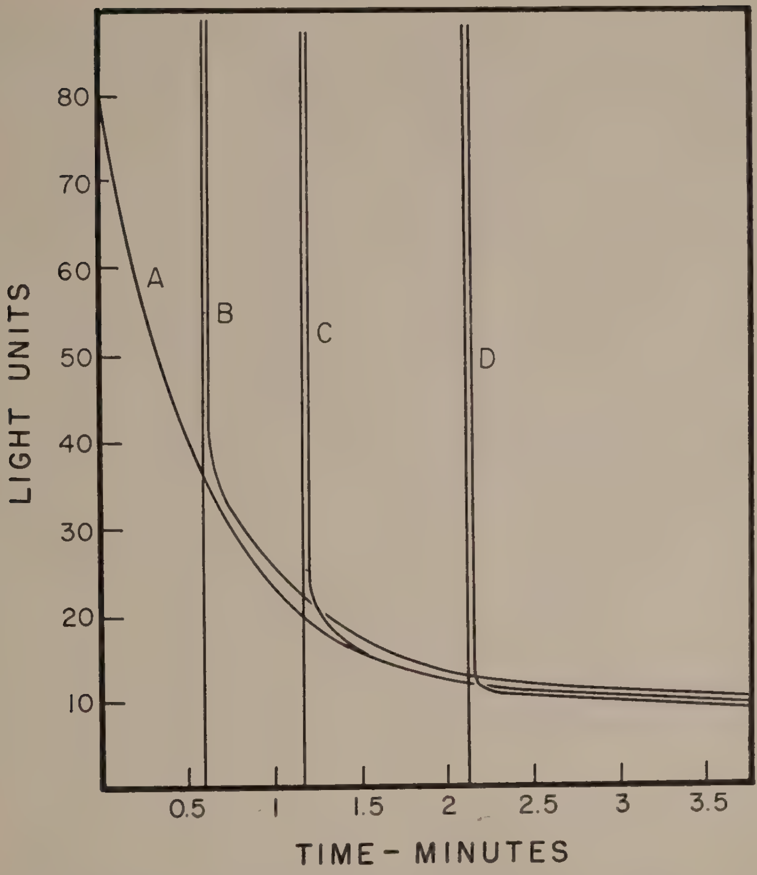

Fig. 5 Effect of mixing reactants anaerobically and adding oxygen at different time intervals. Ordinate, light intensity, abscissa time. Curve A is a control run in air. In curves B, C, and D, reactants were mixed anaerobically and air was added to start reaction at the time intervals shown. Initial flash is brighter and faster than may be shown here, but has the same shape as the one shown in figure 2.

DISCUSSION

The results presented above can be seen to lend additional support to the scheme outlined in the introduction. In particular, it seems certain that the enzyme is bound into some sort of inactive complex. The experiments last mentioned are equivalent to changing the order of addition of the components of the reaction. If either ATP, LH_2, or LH_2ase are added last, the reaction proceeds as the controls shown in figure 5. If oxygen is added last, however, the intensity level, following the very short flash, depends upon the time which the other components have been incubated. The fact that the very bright flash occurs upon the admission of oxygen appears logical since, under the scheme outlined, it might be expected that in the absence of oxygen a higher concentration of the active intermediate would accumulate than under steady state conditions with oxygen not limiting.

The quantitative relationship between oxygen concentration and light intensity also lends support to the scheme given above. If the reaction occurred by the formation of an active intermediate followed only by the oxidative reaction, the relationship between O_2 and light intensity would be expected to have the shape of a rectangular hyperbola (see Hastings, '52a). A more detailed conclusion from the quantitative aspects of the relationship is not possible at the present time since several factors — in particular the activating metal — can be shown to change this relationship. The data do, however, provide a good idea of the concentrations of oxygen which are effective in limiting light production as well as the concentrations which are required for a flash to take place upon the readmission of oxygen (table 1).

One cannot fail to remark how striking is the resemblance between the flash obtained in this manner and the flash normally exhibited by the live firefly (Snell, '32; Alexander, '43). Many workers in the past have offered the suggestion that the firefly regulates flashing by liberating oxygen into the photogenic cells. The various hypotheses in this regard need not be discussed here.[3] A more detailed study of the factors which affect the oxygen flash is being undertaken and will be published subsequently. For the present, we feel that it is important to point out certain general characteristics of the firefly reaction which the present study reveals.

---

[3] A detailed account of the numerous studies and discussions of the firefly flash may be found in Harvey's ('52) monograph.

First, under the conditions in the laboratory, where the components of the reaction have been separated and partially purified before being added back together, the reaction does not proceed at anywhere near its maximum rate. This is also evidently true in the intact organism when flashing is not taking place. With the exception of oxygen, the components which must be present for the light reaction to occur at all are precisely those components which are required for the formation of the inactive complex which results in this very low light production. Thus, for a maximal or near maximal light production to occur — such as most likely occurs when the firefly flashes — this inactive intermediate must in some way be "broken," so that high concentrations of the active intermediate are available for reaction with oxygen. The present study shows that by limiting or excluding oxygen this inactive intermediate may in fact be "broken" very adequately. For the active intermediate to accumulate, the oxygen need only be excluded from the reactants, resulting in a new equilibration between the active and inactive intermediates. For the light intensity to return to its low basal level after oxygen has been added, the active intermediate which was present at the time oxygen was admitted need only be utilized in its very rapid reaction with oxygen.

Should we propose that flashing in the intact firefly, which is ultimately under nervous regulation, is controlled in the organ by oxygen, we must then visualize (a) that there is some very efficient and rapid mechanism for removing oxygen from the photogenic cells and that (b) there is some mechanism under nervous control which can very rapidly bring back the oxygen concentration in solution to a fairly high level. From the present study it would appear that a concentration of the order of 5 to 10% oxygen would have to be reached within less than one-thirtieth of a second. With reference to point (a) it can be recalled that numerous species of fireflies produce flashes in rapid succession, one flash following the previous one by less than one second (see Harvey, '52), so that oxygen removal would not only have to be complete but also fast. It should also be pointed out that the time for the flash in solution to occur is of the order of 5 to 15 times as long as the typical flash of the intact firefly. While this in itself is not too serious a drawback, still the flash in solution appears more like the pseudoflash[4] first described by Snell ('32), later by Alexander ('43), and confirmed in our laboratory.

While the conditions specified above appear to be such that it would be unlikely that oxygen could serve as the controlling mechanism in the intact firefly, still the experiments are of value in giving us a better idea of the general characteristics of the reaction. The system is a rather interesting, if not an exceptional one, where all the components of the reaction may be present without any appreciable reaction occurring. For the reaction to occur, the components must be displaced from an inactive to an active intermediate complex, the latter of which will react with oxygen in the last step before the formation of an excited electronic state. The exclusion of oxygen is one condition under which a temporary high concentration of the active intermediate may occur. However, numerous inorganic and organic pyrophosphate compounds are also able to displace the inactive to the active form (McElroy, '51). When sodium triphosphate, for example, is added to a system luminescing at a low intensity, a temporary increase in light intensity results. While the flash which results from the addition of these compounds does not simulate the firefly flash closely, still they appear to be likely examples of how such compounds might function.

SUMMARY

The bioluminescent reaction in the firefly *Photinus pyralis* requires in partially purified extracts at least 5 components, luciferin, luciferase, adenosine triphosphate, an inorganic ion and oxygen. When these components are mixed together the

---

[4] If a live firefly is put under partially anaerobic conditions (0.2–0.5% oxygen), a flash, called the pseudoflash, is observed following the readmission of air, which has a duration of about 10 times that of the normal flash.

light intensity, which is presumed to be proportional to the overall reaction velocity, decreases to about 5–15% of its initial intensity within about one minute. Previous studies have shown that this decrease does not come about by the utilization of any of the reactants but rather as the result of a complexing reaction which binds the enzyme in an inactive form. The experiments reported have shown that if the components in the system are mixed anaerobically, no light appears but the reactions which result in the formation of the inactive intermediate proceed in the same manner as in the control. It has been further shown that the removal of oxygen from the system at any time results in the formation of a high concentration of an active intermediate which reacts oxidatively when air is admitted to give a bright flash, similar to the flash of the intact firefly. The conditions under which this flash may occur are described and the possibility that oxygen may function in the flashing mechanism in the intact firefly is discussed. The effect of lowered oxygen concentrations upon the steady state light intensity in extracts has been described. An oxygen concentration of about 0.01% decreases the light intensity by about 50%.

ACKNOWLEDGMENTS

We would like to express our appreciation to Prof. John Hervey, Dr. Edward MacNichol and Mr. Jay Jacobs for their help in the design and construction of the multiplier phototube assembly.

LITERATURE CITED

Alexander, R. S. 1943 Factors controlling firefly luminescence. J. Cell. and Comp. Physiol., *22:* 51–70.

Harvey, E. N. 1952 Bioluminescence. Academic Press, Inc., New York.

Hastings, J. W. 1952a Oxygen concentration and bioluminescence intensity. I. Bacteria and fungi. J. Cell. and Comp. Physiol., *39:* 1–30.

——— 1952b Oxygen concentration and bioluminescence intensity. II. Cypridina hilgendorfii. J. Cell. and Comp. Physiol., *40:* 1–9.

McElroy, W. D. 1951a Properties of the reaction utilizing adenosine triphosphate for bioluminescence. J. Biol. Chem., *191:* 547–557.

—— —— 1951b Phosphate bond energy and bioluminescence in Phosphorus Metabolism, Vol. I, edited by W. D. McElroy and H. B. Glass, Johns Hopkins Press, Baltimore.

McElroy, W. D., and B. L. Strehler 1949 Factors influencing the response of the bioluminescent reaction to adenosine triphosphate. Arch. Biochem., *22:* 420–433.

McElroy, W. D., and Jane Coulombre 1952 The immobilization of adenosine triphosphate in the bioluminescent reaction. J. Cell. and Comp. Physiol., *39:* 475–486.

Snell, P. A. 1932 The control of luminescence in the male lampyrid firefly, *Photuris pennsylvanica*, with special reference to the effect of oxygen tension on flashing. J. Cell. and Comp. Physiol., *1:* 37–51.

BIOCHEMICAL AND PHYSIOLOGICAL DIFFERENTIATION DURING MORPHOGENESIS

XVI. CYTOCHROME OXIDASE, SUCCINIC DEHYDROGENASE AND SUCCINOXIDASE IN THE DEVELOPING CEREBRAL CORTEX AND LIVER OF THE FETAL GUINEA PIG [1]

LOUIS B. FLEXNER, ELSTON L. BELKNAP, JR.,[2] AND
JOSEFA B. FLEXNER

Department of Anatomy, School of Medicine, University of Pennsylvania,
Philadelphia, and Department of Embryology,
Carnegie Institution of Washington,
Baltimore, Maryland

SIX FIGURES

Evidence is now at hand that the period between the 41st and 45th days of gestation (term 66 days) is critical in the differentiation of the nerve cells of the frontal cerebral cortex of the fetal guinea pig. During this time the enzymes adenyl pyrophosphatase (Flexner and Flexner, '48) and less clearly cholinesterase (Kimel and Kavaler, '52) have been found to begin to increase to the adult level, there is evidence of change in permeability of the cell membrane (Flexner and Flexner, '49), and these biochemical changes have been correlated with a series of cytological changes (Peters and Flexner, '50) and with the first evidence of functional differentiation (Flexner, Tyler and Gallant, '50; Kimel and

---

[1] This investigation was supported by a research grant from the Division of Research Grants and Fellowships of the National Institutes of Health, U. S. Public Health Service, and by a grant from the American Cancer Society recommended by the Committee on Growth of the National Research Council.

[2] Henry Strong Denison Scholar for 1948–49, Johns Hopkins University School of Medicine.

Kavaler, '51). The evidence is less clear and less extensive for the liver of the fetal guinea pig but suggests that adenyl pyrophosphatase and acid phosphatase begin to increase in activity at approximately the same period as is critical for the cortex (Flexner and Flexner, '48). These observations have raised the following question: Does differentiation at the critical period affect simultaneously a series of basic enzyme systems and so suggest a key mechanism which controls them all? The work reported here on the two respiratory enzymes, succinic dehydrogenase and cytochrome oxidase, is directed toward this question. The observations on the enzyme system, succinoxidase, are of interest because of the added evidence they give of a change in permeability of cortical cells at the critical period.

METHODS

Pregnant guinea pigs were killed by injection of air into the heart. Fetuses were removed immediately. Where possible, tissue for analysis was taken only from Fortuyn's ('14) areas f and f¹ of the cerebral cortex. In an effort to minimize irregularity of activities measured in liver, tissue was taken from the free edge of the same lobe from one experiment to another. The activity of succinic dehydrogenase was determined by the method previously described (Flexner and Flexner, '46) in which homogenized tissue is used in the presence of an excess of ferricyanide which serves as final electron-acceptor from succinate. Some of the samples of cortex were frozen and kept on dry ice up to a period of a month without affecting the activity of the enzyme. This procedure is not acceptable, however, for liver and consequently only fresh liver was used for the assays. Cytochrome oxidase was estimated on fresh tissue by the method of Schneider and Potter ('43), using ascorbic acid as substrate (Umbreit, Burris and Stauffer, '45). In view of the observations of Slater ('49) cytochrome oxidase activities have been checked by the spectrophotometric method used by Albaum, Tepperman and

Bodansky ('46) and by Stannard and Horecker ('48). Succinoxidase activity was measured as previously described (Flexner and Flexner, '46). Activities of succinic dehydrogenase and cytochrome oxidase in both cerebral cortex and liver are referred to a milligram wet weight of cellular phase (Flexner and Flexner, '49).

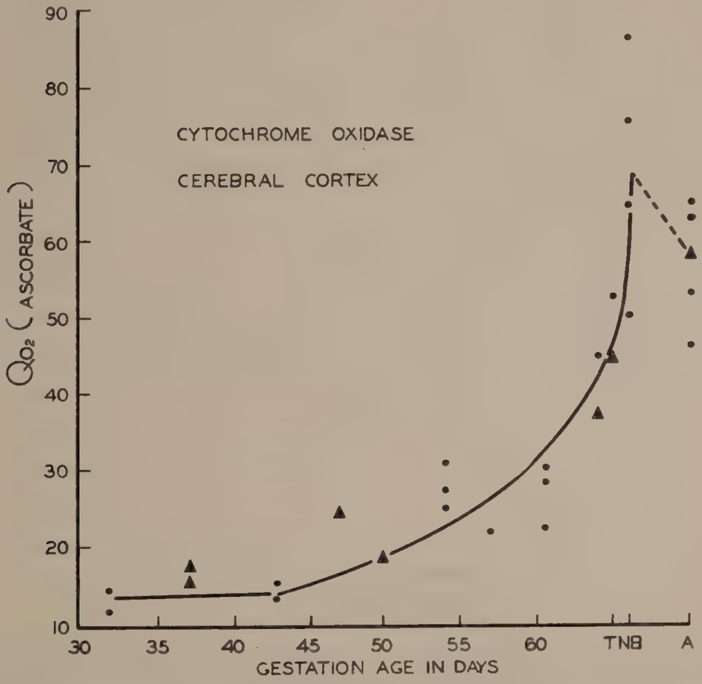

Fig. 1 Cytochrome oxidase activity of fetal and adult frontal cerebral cortex. Results with the method of Schneider and Potter ('43) are expressed in terms of cubic millimeters of oxygen consumed per milligram wet weight of cell phase per hour and are indicated by circles. Check results with the spectrophotometric method are indicated by circles within triangles and have been plotted by placing the adult value at the average Q_{O_2} (ascorbate) value of the adult. T = term; N.B. = newborn; A = adult.

RESULTS

Cerebral cortex. The results of assay of the cerebral cortex for cytochrome oxidase activity are given in figure 1. It will be noted that there is satisfactory agreement between the two methods of assay. The enzyme has a relatively low and constant level of activity up to about the 43rd day of gestation; then begins to increase to the fivefold greater activity found at term and in the adult.

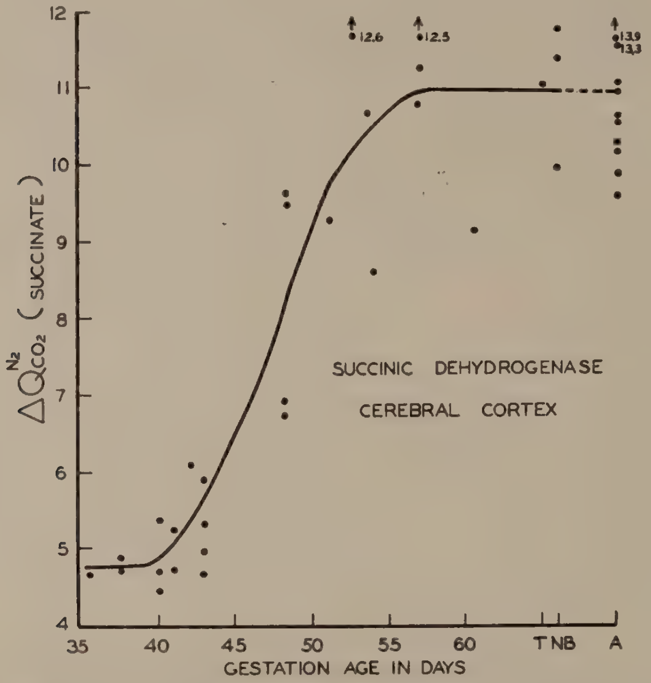

Fig. 2 Succinic dehydrogenase activity of fetal and adult frontal cerebral cortex. CO_2 production is in terms of cubic millimeters CO_2 per milligram wet weight of cell phase per hour, as observed with method utilizing homogenized tissue and ferricyanide.

The measurements of activity of succinic dehydrogenase, which show considerable variation, are given in figure 2. The enzyme appears to have a relatively low and constant level of activity up to the period between 40 and 45 days and then begins to increase to the two- or threefold greater activity found after the 55th day of gestation.

Our experience with succinoxidase activity in the fetal guinea pig was much like that previously reported for the fetal pig (Flexner, Flexner and Straus, '41). As shown in figure 3, at relatively early stages of gestation the increment of oxygen consumption on addition of succinate to minced cortex is so small as to be uncertain. This low activity might be because of several factors, among them a very low concentration of cyotchrome c, the presence of an inhibitor or failure of the succinate to penetrate the cell wall. Various methods failed to extract cytochrome c from the cortex of the guinea pig and we are consequently unable to make quantitative statements regarding its concentration during development. To test for the presence of an inhibitor, homogenates

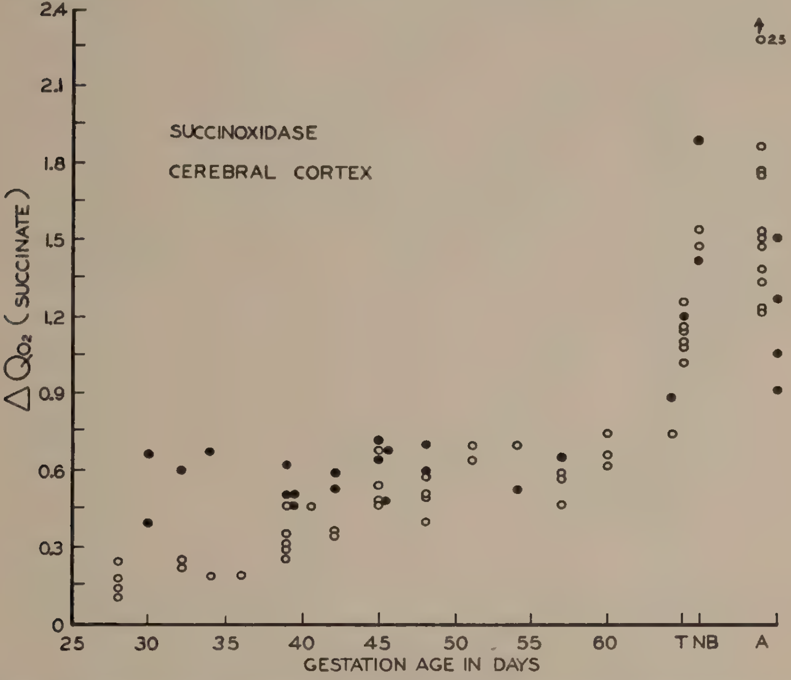

Fig. 3 Succinoxidase activity of minced and homogenized fetal and adult frontal cerebral cortex. Results are expressed in terms of the increment, on addition of succinate, in cubic millimeters of oxygen consumed per milligram wet weight per hour. Solid circles = homogenized cortex; open circles = minced cortex.

of fetal cortex were made with saline, centrifuged and the supernatant then added to a concentrated homogenate of adult cortex. The saline extract failed to reduce the oxygen consumption of the homogenate. To test for the possibility that the low activity might be because succinate failed to penetrate the cell wall, measurement was made of the response of an homogenate (in which the cell membranes were disrupted) to the addition of succinate. To minimize dilution effects as concentrated an homogenate as practical was used. Except for the cortex of the smaller fetuses, where 300 mg of tissue were taken, the homogenate contained 200 mg in 0.5 ml of fluid. As shown in figure 3, the response of the homogenate to succinate was definitive and considerably greater than with

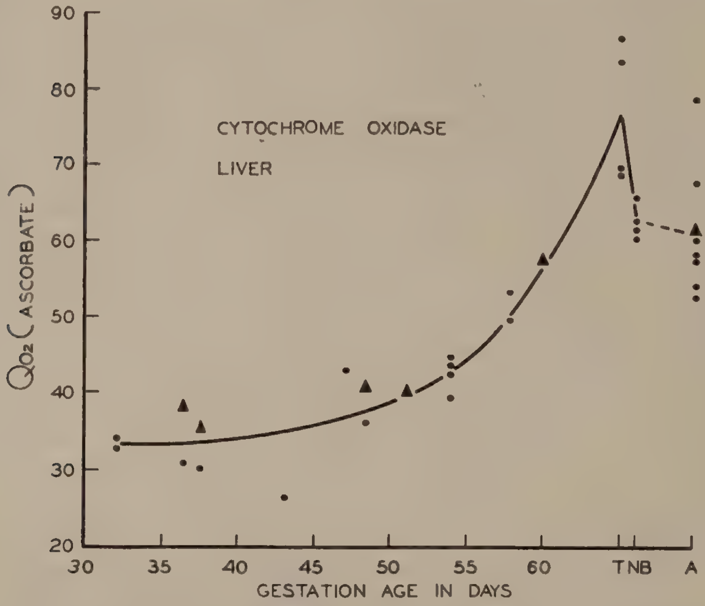

Fig. 4 Cytochrome oxidase activity of fetal and adult liver. Results with the method of Schneider and Potter ('43) are expressed in terms of cubic millimeters of oxygen consumed per milligram wet weight of cell phase (fat and glycogen free) per hour and are indicated by circles. Check results with the spectrophotometric method are indicated by triangles and have been plotted by placing the adult value at the average Q_{O_2} (ascorbate) of the adult.

the minced tissue. Minced tissue continued to give clearly a lower response than homogenates up to the 45th day. We explain this behavior by assuming that the cell membrane at early stages of development is relatively impermeable to succinate and that maturation is accompanied by an increase in permeability.

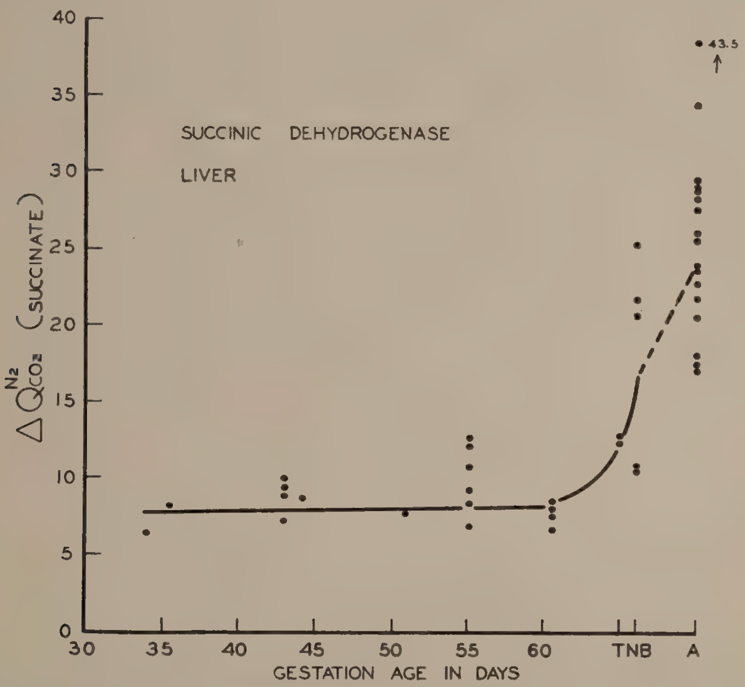

Fig. 5 Succinic dehydrogenase activity of fetal and adult liver CO_2 production is in terms of cubic millimeters CO_2 per milligram wet weight of cells (fat and glycogen free) per hour, as observed with method utilizing homogenized tissue and ferricyanide.

Liver. Results of assay of liver for cytochrome oxidase activity are given in figure 4. The two methods of assay were in satisfactory agreement. The enzyme has a relatively low level of activity in the earlier stages of gestation; it approximately doubles in amount to term where it appears to be somewhat higher than in the adult.

Measurements of activity of succinic dehydrogenase are given in figure 5. From the 34th to the 60th day the activities appear to fluctuate about a relatively low and constant level and then to begin to increase to the threefold higher average of the adult.

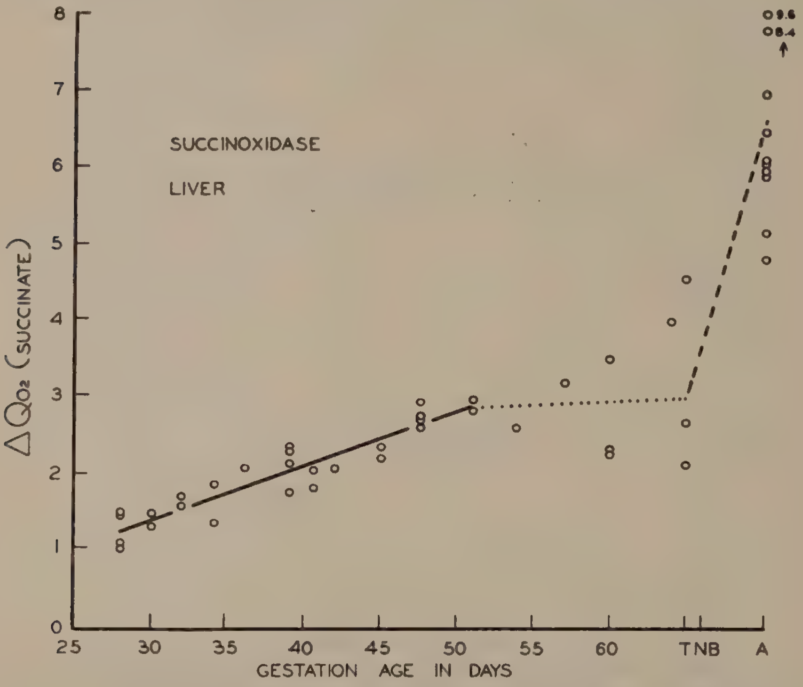

Fig. 6 Succinoxidase activity of minced fetal and adult liver. Results are expressed in terms of the increment, on addition of succinate, in cubic millimeters of oxygen consumed per milligram wet weight of cells (fat and glycogen free) per hour.

The succinoxidase activity of minced liver is given in figure 6. From the 28th to the 50th day there is a linear increase in activity; the observations to term then become indeterminate. The over-all increase in activity from the 30th day to the adult is about 6 times. Unlike the cortex, concentrated homogenates of fetal liver give succinoxidase activities 50 to 60% lower than the mince as in the adult; in the fetal liver there is no evidence of permeability effects.

DISCUSSION

Cerebral cortex. Observations previously reported on the rat (Potter, Schneider and Liebl, '45) and on the pig (Flexner, Flexner and Straus, '41) have shown that there is a critical time at which the activity of the succinic dehydrogenase of whole brain or cerebral cortex begins to increase rapidly to the adult level. In the brain of the rat this increase from a relatively low and constant level of activity occurs at the 7th day of postnatal life; in the cerebral cortex of the pig, at the beginning of the second half of gestation. The same pattern is evident during the development of the frontal cerebral cortex of the guinea pig, the increase taking place at the beginning of the last trimester of pregnancy.

Cytochrome oxidase activity in the guinea pig begins to increase to the adult level at approximately the same time as does succinic dehydrogenase. This is unlike the findings on the pig where a less reliable method of assay indicated a constant and low level of activity during the last three-fourths of prenatal life.

The assays of succinoxidase activity give evidence that the cell membrane increases in permeability to succinate at the critical period. This observation strengthens the deduction previously made (Flexner and Flexner, '49) that there is an increase in permeability to sodium-ion at this same time when the cell membrane appears to acquire at least some of its adult characteristics. In the pig, the corresponding period is characterized by an apparent increase in permeability to p-phenylenediamine (Flexner, Flexner and Straus, '41).

In answer to the question raised in the introduction to this report, it does appear that differentiation of the cerebral cortex of the guinea pig at the critical period affects simultaneously several enzymes. Succinic dehydrogenase and cytochrome oxidase in addition to adenylpyrophosphatase and, less clearly, cholinesterase begin to increase in activity at this time. The amount of protein per unit weight of cell phase remains constant throughout gestation (Flexner and Flexner, '50). The increase in enzyme activity per unit weight of cell phase consequently indicates that, beginning at the critical period, an increasing proportion of protein is diverted to the synthesis of these enzymes. The change in their activity is closely related temporally to a series of cytological, functional and other biochemical changes. Of most significance for present comment is the finding that increase in rate of synthesis of neuroplasm, as evidenced by the sprouting and growth of processes and the onset of functional activity, occurs coincidentally with increase in activity of some respiratory enzymes. This suggests that the added need for energy for growth and function is met by increase in the part played by aerobic metabolic processes.

Liver. The characteristics of increase of cytochrome oxidase activity in the liver differ from the cerebral cortex. During the last half of gestation, the oxidase activity of the cortex increases fivefold; that of the liver only doubles. Unlike the cortex where activity begins to increase at a critical period from a relatively constant level, hepatic activity progressively increases throughout that part of pregnancy which has been studied. This difference with respect to a critical period is also evident in the observations of Potter, Schneider and Liebl ('45) on succinic dehydrogenase and ATPase activities in the brain and liver of the developing rat. Reexamination of our results on adenylpyrophosphatase and acid phosphatase activities of the liver of the fetal guinea pig in the light of these experiences leads us to conclude that, contrary to our first interpretation, these enzymes also increase progressively during the last half of gestation without clear evidence of the sudden increase characteristic of the cortex. A critical period is, however, evident in the development of succinic dehydrogenase activity in the liver of the fetal guinea pig. Here the activity is relatively constant up to the 60th day of gestation and then begins to double in value to term.

SUMMARY

The activities of cytochrome oxidase and succinic dehydrogenase have been measured in cerebral cortex and liver of

the fetal guinea pig during the last half of gestation. In the cortex, these enzymes like others previousy studied begin to increase in activity at a common critical period. Except for succinic dehydrogenase such a critical period is not evident for those enzymes of the liver which have been studied.

Measurement of succinoxidase activity in the cortex gives evidence of an increase in permeability of its cells to succinate at the critical period.

LITERATURE CITED

Albaum, H. G., J. Tepperman and O. Bodansky 1946 J. Biol. Chem., *163:* 641.

Flexner, L. B., and J. B. Flexner 1946 J. Cell. and Comp. Physiol., *27:* 35.

Flexner, J. B., and L. B. Flexner 1948 J. Cell. and Comp. Physiol., *31:* 311.

Flexner, L. B., and J. B. Flexner 1949 J. Cell. and Comp. Physiol., *34:* 115.

Flexner, J. B., and L. B. Flexner 1950 Anat. Rec., *106:* 413.

Flexner, J. B., L. B. Flexner and W. L. Straus, Jr. 1941 J. Cell. and Comp. Physiol., *18:* 355.

Flexner, L. B., D. B. Tyler and L. J. Gallant 1950 J. Neurophysiol., *13:* 427.

Fortuyn, A. B. D. 1914 Arch. Neurol. and Psychiat. (Path. Lab., London County Asylums, Clayburg, Essex), *6:* 221.

Kavaler, F., and V. M. Kimel 1952 J. Comp. Neur., *96:* 113.

Kimel, V. M., and F. Kavaler 1951 J. Comp. Neur., *94:* 257.

Peters, V. B., and L. B. Flexner 1950 Am. J. Anat., *86:* 133.

Potter, V. R., W. C. Schneider and G. J. Liebl 1945 Cancer Research, *5:* 21.

Schneider, W. C., and V. R. Potter 1943 J. Biol. Chem., *149:* 217.

Slater, E. C. 1949 Biochem. J., *44:* 305.

Stannard, J. N., and B. L. Horecker 1948 J. Biol. Chem., *172:* 599.

Umbreit, W. W., R. H. Burris and J. F. Stauffer 1945 Manometric Techniques and Tissue Metabolism. Burgess Publ. Co., Minneapolis.

NOTICE TO CONTRIBUTORS

The Journal of Cellular and Comparative Physiology, appearing bimonthly, is intended as a medium for the publication of papers which embody the results of original research of a quantitative or analytical nature in general and comparative physiology, including both their physical and chemical aspects. Short preliminary notices are not desired and papers will not be accepted for simultaneous publication or which have been previously published elsewhere. While not specifically excluding any particular branch of physiology, contributors should recognize that excellent journals already exist for publication in the field of experimental and physiological zoology, dealing particularly with genetics, growth, behavior, developmental mechanics, sex determination, and hormonal interrelationships, and also for pure mammalian functional physiology and the physical chemistry of non-living systems. Preference will be given to analyses of fundamental physiological phenomena whether the material is vertebrate or invertebrate, plant or animal. Since the journal is restricted, it is not possible to publish more than a limited number of papers which must be short and concise.

It is recognized that prompt publication is essential, and the aim will be to issue papers within three months of acceptance.

Manuscripts and drawings should be sent to the Managing Editor, Detlev W. Bronk, Office of the President, The Johns Hopkins University, Baltimore 18, Maryland.

The paper must be accompanied by an author's abstract **not to exceed 225 words in length**, which will appear on the advance abstract cards of the Bibliographic Service of The Wistar Institute in advance of complete publication. **Nothing can be done with the manuscript until the abstract is received.**

Manuscripts should be typewritten in double spacing on one side of paper 8½ × 11 inches, and should be packed flat — not rolled or folded. The original, not carbon, copy should be sent. The original drawings, not photographs of drawings, should accompany the manuscript. Authors should indicate on the manuscript the approximate position of text figures.

Manuscripts and drawings should be submitted in complete and finished form with the author's complete address. All drawings should be marked with the author's name. The Wistar Institute reserves the privilege of returning to the author for revision approved manuscript and illustrations which are not in proper finished form for the printer. **When the amount of tabular and illustrative material is judged to be excessive, or unusually expensive, authors may be requested to pay the excess cost.**

The tables, quotations (extracts of over five lines), and all other subsidiary matter usually set in type smaller than the text, should be typewritten on separate sheets and placed with the text in correct sequence. Footnotes should not be in with the text (reference numbers only), but typewritten continuously on separate sheets, and numbered consecutively. Explanations of figures should be treated in the same manner, and, like footnotes, should be put at the end of the text copy. **A condensed title for running page headlines, not to exceed thirty-five letters and spaces, should be given.**

Figures should be drawn for reproduction as line or halftone engravings, unless the author is prepared to defray the additional cost of a more expensive form of illustration. All colored plates are printed separately and cost extra. In grouping the drawings it should be borne in mind that, after the reduction has been made, text figures are not to exceed the dimensions of the printed matter on the page, 4¼ × 6¾ inches. Single plates may be 5 × 7½ inches, or less, and double plates (folded in the middle), 11½ × 7½ inches. Avoid placing figures across the fold, if possible.

Figures should be numbered from 1 up, beginning with the text figures and continuing through the plates. **The reduction desired should be clearly indicated on the margin of the drawing.**

All drawings intended for photographic reproduction either as line engravings (black-ink pen lines and dots) or halftone plates (wash and brush work) should be made on white or blue-white paper or bristol board — not on cream-white or yellow-tone. Photographs intended for halftone reproduction should be securely mounted with colorless paste — never with glue, which discolors the photograph.

Galley proofs and engraver's proofs of figures are sent to the author. All corrections should be clearly marked thereon.

The journal furnishes the author fifty reprints, with covers, of the paper gratis. Additional copies may be obtained according to rates which will be sent the author as soon as the manuscript has been examined at The Wistar Institute, after acceptance.

JOURNAL OF
CELLULAR AND COMPARATIVE
PHYSIOLOGY

VOL. 42 AUGUST 1953 No. 1

CONTENTS

B. W. SHUMWAY, M. SABLE AND H. R. BIERMAN. The electrical potentials produced by the chick embryo during its incubation period. Six figures ... 1

FRITIOF S. SJÖSTRAND. The ultrastructure of the outer segments of rods and cones of the eye as revealed by the electron microscope. Twelve figures .. 15

FRITIOF S. SJÖSTRAND. The ultrastructure of the inner segments of the retinal rods of the guinea pig eye as revealed by electron microscopy. Eleven figures ... 45

P. D. BOYER. The activation by K^+ and occurrence of pyruvic phosphoferase in different species. One figure ... 71

H. P. JENERICK AND R. W. GERARD. Membrane potential and threshold of single muscle fibers. Eight figures ... 79

ROBERT E. TAYLOR. The contractile process is not associated with potential changes. Seven figures ... 103

EUGENE BELL. The origin and nature of granules found in macrophages of the white mouse following intravenous injection of Thorotrast. Four figures ... 125

J. WOODLAND HASTINGS, WILLIAM D. MCELROY AND JANE COULOMBRE. The effect of oxygen upon the immobilization reaction in firefly luminescence. Five figures ... 137

LOUIS B. FLEXNER, ELSTON L. BELKNAP, JR., AND JOSEFA B. FLEXNER. Biochemical and physiological differentiation during morphogensis. XVI. Cytochrome oxidase, succinic dehydrogenase and succinoxidase in the developing cerebral cortex and liver of the fetal guinea pig. Six figures .. 151

PRESS OF
THE WISTAR INSTITUTE
OF ANATOMY AND BIOLOGY
PHILADELPHIA

Printed in the United States of America